From the Department of Hematology and Oncology
Medical Faculty
Otto-von-Guericke-University Magdeburg

A study on the effects of calreticulin del52 mutation on neutrophil adhesion: Results from CALRdel52 knock-in mice and characterization of a novel CALRdel52 Catchup mouse model

D i s s e r t a t i o n

to obtain the degree of

Dr. med.

(doctor medicinae)

in the Medical Faculty of the
Otto-von-Guericke-University Magdeburg

presented by Emmanouil Charakopoulos

from Athens, Greece

Magdeburg 2023

Bibliographic Description

Charakopoulos, Emmanouil:

A study on the effects of calreticulin del52 mutation on neutrophil adhesion: Results from CALRdel52 knock-in mice and characterization of a novel CALRdel52 Catchup mouse model.
- 2023. – 60 pages, 17 figures, 2 tables, 11 supplements

Abstract

In the pathophysiology of classical Philadelphia-negative myeloproliferative neoplasms (MPNs), JAK2-V617F represents the most prevalent underlying disease driver mutation followed by deletion mutations in the gene encoding the endoplasmatic reticulum chaperone calreticulin (CALR). Patients harboring CALRdel mutations are at a lower risk of thrombosis as opposed to JAK2-V617F mutation carriers, but this difference in thrombotic risk has yet not been clarified at the molecular level. Our research group has shown for the first time that a JAK2-V617F-mediated shift of neutrophil-bound integrins to the high-affinity conformation leads to increased thrombus formation by strengthening neutrophil adhesion to the endothelial adhesion molecule vascular cell adhesion molecule 1 and lymphocyte function-associated antigen 1. Contrary to JAK2-V617F, much remains unknown regarding the effect CALRdel on neutrophil biology. In this doctoral thesis, we employ a novel neutrophil-specific CALRdel Catchup model and a hematopoietic-specific VavCre CALRdel mouse model to evaluate the impact of CALRdel on neutrophil function. In both murine models, CALRdel was not associated with increased integrin-mediated adhesion. Interestingly, a decreased binding of CALR-mutated neutrophils to E-selectin under flow and partially under static conditions was observed. In addition, CALRdel-expressing neutrophils were not capable of inducing a chronic myeloproliferative phenotype as assessed by similar blood counts and spleen size of $CALR^{del/+}$ Catchup mice compared to their wild-type counterparts. As opposed to a recently described JAK2-V617F Catchup mouse model, $CALR^{del/+}$ Catchup mice did not exhibit elevated levels of key pro-inflammatory cytokines, which points towards a minor role of CALRdel-expressing granulocytes in chronic non-resolving inflammation of MPNs. Our findings indicate that JAK2-V617F and CALRdel differentially regulate neutrophil-related adhesion and inflammation in the pathogenesis of MPNs.

Key Words: CALRdel52, calreticulin, myeloproliferative neoplasm, neutrophil, cell adhesion, thrombosis

Table of Contents

Bibliographic Description

Table of Contents

Abbreviations

1. Introduction 1

1.1. An overview of classical Myeloproliferative Neoplasms (MPNs) 1

1.1.1. Classification of MPNs and characteristics of classical MPNs 1

1.1.2. Quantitative and qualitative changes in blood cells drive thrombosis in classical MPNs 3

1.1.3. MPNs serve as a model of onco-inflammation 5

1.1.4. The role of CALR mutations in classical MPNs 8

1.1.5. JAK2- and CALR-mutated MPNs exhibit differences in clinical presentation, disease-driving mechanism and thrombotic risk 10

1.2. The role of leukocyte-endothelial cell adhesion in thrombosis 11

1.2.1. Activation of the leukocyte adhesion cascade is a major event during venous thrombosis 11

1.2.2. Integrin-mediated neutrophil adhesion to the vascular endothelium drives thrombosis in JAK2-mutated MPNs 13

1.3. Revealing the role of neutrophils in the pathophysiology of MPNs: The Catchup mouse model 15

1.3.1. The murine lymphocyte antigen 6 complex, locus G (Ly6g) gene allows for generation of a mouse model with high neutrophil-specificity 15

1.3.2. $JAK2^{VF/+}$ Catchup mice develop an ET phenotype and exhibit increased integrin-mediated neutrophil adhesion 17

1.4. Hypothesis 18

1.5. Aims and Objectives 20

2. Materials and methods 20

2.1 Animals 20

2.2. Blood counts 21

2.3. Polymerase chain reaction (PCR) genotyping strategy 21

2.4. Hematopoietic cell isolation 22

2.5. Neutrophil isolation 22

2.6. Cytospins 23

2.7.1. Hematoxylin and eosin (H&E) staining 23

2.7.2. Reticulum staining 23

2.8. Flow cytometry 23

2.8.1. Measurement of β integrin and PSGL-1 expression 24

2.8.2. Soluble ligand binding 24
2.8.3. Hematopoietic stem and progenitor cell measurement 24
2.8.4. Measurement of MPL expression 25
2.8.5. Measurement of intracellular phosphorylated STAT1, STAT3 and STAT5 26
2.9. Static adhesion assay 26
2.10. Time lapse assay 27
2.11. Cytokine measurement 27
2.12. Quantitative reverse transcription PCR (qRT-PCR) 27
2.13. Data analysis, representation, and statistical methodology 28
2.14. Study approval 28
3. Results 29
3.1. Negative immunomagnetic isolation of murine WT BM neutrophils yields a cell population with high neutrophil purity 29
3.2. PCR genotyping of VavCre CALR mice 31
3.3. VavCre CALR$^{del/+}$ mice develop a phenotype resembling human ET 31
3.4. Granulocytes isolated from VavCre CALR$^{del/+}$ mice do not demonstrate increased integrin-mediated adhesion 33
3.5. PCR genotyping of CALR Catchup mice 34
3.6. Neutrophil-specific expression of CALRdel52 is not sufficient to induce a chronic myeloproliferative disease 35
3.7. CALR$^{del/+}$ Catchup mice do not show increased expression of inflammatory mediators in serum 41
3.8 Neutrophils isolated from CALR$^{del/+}$ Catchup mice express MPL and exhibit increased TPO-induced STAT5 phosphorylation 43
3.9. Granulocytes isolated from CALR$^{del/+}$ Catchup mice do not demonstrate increased integrin-mediated adhesion 45
3.10. Migration of CALR$^{del/+}$ tdTomato^{+} granulocytes 46
4. Discussion 48
4.1. Hematopoietic expression of CALRdel52 affects primarily but not exclusively the megakaryocytic lineage 48
4.2. Absence of increased integrin-mediated adhesion in neutrophils isolated from VavCre CALR$^{del/+}$ mice 49
4.3. Impaired adhesion of neutrophils isolated from VavCre CALR$^{del/+}$ mice to E-selectin 51
4.4. Different phenotypes of JAK2$^{VF/+}$ Catchup and CALR$^{del/+}$ Catchup models indicate a differential role of CALRdel52 and JAK2-V617F in neutrophil biology 53
4.5. Absence of increased integrin-mediated adhesion in neutrophils isolated from CALR$^{del/+}$ Catchup mice 54

4.7. Neutrophil-specific expression of CALRdel52 does not alter migration of granulocytes in vitro 57
4.8. Limitations 58
4.9. Implications for future research 59
5. Summary 60
German summary
References
Acknowledgments
Ehrenerklärung
Curriculum vitae
Supplements

Abbreviations

-R	-receptor
-RA	-receptor antagonist
APC	Allophycocyanin
BM	Bone marrow
BV	Brilliant violet
CALR	Calreticulin
CCL	C-C motif ligand
CI	Confidence interval
CMP	Common myeloid progenitor
CRD	Carbohydrate recognition domain
Cre	Cyclic recombinase
CRP	C-reactive protein
CXCL	C-X-C motif ligand
DVT	Deep vein thrombosis
EGF	Epidermal growth factor
EpoR	Erythropoietin receptor
ER	Endoplasmatic reticulum
ESL	E-selectin ligand
ET	Essential thrombocythemia
FACS	Fluorescence-activated cell sorting
FBS	Fetal bovine serum
FCS	Fetal calf serum
FSC	Forward scatter
G-CSF	Granulocyte colony stimulating factor
GM-CSF	Granulocyte-macrophage colony stimulating facor
GMP	Granulocyte-macrophage progenitors
GP	Glycoprotein
Gr-1	Granulocyte differentiation antigen
GRO	Growth-regulated protein
GTPase	Guanosine triphosphatase
H&E	Hematoxylin and eosin
Hb	Haemoglobin
HBSS	Hank's balanced salt solution
Hct	Haematocrit
HPRT	Hypoxanthine phosphoribosyltransferase
HSC	Hematopoietic stem cell
ICAM	Intercellular cell adhesion molecule
IFN	Interferon
IL	Interleukin
IP	Interferon-inducible protein
IRE1α	Inositol-requiring enzyme 1 alpha
IVC	Inferior vena cava
JAK2	Janus Kinase 2
JAK-STAT	Janus kinase-Signal transducer and activator of transcription

KC	Keratinocytes-derived chemokine
Ki-PCR	Knock-in PCR
LFA	Lymphocyte function-associating antigen
LIF	Leukemia inhibitory factor
LIX	Lipopolysaccharide-induced CXC chemokine
loxP	Locus of crossover in P1
LT-HSC	Long term HSC
Ly6x	Lymphocyte antigen 6 complex, locus X
MACS	Magnetic-activated cell sorting
MCHC	Mean cell haemoglobin concentration
MCP	Monocyte chemoattractant protein
MCV	Mean corpuscular volume
MEP	Megakaryocyte-erythroid progenitor
MF	Myelofibrosis
MFI	Mean fluorescence intensity
MIG	Monokine induced by gamma
MIP	Macrophage inflammatory protein
MK	Megakaryocyte
MkP	Megakaryocyte progenitor
MP	Myeloid progenitor
MPL	Myeloproliferative leukemia virus
MPN	Myeloproliferative neoplasm
MPP	Multipotent progenitor
MPV	Mean platelet volume
MSFI	Mean subtracted fluorescence intensity
NET	Neutrophil extracellular trap
NK	Natural killer
NO	Nitric oxide
NTL	Neutrophil-to-lymphocyte
OS	Overall survival
PBS	Phosphate buffered saline
PCR	Polymerase chain reaction
PDGF	Platelet-derived growth factor
PE	Phycoerythrin
PLT	Platelet
PMF	Primary myelofibrosis
PSGL-1	P-selectin glycoprotein ligand
PV	Polycythemia vera
qRT-PCR	Quantitative reverse-transcription PCR
RANTES	Regulated on Activation, Normal T Cell Expressed and Secreted
Rap	Ras-related protein
RBC	Red blood cell
RDW	Red cell distribution width
ROS	Reactive oxygen species
Sca	Stem cell antigen
SCF	Stem cell factor
SDF	Stromal cell-derived factor
SEM	Standard error of the mean

sLe^X	Sialyl $Lewis^x$
SOCE	Store-operated calcium entry
SSC	Side scatter
ST-HSC	Short term HSC
TF	Tissue factor
TGF	Transforming growth factor
TNF	Tumor necrosis factor
TPO	Thrombopoietin
UPR	Unfolded protein response
VCAM	Vascular cell adhesion molecule
VEGF	Vascular endothelial growth factor
VLA	Very late antigen
WBC	White blood cell
WT	Wild-type
XBP1	X-box binding protein 1

1. Introduction

1.1. An overview of classical Myeloproliferative Neoplasms (MPNs)

1.1.1. Classification of MPNs and characteristics of classical MPNs

MPNs constitute a group of hematopoietic diseases that are believed to originate from clonal expansion of hematopoietic stem and progenitor cells. The main common features of these clinical entities are their chronic clinical course and the overproduction of differentiated myeloid cells.(1) According to the 2016 World Health Organization classification and diagnostic criteria, MPNs are comprised of seven clinicopathological entities. These include the classical or Philadelphia-negative MPNs [polycythemia vera (PV), essential thrombocythemia (ET) and primary myelofibrosis (PMF)], BCR-ABL1-positive chronic myeloid leukemia, chronic neutrophilic leukemia, chronic eosinophilic leukemia – not otherwise specified and MPN-unclassifiable.(2)

Classical MPNs are characterized by cellular hyperproliferation in the erythroid, megakaryocytic or granulocytic lineage and have overlapping clinical and laboratory spectra.(3) Classical MPN patients are at increased risk of thrombosis or hemorrhage and disease transformation into post-PV or post-ET myelofibrosis (MF) and acute myeloid leukemia (blast phase).(4-6) The annual incidence of PV and ET has been estimated to be up to 2-3 cases per 100,000 population, whereas up to one case of PMF is diagnosed per 100,000 people each year.(7) PV, the most common MPN, is characterized by an elevated haematocrit (Hct), which can also be accompanied by an increased number of neutrophils and platelets (PLTs).(8) Patients may be asymptomatic or present with splenomegaly and even constitutional symptoms in late stages (loss of weight, weakness, night sweating, pruritus or diffuse osteodynia).(9) In PV, there is a particularly high risk of mortality due to thrombosis, especially in the presence of additional risk factors, for example age > 60 years, history of thrombosis or increased leukocyte counts, with a median survival of about 14 years.(5, 10) The hallmark of ET is persistent thrombocytosis due to bone marrow (BM) megakaryocytic hyperplasia. Patients with ET are frequently asymptomatic; they are however at risk of developing thrombo-hemorrhagic complications.(9) Among classical MPNs, ET is associated with the most favorable median survival (approximately 18-20 years).(5, 11) PMF is associated with more severe symptomatology and less favorable prognosis (median overall survival of approximately 5-6 years) compared to ET and PV as a result of elevated risk of leukemic transformation, thrombosis or hemorrhage, infection and portal hypertension.(5, 12-14) The main feature of PMF is BM

reticulin fibrosis.(1) BM fibrosis results in BM failure and reduction of blood counts in one, two or all three blood cell lines (most commonly anemia), although leukocytosis and thrombocytosis can also be observed. Splenomegaly and constitutional symptoms are common clinical manifestations of PMF.(9)

PV, ET and PMF were known as distinct clinical entities until 1951, when they were grouped under the common term “myeloproliferative disorders” by William Dameshek.(15) In 2005, hematopoietic-specific expression of the activating Janus Kinase 2 (JAK2) V617F mutation, resulting from a valine to phenylalanine substitution in codon 617 of the JAK2 tyrosine kinase, was identified in most patients with classical MPNs.(16-19) More specifically, the JAK2-V617F mutation can be found in the vast majority of patients with PV (>90%) and in approximately 50% of ET and PMF cases.(20) Interestingly, rare mutations of the JAK2 exon 12 are present in the small percentage of patients with JAK2-V617F-negative PV.(21) In addition, it was known since 2006, that a small proportion of patients with JAK2-V617F-negative ET and PMF (approximately 5-10%) express gain-of-function mutations of the myeloproliferative leukemia virus (MPL) gene, which encodes the thrombopoietin (TPO) receptor.(22) It was not until 2013, when two independent exome sequencing studies demonstrated that 70-80% of patients who are diagnosed with non-JAK2 or MPL-mutated ET and PMF exhibit a mutation in the exon 9 of calreticulin (CALR). Overall, CALR mutations are present in about 25% of patients with ET and 35% of patients with PMF.(23, 24) There remains 20% of ET and 10-15% of PMF patients in the case of which neither of the aforementioned mutations can be identified (triple-negative MPN).(2)

The treatment of classical MPNs aims at thrombosis prevention, blood count reduction, constitutional symptom amelioration and improvement of splenomegaly. Low dose aspirin (81 mg/day) is initiated in ET and PV patients. In PV, the primary target of treatment is reduction of Hct levels, which can be achieved by phlebotomy and/or cytoreductive therapy with hydroxyurea.(9, 25) In high-risk ET patients, normalization of PLT counts with cytoreduction and/or inhibition of megakaryocyte differentiation by anagrelide has been proven to reduce thrombotic risk.(26, 27) Inhibition of the Janus kinase-Signal transducer and activator of transcription (JAK-STAT) pathway, mainly with oral administration of the JAK1/2 inhibitor ruxolitinib, represents the mainstay of treatment in PMF, but is also used in hydroxyurea-resistant PV.(9) JAK inhibitors are effective in reducing splenomegaly and constitutional symptoms of MPN patients.(28) Importantly, there is currently no mutation-specific treatment strategy and ruxolitinib can be used in all driver mutation types (JAK2, CALR and MPL) because they all converge to hyperactivation of JAK-STAT signaling.(29) Supportive treatment of PMF involves blood transfusions in the case of severe anemia, while allogeneic stem cell transplantation remains the only curative option.

Finally, interferon-α and alkylating agents, for example busulfan, can be used as second- and third line medications in MPNs.(9) Clinical, epidemiological and laboratory features of MPNs are summarized in Table 1.

Table 1. Clinical, epidemiological and laboratory characteristics of classical Philadelphia-negative MPNs.(2,7,30)

	PV	**ET**	**PMF**
Annual incidence rate per 100,000 (95% CI) (7)	0.84 (0.70 – 1.01)	1.03 (0.58 – 1.80)	0.47 (0.34 - 0.65)
Hemoglobin, median (range), g/dL (7)	18.4 (15.1 – 24.5)	13.9 (6.9 – 17.9)	10.6 (5.8 – 16.1)
Leukocytes, median (range), x 10^9/L (7)	11.8 (3.8 – 171.6)	9.6 (2.8 – 53.4)	8.6 (0.8 – 146.6)
Platelets, median (range), x 10^9/L (7)	467 (37 – 1720)	1000 (454 – 3460)	253 (12 – 2466)
Bone marrow changes (2)	Hypercellularity with trilineage growth	Megakaryocytic hyperproliferation with large, mature and hyperlobulated megakaryocytes	Megakaryocytic hyperproliferation and atypia Reticulin and/or collagen fibrosis grade 2 or 3
Driver mutation (7)	JAK2-V617F or JAK2 exon 12	JAK2-V617F, CALR mutations, MPL W515L/K	JAK2-V617F, CALR mutations, MPL W515L/K
Median overall survival (years) (7)	13.7	19.8	5.9
Prevalence of thrombosis at diagnosis (95% CI) (30)	28.6 (22.0 – 36.3)	20.7 (16.6 – 25.5)	9.5 (5.0 – 17.4)

CI: Confidence Interval

1.1.2. Quantitative and qualitative changes in blood cells drive thrombosis in classical MPNs

The increase in blood counts resulting from chronic myeloproliferation, more specifically erythrocytosis, thrombocytosis and leukocytosis, are all thought to contribute to the procoagulant state of MPNs.(31, 32) Leukocytosis is a well-established independent risk factor for arterial thrombosis in PV and ET. (11, 33-35) Regarding the role of erythrocytosis in thrombotic risk there exists conflicting evidence; a prospective randomized study in 2013 was able to detect a significant correlation between Hct elevation and thrombosis in PV as opposed to what was demonstrated by previous studies.(36-39) It is currently

thought that increased Hct levels induce thrombus formation through hyperviscosity at low values of shear rate (eg in the venous system), and shear-induced PLT activation due to displacement of PLTs towards the endothelial surface at high shear rate values, such as in the arterial network.(40, 41) There is currently no data supporting a role of thrombocytosis in the increased thrombotic risk of patients with MPN, with some studies showing that extreme thrombocytosis is associated with a higher risk of hemorrhage rather than thrombosis.(42)

However, the pathophysiological mechanism of increased thrombotic risk in MPN is multifaceted and goes beyond mere increases in blood cell counts. Functional and structural abnormalities of blood and endothelial cells are additional factors that mediate thrombosis in MPNs.(31, 32) Contrary to the low importance of PLT number in MPN thrombosis, qualitative changes in PLTs are considered as one of the most important mediators of the procoagulant phenotype.(43) As a result of the mutation-driven hyperactivation of the JAK2-signaling pathway in hematopoietic progenitor cells, PLTs shift into an activated state, as demonstrated by the upregulation of membrane bound P-selectin and tissue factor (TF) and increased phagocytosis rate by circulating leukocytes.(44-46) Increased levels of PLT activation markers, such as β-thromboglobulin, platelet factor 4, platelet-derived growth factor (PDGF) and thromboxane B2 can be detected in the blood and/or urine of MPN patients.(47-49) In PV, structural abnormalities of the red blood cell (RBC) membrane and increased RBC adhesion to the basement membrane protein laminin facilitate the formation of RBC aggregates on the vessel wall, which subsequently participate in thrombus propagation.(41, 50)

Neutrophil activation, as assessed by increased expression of membrane-bound integrin αM (CD11b), is a well-known characteristic of MPN and plays a major role in thrombus formation.(51) Upregulation of CD11b on neutrophils enhances adhesion to PLTs and formation of neutrophil-PLT aggregates, which can be attributed to the role of the PLT glycoprotein (GP) Ibα as a counter-receptor for CD11b.(31, 52, 53) The interaction between PLTs and neutrophils contributes to the prothrombotic state by reciprocally promoting further activation of both cell types.(43) Activated neutrophils release primary granule proteins (eg cathepsin G, elastase and myeloperoxidase) and reactive oxygen species (ROS), which are able to cleave coagulation factors and activate PLTs and endothelial cells.(54) Neutrophil-induced endothelial damage leads to detachment and activation of endothelial cells, which in turn release factors that facilitate cell aggregation, such as selectins, von Willebrand factor (vWF) and thrombomodulin.(55-57) In addition, endothelial synthesis of nitric oxide (NO), which plays a key role in thrombosis by inhibiting PLT conglomeration and adhesion, becomes impaired.(57, 58) Finally, activation

of cell-surface β_1 and β_2 integrins on JAK2-V617F-mutant neutrophils facilitates thrombus formation by strengthening adhesion to vascular cell adhesion molecule 1 (VCAM-1) and intercellular adhesion molecule 1 (ICAM-1) normally expressed on the vascular endothelium.(59-61)

An additional mechanism of neutrophil-mediated thrombosis in MPNs lies in the formation of neutrophil extracellular traps (NETs), chromatin complexes composed of primary granule proteins, DNA and histones. It has been demonstrated, that JAK2-mutated neutrophils exhibit increased formation of NETs, which are capable of further propagating thrombosis by serving as scaffolds for coagulation factors, PLTs and red blood cells.(62, 63) The process of NET formation and extracellular release is a specialized form of cell death which does not fulfill the criteria neither for necrosis nor apoptosis and involves stimulus-induced intracellular signal transduction.(64) Characteristic features of NETosis are chromatin decondensation, which is induced by neutrophil elastase and protein arginine deiminase 4 through histone cleavage and citrullination respectively, nuclear swelling and eventually compromise of nuclear and cellular membrane integrity.(63-66)

1.1.3. MPNs serve as a model of onco-inflammation

The term “onco-inflammation” refers to the complex interaction between tumor cells and their inflammatory milieu.(67) Tumor cells are able to secrete pro-angiogenic factors [eg vascular endothelial growth factor (VEGF)] and immunosuppressive cytokines [mainly interleukin (IL)-10 and transforming growth factor beta (TGF-β)], which allows them to escape immunosurveillance from adjacent stroma and immune cells. Simultaneously, a chronically inflamed microenvironment contributes to malignant transformation through increased levels of tumor necrosis factor alpha (TNF-α), IL-6 and IL-8, which exhibit anti-apoptotic properties and increase cell proliferation. Tumor cells readily secrete inflammatory cytokines, which further enhance inflammation in the neighboring tumor microenvironment. In this way, a vicious circle between inflammation and tumorigenesis is maintained.(68, 69)

In the case of MPNs, driver mutations lead to clonal proliferation and induce increased secretion of inflammatory mediators from the affected malignant clone. Elevated cytokine levels are responsible for generation of chronic inflammation locally (in the BM microenvironment) and systemically. In the context of a chronically inflamed microenvironment, constitutively active immune cells induce tissue damage and fibrosis and readily secrete ROS and NO. In the resulting hostile cellular milieu, cells that acquire mutations which confer an increased survival advantage are able to proliferate (selective

pressure). Inflammation-driven selective pressure can further promote malignant transformation through genomic instability and emergence of DNA mutations and can be exerted either on malignant cells, therefore promoting evolution of ET or PV to post-ET and post-PV MF respectively, or on healthy cells, thus giving rise to secondary malignancies. Due to the central role of inflammation in progression of MPNs, the pathophysiology of MPNs is currently considered to be a paradigm of onco-inflammation.(70-72)

The JAK-STAT pathway has been shown to play a pivotal role in cytokine signaling and immune cell function and is constitutively activated by all three MPN mutation types. Hyperactivation of the JAK-STAT pathway in the context of MPNs leads to cytokine-independent proliferation and cytokine hyperresponsiveness.(73) Therefore, the JAK-STAT pathway represents a biological link between the disease driving mechanism of MPNs and cytokine signaling.(74) The elevated inflammatory mediator profile in MPNs is responsible for the systemic symptoms that typically appear in MPNs, for example fatigue, fever, weight loss, pruritus and night sweats, especially in advanced PMF, and contributes to the increased atherosclerotic and thrombotic risk, as well as to the increased probability of secondary malignancy emergence in MPN patients.(70, 71, 75-77)

A large number of studies have tried to define the pattern of cytokine elevation in classical-Philadelphia negative MPNs and to elucidate the prognostic significance of specific cytokines. More specifically, elevated serum levels of pro-inflammatory cytokines, including IL-1β, IL-2, IL-2R, IL-5 (in ET and PV), IL-6, IL-7 (in PV), IL-12, IL-13 (in PV and PMF), IL-15 (in PMF), IL-17 (in PMF), IL-23 (in PV), TNF-α, interferon alpha (IFN-α) and IFN-γ (in PV and PMF), anti-inflammatory cytokines, including IL-1RA (in PV and PMF), IL-4, IL-10, IL-11 (in PV) and IL-13 (in PV and PMF), chemokines, including monocyte chemoattractant protein-1 (MCP-1), macrophage inflammatory protein 1-alpha (MIP-1α), MIP-1β, IL-8, regulated on activation, normal T cell expressed and secreted (RANTES) (in ET and PMF), interferon-induced protein (IP)-9, IP-10 (in PV and PMF), monokine induced by gamma (MIG) (in PV and PMF), growth-regulated protein alpha (GRO-α) and C-C motif chemokine ligand (CCL)11 (in ET and PV) and growth factors, including granulocyte-macrophage colony-stimulating factor (GM-CSF), granulocyte colony-stimulating factor (G-CSF) (in PMF), hepatocyte growth factor (in PV and PMF), PDGF, VEGF (in PV and PMF), epidermal growth factor (EGF), TPO (in PMF), stem cell factor (SCF) (in ET) and TGF-β (in PMF) have been reported in patients with MPNs.(78-93) Reductions in inflammatory biomarker concentrations were controversial and very rarely observed by a few studies, more specifically decreased levels of IFN-γ in PMF and RANTES as well as EGF in PV.(85, 86)

The pattern of inflammatory mediator expression is different among the three Philadelphia-negative MPNs. In general, PMF is associated with a larger increase of inflammatory biomarkers compared to PV and ET, with the exception of IL-7, VEGF, MIG, GRO-α and CCL11, which are found in lower levels in PMF. Interestingly, pro-fibrotic cytokine concentrations, for example MCP-1, fibroblast growth factor and TGF-β, display higher concentrations in PMF compared to ET and PV.(80, 86, 87, 90-92) In general, ET and PV demonstrate a similar inflammatory biomarker profile, with the exception of some chemokines and growth factors that are found in higher concentrations in ET compared to PV, namely MCP-1, IL-8, RANTES, GRO-α, GM-CSF, PDGF and VEGF.(79, 80, 83, 84, 87, 90, 94)

Inflammatory mediators correlate with different stages of disease evolution, constitutional symptoms and treatment response and might be of prognostic significance in MPNs. A further increase in the concentration of IL-6, IL-2 and sIL-2Rα accompanies transformation of PV and ET to MF and MF to AML. Symptom improvement after initiation of treatment with the JAK2-inhibitor ruxolitinib is correlated with significant decreases in TNF-α, C-reactive protein (CRP), IL-1RA, MIP-1β, and IL-6.(95) In MF, levels of IL-8 independently predict leukemia-free survival and constitutional symptoms. In addition, IL-2R and IL-12 levels are predictive of transfusion need. Moreover, IL-8, IL-2R, IL-15 and IL-12 are associated with a more dismal overall survival independently of prognostic risk.(85) In PV, MIP-1β was found to be the only inflammatory biomarker that is associated with inferior survival in multivariate models and IL-12 levels were demonstrated to be positively correlated with Hct.(86)

Whether some cytokines are elevated in the context of a specific driver mutation has not been extensively investigated. TNF-α and PDGF tend to be increased particularly in JAK2-mutated PV and ET.(94) In addition, elevation of IP-10 levels and prognostic significance of sIL-2Rα have been demonstrated only in JAK2-mutated PMF.(87, 89) In a study of serum cytokine profiling in JAK2- and CALR-mutated PMF patients, IL-12, along with IL-13, were significantly upregulated only in JAK2-mutated patients, whereas increased IL-17 and lower IFN-γ levels were shown specifically in CALR-mutated patients.(96) A threefold elevation of TGFβ-2 serum levels was detected particularly in MPL-mutated patients.(92) In CALR-mutated PMF patients, a correlation between CALR and IL-6 serum levels has been observed, and recently IL-6 signaling blockade has been proposed as a potential therapeutic target of CALR-mutated MPNs based on hyperactivation of IL-6 pathway in UT7 and UT7/mpl cell lines harboring the CALRdel52 mutation.(97, 98)

1.1.4. The role of CALR mutations in classical MPNs

CALR is an endoplasmatic reticulum (ER) Ca^{2+} binding chaperone of 46kDa in size which plays a key role in supporting the folding of proteins that travel across the ER and regulating Ca^{2+} levels in the ER lumen.(99) The tertiary structure of CALR is comprised of a globular N-domain, a proline-rich P-domain and a negatively-charged C-domain.(100) Specific oligosaccharide- and polypeptide-binding regions of both the N-domain and the P-domain are required for the protein to perform its function as a chaperone.(101) ER luminal Ca^{2+} binds mainly to the C-domain and to a lesser extent to the P-domain.(102) The transport of CALR in the ER is guided by a signaling amino acid sequence in the N-terminal end, whereas a KDEL motif in the C-terminal end ensures that CALR remains inside the ER.(99) CALR is involved in a variety of cellular functions, including cell adhesion, programmed cell death, antitumor immunity and wound healing.(100) Moreover, CALR is essential for cardiac and neural development, as CALR knock-out in mice is embryonically fatal due to cardiac defects and exencephaly.(103, 104)

More than 50 different CALR-mutated variants have been identified in patients with MPNs, all of which represent insertion-deletion mutations that result in a +1 base-pair frameshift in exon 9, thus shifting transcription to the alternative reading frame 1 and generating a C-terminal end with a novel amino acid sequence. The 52-bp deletion L367fs*46 (type 1) and the 5-bp insertion K385fs*47 (type 2) are the two most common mutated variants and constitute 80% of CALR mutated cases. In the new mutated C-terminal end the KDEL retention sequence is eliminated. In addition, the mutant C-terminal end becomes less acidic, harbors fewer Ca^{2+} binding sites and carries a positive charge. CALR mutations are predominantly heterozygous.(23, 24, 105) Homozygous CALR mutations are very rare and usually associated with high allelic burden and/or accelerated disease progression. In about one-fifth of homozygous cases the underlying mechanism is copy neutral loss of heterozygosity of the chromosomal region 19p13.(106) The CALR mutation is expressed in hematopoietic multipotent progenitors capable of giving rise to blood cells of myeloid and erythroid lineage and has been demonstrated to be the earliest arising mutation, which points towards a role of the CALR mutation as a driver mutation in the pathogenesis of MPNs.(23)

It is noteworthy that the type of CALR mutation is associated with different clinical characteristics. Type-1 mutations appear more frequently in PMF, whereas type-2 predominate in ET.(107, 108) In ET, clinical features and overall prognosis are generally independent of the type of CALR mutation, with the

exception of higher PLT counts in the case of type-2 mutations.(108) Unlike ET, PMF patients with type-2 CALR mutations present with more severe splenomegaly, leukocytosis, anemia and thrombocytopenia, as well as decreased overall survival (OS), compared to patients harboring type-1 mutations.(108-111)

The underlying pathophysiological mechanism of chronic myeloproliferation in CALR-mutated MPNs is based on the loss of the KDEL retention motif in the C-terminal end of mutated CALR, which results in the entry of mutated CALR in the ER secretory pathway. After exiting the ER, mutated CALR binds firmly to N-glycosylated sites of the immature MPL, therefore allowing protection against protein quality surveillance and escape from modifications that would have normally taken place. The two proteins are transported as a complex along the secretory pathway while immature N-glycosylated sites remain attached to the amino acid sequence of MPL up to the cell membrane. The ultimate outcome of mutant CALR binding to MPL is ligand-independent constitutive activation of the JAK2-STAT5 pathway through dimerization of the receptor's cytoplasmic tails (Figure 1B). For complete stabilization and activation of MPL by CALR, a hydrophobic extracellular motif in the amino sequence of MPL (not directly interacting with CALR), N-glycosylation and full cell membrane transport are required.(112) Moreover, loss of ER retention signals leads to accumulation of mutant CALR in the nucleus and excretion to the extracellular space.(113)

Apart from MPL-dependent JAK-STAT activation, further mechanisms drive chronic myeloproliferation in the presence of mutant CALR. Because of the central role of CALR in regulating calcium homeostasis and folding of immature proteins in the ER, CALR mutations have been associated with activation of the unfolded protein response (UPR) due to accumulation of misfolded proteins in the ER. In this regard, loss of Ca^{2+} binding sites associated particularly with type I CALR mutations promote cell survival by activating the inositol-requiring enzyme 1 alpha (IRE1α)/ x-box binding protein 1 (XBP1) branch of the UPR.(114-116) Apart from dysregulations in UPR, impairments in oxidative stress responses were identified in K562 cells harboring CALR mutations.(114) Moreover, impaired interaction of mutant CALR with the store-operated calcium entry (SOCE) machinery in megakaryocytes results in megakaryocyte hyperproliferation.(117) Finally, further disease-driving mechanisms of mutant CALR might lie in formation of abnormal complexes between the C-terminal domain of CALR and known but yet unidentified proteins as assessed by JAK-STAT signaling abrogation in CALR-mutant cells incubated with a synthetic peptide mimicking the C-terminal sequence.(118)

1.1.5. JAK2- and CALR-mutated MPNs exhibit differences in clinical presentation, disease-driving mechanism and thrombotic risk

Clinical features and outcomes of MPN patients are influenced by type of driver mutation. Patients who present with CALR-mutated ET and PMF are younger and exhibit lower white blood cell (WBC) counts and more pronounced thrombocytosis compared with JAK2-mutated patients. Specifically in the case of CALR-mutated ET, increased male predominance in comparison to JAK2-mutated ET has been observed. Furthermore, CALR mutations are accompanied by lower haemoglobin (Hb) levels in ET and higher Hb levels in PMF compared with JAK2-V617F.(5, 23, 24, 119-123)

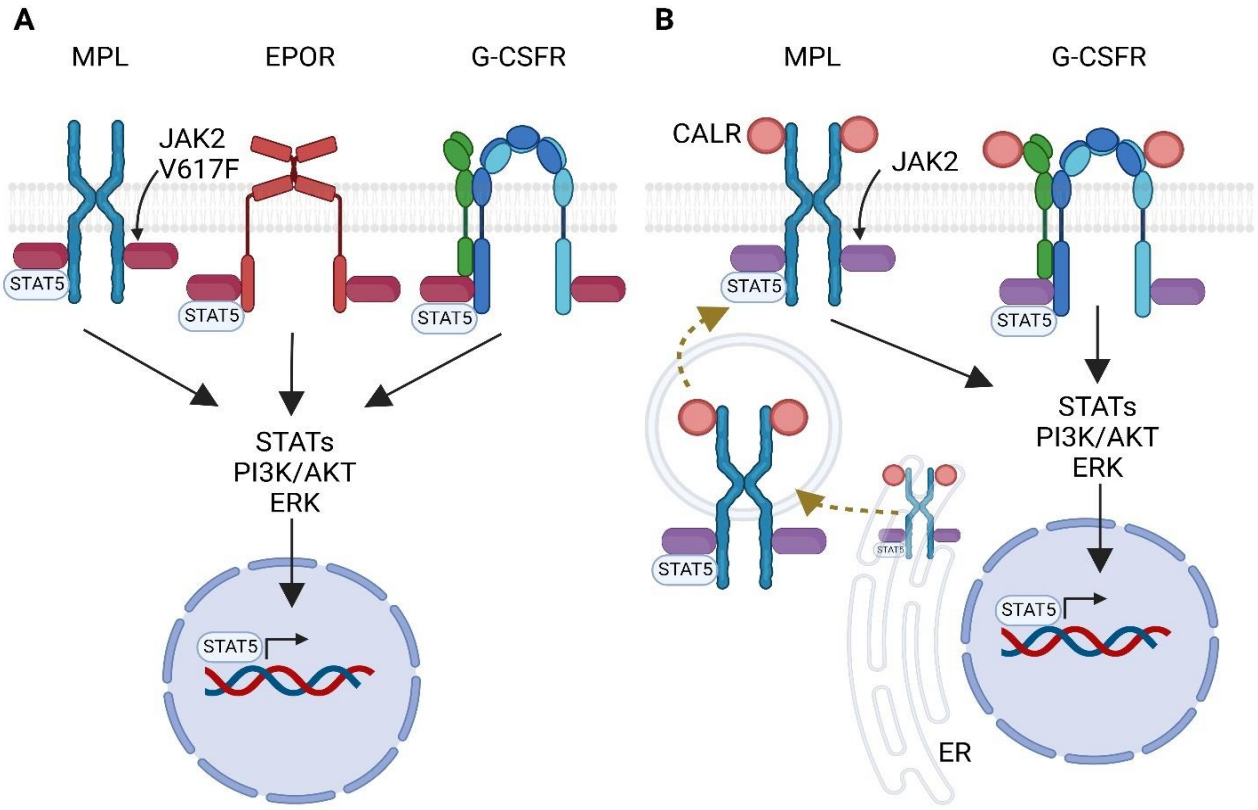

Figure 1. JAK2-V617F and CALRdel52 mutations demonstrate different patterns of hematopoietic growth factor receptor activation. (A) JAK2-V617F induces activation of downstream signaling pathways through constitutive activation of the three main receptors involved in proliferation of the erythrocytic, granulocytic and megakaryocytic lineage, namely EpoR, G-CSFR and MPL respectively. (B) CALR mutants primarily bind and activate MPL and to a lesser extent G-CSFR. Constitutive activation of the JAK2 signaling pathway specifically associated with MPL by CALR mutants explains the thrombocytosis of patients harboring CALR mutations. Mutated CALR exits the ER due to loss of the KDEL ER retention sequence and traffics to the cell membrane by remaining bound to immature forms of MPL. This image was created with BioRender.com and is modified from illustrations published by Vainchenker & Kralovics.(124)

Interestingly, there are no significant differences regarding clinical presentation of CALR-mutated and MPL-mutated ET patients, which both have a tendency towards higher PLT counts in comparison to JAK2-mutated ET patients.(5, 122) This is in accordance with the pathophysiological mechanism of diffuse myeloid growth factor receptor activation [erythropoietin receptor (EpoR), G-CSF receptor and MPL] by the JAK2-V617F mutation as opposed to specific MPL activation induced by CALR and MPL mutations (Figure 1).(124) Despite the different pattern of receptor activation between CALR and JAK2 mutations, the treatment of classical MPNs is currently not mutation-specific. Ruxolitinib has been shown to be equally effective when administered in CALR-mutated and JAK2-mutated disease, most certainly because constitutive activation of the MPL receptor in CALR-mutated disease is JAK2 dependent.(105, 125)

There exists convincing evidence that CALR-mutated ET patients have decreased venous and arterial thrombotic risk compared with JAK2-mutated ET patients. In a meta-analysis, it was shown that ET patients bearing the JAK2-V617F mutation exhibit 2.35 times increased odds of thrombotic disorders [95% confidence interval (CI) = 1.83 - 3.02] compared to CALR-mutated patients.(126) Unlike thrombotic risk, OS does not appear to be affected by mutation status in ET.(119, 122, 127, 128) Relevant data in the case of PMF also point towards a decreased thrombotic risk in CALR-mutated PMF. In contrast to ET, however, in PMF it is well established that CALR mutation confers an improved median OS (ca. 17 years) compared with the JAK2-V617F mutation (ca. 9 years).(120, 123)

1.2. The role of leukocyte-endothelial cell adhesion in thrombosis

1.2.1. Activation of the leukocyte adhesion cascade is a major event during venous thrombosis

In response to inflammatory signals, leukocytes adhere to the vascular endothelium in a multistep process. Initially, cell rolling is mediated by a group of Ca^{2+} dependent lectins, called selectins. There are currently three known types of selectins, namely E- selectin (CD62E), P-selectin (CD62P) and L-selectin (CD62L). All selectins bind to sialyl Lewis^x (sLe^x) tetrasaccharides through a common Ca^{2+} dependent carbohydrate recognition domain (CRD).(129) Unlike E-selectin, P- and L-selectin can also bind to sulfated tyrosine residues.(130, 131) P-selectin is expressed by PLTs and endothelial cells, where it is stored in α granules and Weibel-Palade bodies respectively.(132, 133) E-selectin is not stored and is expressed by endothelial cells after stimulation by chemokines.(134) L-selectin can be found on the

surface of neutrophils, monocytes and lymphocytes and mediates homing to lymph nodes via binding of carbohydrate groups on high endothelial venules.(135) Upon inflammation, levels of P- and E-selectin expression on activated endothelial cells are increased.(129) Subsequently, weak bonds are formed between the CRD of selectins and P-selectin glycoprotein ligand 1 (PSGL-1), an sLe^x containing mucin on the surface of leukocytes.(129, 130) In the case of E-selectin, additional ligands have been identified, namely CD44 and E-selectin ligand-1 (ESL-1).(131)

The initial interaction between P- and E-selectin and PSGL-1 enables leukocytes to decelerate and roll along the endothelial surface, which is a prerequisite for firm adhesion and subsequently transmigration.(135) Tight adhesion and transmigration are mediated by integrins, a family of heterodimeric transmembrane proteins composed of an α- and a β-subunit. In total, 18 α-subunits and eight β-subunits have been described, which are known to form 24 integrin subtypes. Leukocytes express seven different integrins, among which very late antigen 4 (VLA-4, $\alpha_4\beta_1$ integrin) and lymphocyte function-associating antigen 1 (LFA-1, $\alpha_L\beta_2$ integrin). VLA-4 is capable of binding to VCAM-1 and mucosal vascular addressin cell adhesion molecule 1, whereas LFA-1 binds to ICAM-1 and ICAM-2.(136) Integrins can exist in three different conformations: a bent inactive conformation, an extended conformation with a closed headpiece and intermediate affinity for ligand and an extended conformation with open headpiece and high affinity for ligand.(137)

During leukocyte rolling, integrin conformational status is regulated by selectin- and chemokine-induced signals.(135) Binding of leukocytes to selectins leads to activation of an intracellular protein kinase cascade, the end point of which is recruitment of talin, a cytoskeletal protein that upon activation disrupts the α-β tail of the integrin transmembrane complex (inside-out signaling).(138) This results in a transition from the bent to the intermediate affinity integrin conformation and subsequently weak binding to ICAM-1, which reduces leukocyte rolling velocities but does not cause arrest.(139) Leukocyte deceleration increases the probability of interaction with chemokines immobilized on the endothelial surface, for example C-X-C motif ligand 1 (CXCL1).(140) Finally, chemokine signals induce strong binding to ICAM-1 and firm adherence to the endothelium by causing a shift towards the open high-affinity conformation.(141) Although integrin activation triggered by inflammatory mediators has been most extensively described for binding of $\alpha_L\beta_2$ integrin to ICAM-1,(135) similar mechanisms orchestrate binding of $\alpha_4\beta_1$ integrin to VCAM-1.(142)

Leukocyte rolling and adhesion to the vascular endothelium are well-recognized events during venous thrombosis.(143) In a deep vein thrombosis (DVT) flow restriction mouse model with partial ligation of

the inferior vena cava (IVC) and no endothelial compromise, von Brühl and colleagues showed that flow restriction triggers increased expression of adhesion molecules and IL-6 by endothelial cells, as well as excretion of P-selectin stored in endothelial Weibel Palade bodies. Presence of P-selectin was found to be a *sine qua non* for leukocyte crawling, which was followed by firm adhesion. Leukocytes were recruited to the endothelium one hour after stasis, while complete covering of the endothelial surface could be observed within six hours. The majority of recruited cells were neutrophils (~70%) and to a lesser extent monocytes (~30%). Following adhesion to the endothelium, it was demonstrated that recruited neutrophils undergo NETosis, a process which was found to be further enhanced by neutrophil-PLT interactions via the GPIb receptor. Furthermore, it was shown that the resulting NET fiber network became coated with coagulation factors, such as fibrinogen, vWF, TF and factor XII and was able to serve as a substrate on which circulating PLTs and erythrocytes were retained.(144) In the subsequent steps of thrombus development, the thrombotic function of NET components may involve promotion of PLT activation and conglomeration, inhibition of protein C, tissue factor pathway inhibitor cleavage and factor XII activation.(143-146) Finally, a secondary leukocyte-dependent mechanism of thrombus formation, which involved TF expression mainly by monocytes, was revealed by the same authors.(144)

1.2.2. Integrin-mediated neutrophil adhesion to the vascular endothelium drives thrombosis in JAK2-mutated MPNs

A novel mechanism of neutrophil-induced thrombus formation in MPNs has recently come to light by our research group (Figure 2). In a VavCre JAK2-V617F knock-in mouse model, it was shown that JAK2-V617F induces thrombosis through increased binding of murine neutrophils to VCAM-1 and ICAM-1. Upregulation of membrane-bound β_1 and β_2 integrins was detected in all major leukocyte subtypes of VavCre^{+} JAK2$^{VF/+}$ mice with the exception of β_1 integrin on granulocytes and β_2 integrin on B cells, where no significant differences were observed compared to wild-type (WT) mice. Interestingly, while JAK2-mutated murine neutrophils did not exhibit altered total β_1 integrin expression, they harbored elevated levels of activated high-affinity β_1 integrin, which indicates a JAK2-V617F-induced shift of β_1 integrin structure from the closed to the open conformation.(59) Moreover, BaF3 JAK2-V617F cells were demonstrated to exhibit stronger binding to VCAM-1 and ICAM-1 compared to BaF3 JAK2-WT cells while increased adhesion to VCAM-1 could additionally be proven in 32D JAK2-mutated cell lines and JAK2-mutated human granulocytes.(59, 60)

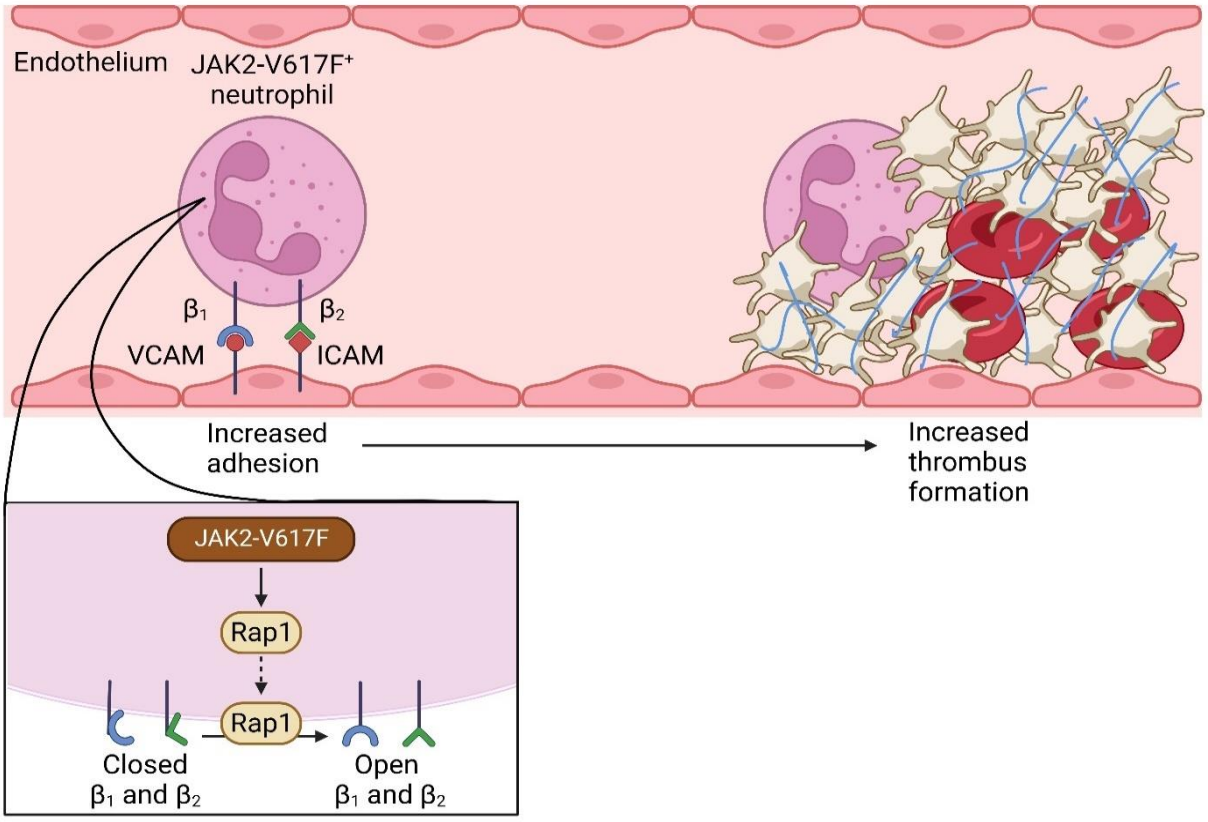

Figure 2. In the pathophysiology of MPN, JAK2 mutations drive thrombosis by enhancing integrin-mediated adhesion of neutrophils to the vascular endothelium. JAK2-V617F induces activation and translocation of the small GTPase Rap1 to the neutrophil surface. Subsequently, Rap1 mediates the inside-out signaling that ultimately leads to a conformational change of cell-surface β_1 and β_2 integrins from the closed to the open high affinity structure. Integrin activation strengthens neutrophil adhesion to VCAM-1 and ICAM-1 normally expressed on the endothelial surface, thus promoting thrombus formation. This image was created with BioRender.com and is modified from illustrations published by Oh.(61)

The small guanosine triphosphatase (GTPase) Ras-related protein 1 (Rap1), a well-studied regulator of β_1 integrin function, was shown to be hyperactivated in JAK2-V617F-mutated murine and human neutrophils (Figure 2). Moreover, in accordance with previous studies showing that regulation of β_1 integrin by Rap1 involves translocation of the GTPase to the cell membrane, 32D JAK2-mutated myeloid progenitors were found to exhibit increased membrane localization and activation of Rap1 compared to 32D WT cells.(59, 60, 147, 148) On the basis of these findings, it was hypothesized that the switch of β_1 integrin to the open high-affinity conformation in the context of JAK2-V617F is driven by Rap1 activation.(61) The resulting stronger integrin-mediated interaction between neutrophils and endothelial cells in VavCre$^+$ JAK2$^{VF/+}$ mice compared to WT mice was revealed to be responsible for increased thrombosis propensity, as assessed by reversibility of enhanced thrombus formation in

VavCre^{+} JAK2$^{VF/+}$ mice when an anti-β_1/β_2 integrin antibody was used *in vivo*. For this reason, integrins are considered to be promising targets in the treatment of patients with JAK2-positive MPN.(59)

1.3. Revealing the role of neutrophils in the pathophysiology of MPNs: The Catchup mouse model

1.3.1. The murine lymphocyte antigen 6 complex, locus G (Ly6g) gene allows for generation of a mouse model with high neutrophil-specificity

The Ly6g protein represents an important member of the murine Ly6 protein family and is expressed at high levels exclusively by murine neutrophils.(149, 150) The Ly6 protein family includes >20 peptides, which are encoded by respective alleles on chromosome 15 and share a common preserved LU motif. In most cases, Ly6 family members are glycosylphosphatidylinositol-anchored membrane-bound proteins.(151) Ly6g is widely used as a marker to distinguish neutrophils from other types of leukocytes. Additional Ly6 proteins used to identify specific cell types are Ly6A [or stem-cell antigen 1 (Sca-1)] and Ly6C in the case of hematopoietic stem cells (HSCs) and monocytes respectively, although Ly6C does not solely exhibit monocytic specificity, because it is expressed to a lesser extent by neutrophils, T-cells, natural killer (NK)-cells or dendritic cells.(149, 150) Ly6G, together with Ly6C, form the granulocyte-differentiation antigen (Gr-1), which can be recognized by the monoclonal antibody RB6-8C5.(152) It is worth mentioning that regarding Ly6G and Ly6C, there is no equivalent genomic region in humans, which indicates that neutrophil-specific Ly6 proteins are products of gene duplication in mice after species divergence during evolution.(150)

By taking advantage of the high neutrophil specificity of Ly6g, Hasenberg and colleagues were able to generate a mouse line, which allows for cyclic recombinase (Cre)-mediated neutrophil-specific expression of a mutation of interest. This mouse model was named by the authors as “Catchup” to indicate that the mutation under study is expressed solely in pathogen-catching neutrophils. In Catchup mice, exon 1 of the Ly6g allele is substituted for a targeting vector containing both the genetic sequence of Cre recombinase and the red fluorescent protein tdTomato, while normal murine gene regulatory elements remain intact (Suppl. Figure 1B). In this way, Cre-mediated excision of a knocked-in floxed gene of interest occurs only in Ly6g^{+} cells, namely in murine neutrophils.(153) Knock-in of the bicistronic Cre-tdTomato allele in the Ly6g locus leads to premature termination of transcription and knock-out of the normal Ly6g gene, which has been associated with β_2 integrin-associated adhesion and migration

defects in the mutated neutrophils by a study that involved antibody-mediated Ly6g blockade.(153, 154) However, a thorough examination of the functional properties of neutrophils isolated from homozygous Catchup mice ($Ly6g^{Cre\text{-}tdTomato/Cre\text{-}tdTomato}$) by Hasenberg and colleagues did not yield any findings indicative of neutrophil dysfunction.(153)

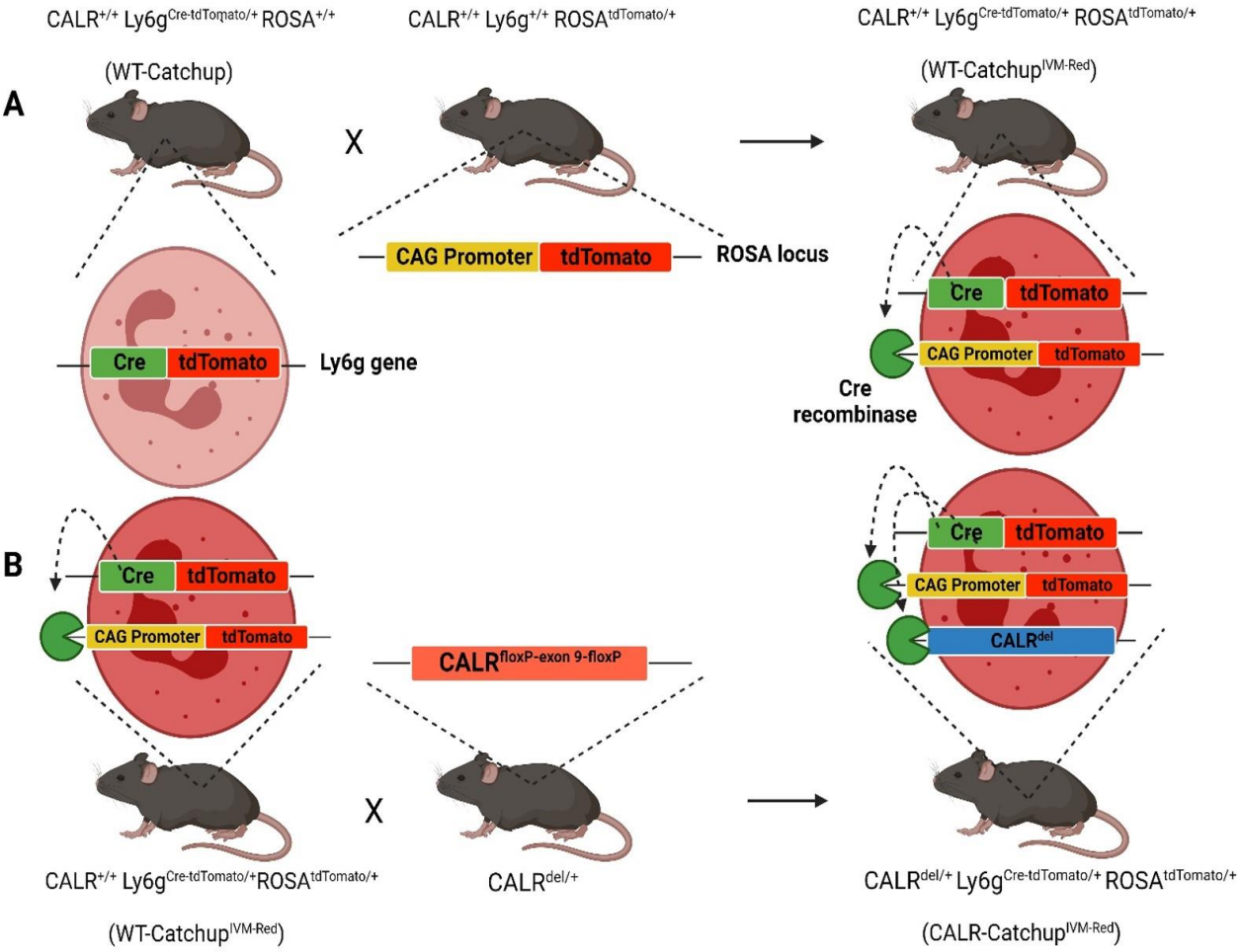

Figure 3. The Catchup mouse model and diagrammatic representation of the breeding strategy employed to generate the $CALR^{del/+}$ Catchup mice. (A) WT Catchup mice are crossed with a reporter mouse line harboring the tdTomato gene in the ROSA locus to generate WT $Catchup^{IVM\text{-}Red}$ mice. (B) WT $Catchup^{IVM\text{-}Red}$ mice are bred with mice harboring the floxed CALRdel allele ($CALR^{del/+}$) to induce Cre-mediated neutrophil-specific expression of CALRdel in the offspring (CALR-$Catchup^{IVM\text{-}Red}$). Created with BioRender.com.

Apart from the ability to induce neutrophil-specific expression of a knocked-in gene, an additional advantage of the Catchup mouse model lies in the fluorescent marking of $Ly6g^{+}$ cells with tdTomato, which enables neutrophil manipulation and visualization.(153) The red fluorescent marker tdTomato has an emission wavelength of 581 nm and can be detected in the phycoerythrin (PE) channel during flow

cytometric analysis.(153, 155) In transgenic animal models, tdTomato allows for *in vivo* imaging of marked cells and serves as a reporter of Cre recombination.(156, 157) In Catchup mice, tdTomato enables flow cytometric identification of untouched granulocytes in one simple step. Expression of tdTomato can be increased by crossing Catchup mice with reporter mice that harbor a secondary Cre-activatable CAG promoter for tdTomato in the ROSA26 locus. The resulting mouse line can be used for intravital microscopy of tdTomato^{+} cells und is thus termed as Catchup$^{IVM\text{-}Red}$ (Figure 3A). In Catchup$^{IVM\text{-}Red}$ mice, tdTomato is expressed in the peripheral blood and hematopoietic tissues almost entirely by neutrophils (defined as CD11b^{+}Ly6g^{bright} cells) and only by a very small number of eosinophils and basophils (< 2% of tdTomato^{+} peripheral blood leukocytes). In contrast to other widely used mouse models for neutrophil studies, namely lysozyme M-Cre and lysozyme-enhanced green fluorescent protein, which exhibit "leakage" of the fluorescent labeling in non-neutrophilic myeloid progenitors, Catchup mice demonstrate absence of fluorescent marking in progenitor cells, including granulocyte-macrophage progenitors (GMPs).(153, 158, 159) It is worth mentioning however, that while practically all tdTomato^{+} cells express neutrophil-specific markers, the opposite is not true, as 20-40% of peripheral blood neutrophils and 10-20% of neutrophils located in the spleen and BM do not express tdTomato.(153)

1.3.2. JAK2$^{VF/+}$ Catchup mice develop an ET phenotype and exhibit increased integrin-mediated neutrophil adhesion

Because of its high neutrophil specificity, the Catchup mouse model can be employed to induce neutrophil-specific expression of an MPN-associated mutation, for example JAK2-V617F or CALRdel52, which can be helpful in determining the role of neutrophils in the pathophysiology of MPNs. A Catchup mouse model with neutrophil-specific expression of JAK2-V617F (JAK2 Catchup) has already been established and described by our research group in an abstracted publication by Haage and colleagues (complete data not yet published). When compared with control WT Catchup mice, JAK2$^{VF/+}$ Catchup mice develop an ET phenotype as assessed by increased BM megakaryopoiesis and mild but significant elevations in PLT numbers (JAK2$^{+/+}$ Catchup: 1146 ± 58.96 Gpt/l vs JAK2$^{VF/+}$ Catchup: 1519 ± 59.03 Gpt/l, P = 0.001).(160) While it is known that hematopoietic-specific expression of JAK2-V617F in mice induces a PV phenotype with marked elevations of Hct and splenomegaly,(161) JAK2$^{VF/+}$ Catchup mice exhibit normal Hct levels and unaltered splenic architecture and size. Moreover, JAK2$^{VF/+}$ Catchup mice do not display any changes in peripheral blood WBC, RBC or neutrophil counts. According to Haage et al, non-significant alterations of BM HSCs and myeloid progenitors (MPs) in JAK2$^{VF/+}$ Catchup mice indicate that

neutrophil-specific expression of JAK2-V617F is not sufficient to induce myeloproliferation in hematopoietic progenitors.(160)

An additional finding in the work of Haage et al was the significantly increased levels of serum inflammatory biomarkers, namely IL-1α, macrophage colony-stimulating factor and IL-12 and upregulation of IL-1β, IL-10, IP-10 and TNF-α mRNA levels in neutrophils isolated from JAK2$^{VF/+}$ Catchup mice, which indicate that neutrophil-specific expression of JAK2-V617F is capable of inducing inflammation and might shed new light on the role of neutrophils in guiding systemic inflammation development in MPN patients. Haage and colleagues hypothesized that thrombocytosis and increased megakaryocyte (MK) number in JAK2$^{VF/+}$ Catchup mice are induced by cytokine secretion from neutrophils. Indeed, IL-1α could be responsible for the development of thrombocytosis in the JAK2 Catchup mouse model due to its central role in PLT production.(162)

In the VavCre JAK2-V617F mouse model, upregulation of β_1 and/or β_2 integrin on the surface of almost all leukocytes subtypes isolated from VavCre JAK2$^{VF/+}$ animals was detected.(59) On the contrary, in the research work of Haage et al β_1 and β_2 integrin levels as well as PSGL-1 expression on neutrophils isolated from JAK2$^{VF/+}$ Catchup mice corresponded to their WT controls. Despite unremarkable surface integrin expression, JAK2$^{VF/+}$ tdTomato^{+} neutrophils displayed significantly increased adhesion to VCAM-1 under flow and static conditions compared to JAK2$^{+/+}$ tdTomato^{+} neutrophils. Increased VCAM-1 binding without upregulation of surface β_1 integrin could indicate a change of integrin conformational status to the active high-affinity structure on neutrophils isolated from JAK2$^{VF/+}$ Catchup mice. Soluble binding of JAK2$^{VF/+}$ tdTomato^{+} neutrophils to P- and E-selectin was unremarkable. By using an *in-vitro* time lapse assay to record neutrophil migration on a pre-coated slide with VCAM-1 and ICAM-1, Haage et al could show that neutrophils isolated from JAK2$^{VF/+}$ Catchup mice exhibited significantly reduced displacement from origin and median migration velocities, which indicated firmer adhesion. In line with this finding, slower movement of JAK2$^{VF/+}$ tdTomato^{+} neutrophils during migration was additionally demonstrated *in vivo* after partial ligation of the great saphenous vein of JAK2$^{VF/+}$ Catchup mice and tracking of fluorescent tdTomato^{+} cells with two-photon microscopy in the stenosed vessel.(160)

1.4. Hypothesis

It is well-known that several aspects of neutrophil biology, including integrin function and cytokine signaling, are dependent on the JAK-STAT pathway, which is constitutively activated in JAK2-V617F-

mutated cells.(163-165) Indeed, several type I and type II cytokine receptors, which transmit intracellular signals via JAK-STAT signaling, are expressed by neutrophils and play an important role in regulation of inflammatory response.(165, 166) Our research group has shown for the first time that constitutive JAK-STAT signaling in JAK2-V617F-mutated neutrophils leads to activation of the small GTPase Rap1, which in turn induces elevated integrin-mediated adhesion by changing integrin conformation to the open high-affinity state. Importantly, increased integrin-mediated adhesion contributes to enhanced thrombus formation *in vivo*.(59) In addition, by generating a JAK2 Catchup mouse model, our team demonstrated that neutrophil-specific expression of JAK2-V617F leads to increased adhesion to VCAM-1 and induces an ET-like myeloproliferative disease with aberrant cytokine expression (Haage et al, yet unpublished data).

Contrary to JAK2-V617F, which leads to diffuse hyperactivation of all major hematopoietic receptors by JAK2-V617F, namely Epo-R, GM-CSFR and MPL, currently available data indicate that activation of the JAK-STAT pathway in the context of CALRdel52 is associated particularly with the MPL receptor.(124) Indeed, MPL represents the only cytokine receptor that has been proven to exhibit significant hyperactivation in the presence of a CALR mutation.(167) As mentioned previously, the underlying pathophysiological mechanism of persistent MPL-associated JAK-STAT signaling lies in defective folding of premature MPL by mutated CALR.(112) Given the minor physiological role of MPL receptor-related signaling in neutrophils, it is plausible to hypothesize that many neutrophil functions that are dependent on JAK-STAT signaling, including integrin function and cytokine signaling, would be left unaffected by CALRdel52. Indeed, stimulation with TPO was not associated with alterations in integrin expression on segmented neutrophils.(168) In line with this hypothesis, our team observed significantly reduced levels of activated Rap1 in neutrophils isolated from CALR-mutated compared to JAK2-mutated patients, which could indicate that CALR mutations do not enhance integrin activation to the same degree as JAK2 mutations.(59)

Taking into consideration the aforementioned data we hypothesize that CALRdel52 mutations in neutrophils are not associated with prominent alterations in integrin-associated adhesion. Moreover, we speculate that neutrophil-specific expression of CALRdel52 is not sufficient to induce chronic myeloproliferative or inflammatory changes. Validation of this hypothesis could pave the way towards unraveling a differential impact of JAK2 and CALR mutations in neutrophil biology and providing an

explanation for the decreased thrombotic risk in CALR-mutated as compared to JAK2-mutated MPN patients.

1.5. Aims and Objectives

The role of neutrophils in MPN-associated thrombosis has gained attention in recent years.(59, 169) Contrary to JAK2-V617F, the impact of CALRdel mutations on neutrophil adhesion has to our knowledge not been examined to date. Moreover, it remains unknown whether neutrophil-specific expression of CALRdel contributes to inflammation development and chronic myeloproliferation of MPNs. The primary focus of this study is to investigate the influence of CALRdel52 mutation on neutrophil binding to integrin ligands normally expressed on the vascular endothelium. An additional aim is to gain an understanding of how neutrophil-specific expression of CALRdel52 contributes to myeloproliferation and inflammation in the pathophysiology of MPNs. For this purpose, we employ two mouse models, namely a VavCre transgenic mouse model, which displays expression of CALRdel52 in hematopoietic and endothelial cells through VavCre-mediated recombination (VavCre CALR) and a novel mouse model with neutrophil-specific expression of CALRdel52 (CALR Catchup) (Figure 3B). In both mouse lines, a locus of crossover in P1 (loxP) flanked chimeric mouse-human CALRdel52 gene is expressed in the tissue of interest via Cre recombination (Suppl. Figure 1A).(170, 171) For all experiments, comparisons are conducted between age- and gender-matched WT and CALR-mutant mice.

2. Materials and methods

2.1 Animals

C57BL/6 mice were used for all experiments. $CALR^{del/+}$ mice were kindly provided by Prof. Dr. Anthony R. Green (Department of Hematology, University of Cambridge, UK). Heterozygous mice harboring the loxP flanked CALRdel52 mouse-human chimeric oncogene in exon 9 ($CALR^{fl/+}$) were crossed with $VavCre^{+}$ transgenic mice (The Jackson Laboratory) to obtain offspring with hematopoietic-specific expression of CALRdel52 (VavCre $CALR^{del/+}$). WT mice (VavCre $CALR^{+/+}$) were either $VavCre^{-}$ $CALR^{fl/+}$, $VavCre^{+}$ $CALR^{+/+}$ or $VavCre^{-}$ $CALR^{+/+}$. $VavCre^{+}$ as well as $VavCre^{-}$ WT mice were included as controls in order to make use of the significant numbers of surplus $VavCre^{-}$ in comparison to $VavCre^{+}$ WT animals. WT $Catchup^{IVM\text{-}Red}$ mice ($Ly6g^{Cre\text{-}tdTomato/+ \text{ or } Cre\text{-}tdTomato/Cre\text{-}tdTomato}$ $ROSA26^{tdTomato/+ \text{ or } tdTomato/tdTomato}$) were obtained from the Institute of Molecular and Clinical Immunology of the Otto von Guericke University (Magdeburg, Germany) and

were crossed with $CALR^{fl/+}$ mice to induce neutrophil-specific expression of CALRdel52 (CALR Catchup). All Catchup mice used in this study exhibited heterozygosity for the Cre recombinase-tdTomato bicistronic allele ($Ly6g^{Cre\text{-}tdTomato/+}$) and were either heterozygous or homozygous for tdTomato in the ROSA26 locus ($ROSA26^{tdTomato/+}$ or $ROSA26^{tdTomato/tdTomato}$). All CALR Catchup mice used were heterozygous for CALRdel52 ($CALR^{del/+}$ Catchup) and were compared with age- and sex-matched WT Catchup mice ($CALR^{+/+}$ Catchup). Cervical dislocation was used for animal euthanasia.

2.2. Blood counts

Blood samples were drawn from the retrobulbar venous plexus, collected in EDTA tubes and analyzed with an ADVIA 2120 blood analyzer (Siemens).

2.3. Polymerase chain reaction (PCR) genotyping strategy

Tissue specimens obtained from ear punch biopsies of 3-weeks old mice were incubated on shaker at 42 °C for 24 hours in buffer containing 100 µl of DirectPCR Lysis Reagent (Viagen) and 5 µl Proteinase K (Merck). Next, inactivation of restriction enzymes was performed at 85°C for 45 minutes. After short centrifugation, the supernatants were collected and 1 µl of isolated DNA was added to 24 µl Master Mix containing 12.5 µl Dream Taq Green PCR Master Mix (Thermo Fischer Scientific), 9.5 µl sterile distilled H_2O and 1 µl of the desired primers per sample. DNA fragments were separated with agarose gel electrophoresis after addition of ethidium bromide in the running buffer and visualized with ultraviolet light exposure. DNA purification from BM samples was conducted with the QIAamp DNA Blood Kit (Qiagen). VavCre recombinase expression was identified using primers 5'-CGTATAGCCGAAATTGCCAG-3' (forward) and 5'-CAAAACAGGTAGTTATTCGG-3' (reverse). Cre-mediated excision of the floxed CALR allele was confirmed with primers 5'-CCTACCTTCTCAGTGCATCAA-3' (forward)/5'-ATCTGAACCTGCCTGGAAAA-3' (reverse). Genotyping of Catchup mice was performed with two separate PCRs: a WT-PCR, where the pair of primers 5'-GGTTTTATCTGTGCAGCCC-3' (forward) and 5'-GAGGTCCAAGAGACTTTCTGG-3' (reverse) is used to amplify exon 1 of the wild-type Ly6g gene and a knock-in PCR (Ki-PCR), which employs primers 5'-ACGTCCAGACACAGCATAGG-3' (forward) and 5'-GAGGTCCAAGAGACTTTCTGG-3' (reverse) to detect the knock-in bicistronic Cre-tdTomato gene contruct. In both PCR strategies, primers 5'-GAGACTCTGGCTACTCATCC-3' (forward) and 5'-CCTTCAGCAAGAGCTGGGGAC-3' (reverse) were included for detection of the wild-type CD79b allele. An additional Rosa-PCR was used to identify the tdTomato knock-in allele in the ROSA26 locus with primers

5’-AAGGGAGCTGCAGTGGAGTA-3’ (forward) and 5’-CCGAAAATCTGTGGGAAGTC-3’ (reverse). The PCR protocols that were applied for each gene are shown in Table 2.

Table 2. PCR genotyping protocols

Gene of interest	Initial denaturation	Cyclic denaturation	Cyclic annealing	Cyclic elongation	Final elongation	Number of circles
VavCre	94 °C, 4 min	94 °C, 25 sec	55 °C, 30 sec	72 °C, 45 sec	72 °C, 5 min	30
CALR	95 °C, 3 min	95 °C, 30 sec	56 °C, 30 sec	72 °C, 1 min	72 °C, 5 min	35
Ly6g	95 °C, 5 min	95 °C, 30 sec	60 °C, 30 sec	72 °C, 1 min	72 °C, 10 min	35
Rosa	95 °C, 10 min	95 °C, 30 sec	58 °C, 20 sec	72 °C, 40 sec	72 °C, 10 min	35

2.4. Hematopoietic cell isolation

Hematopoietic cells were isolated from hind limb bones, spleen and/or the vertebral column of the mice of interest. Muscles and connective tissue attached to the bone were removed with a small wipe. Bone and spleen tissues were smashed, resuspended in 10 ml phosphate buffered saline (PBS) with 1% fetal bovine serum (FBS) and collected in a 50 ml Falcon Conical Tube through a 70μm Cell Strainer. After centrifugation, cells were briefly treated with 5 ml RBC Lysis Buffer (BD Biosciences), re-centrifuged, re-filtered, washed twice with PBS with 1% FBS and finally resuspended in the desired volume.

2.5. Neutrophil isolation

Polymorphonuclear granulocytes were isolated from hematopoietic cells with negative magnetic-activated cell sorting (MACS) as described previously.(172) Murine whole BM cells were labeled with the following biotin-conjugated antibodies: anti-CD5 (Biolegend, Clone: 53-7.3), anti-CD45R/B220 (Biolegend, Clone: RA3-6B2), anti-CD49b (eBioscience, Clone: HMα2), anti-CD117 (Biolegend, Clone: 2 B8), anti-F4/80 (Biolegend, Clone: BM8) and anti-Ter119 (Biolegend, Clone: TER-119) in 1:250 dilution and were left to bind for 45 min at 4 °C on shaker. Subsequently, cells were washed once and resuspended in 6 ml of ice-cold PBS with 1% FBS. 150 μL of Streptavidin Magnetic Particles (BD IMag Streptavidin Particles Plus – DM, BD Biosciences) were diluted in 5 ml of ice-cold PBS with 1% FBS in a 15 ml Falcon Conical Tube and placed on a MACSiMAG^{TM} Separator (Miltenyi Biotec). After 6 minutes, the magnetic beads solution was suctioned leaving the streptavidin particles on the posterior tube wall as a result of the magnetic force. Cells were immediately introduced and mixed well with the streptavidin

particles. After incubation for 45 min at 4 °C on shaker, cells were placed on the MACSiMAG Separator and “non-granulocytes” were left to stick on the posterior tube wall for 6 minutes. “Granulocytes” were collected and re-subjected to magnetic separation. Overall, the separation process of “granulocytes” was performed three times. Finally, isolated neutrophils were washed, resuspended in RPMI-1640 and quantified with Trypan blue staining.

2.6. Cytospins

50,000 cells per slide were cytospun with a D7200 Tuttlingen Centrifuge (Hettich), stained with May-Grünwald-Giemsa and examined under the microscope.

2.7. Histology

2.7.1. Hematoxylin and eosin (H&E) staining

Directly after mouse euthanasia by cervical dislocation, the sternum and spleen were removed and stored in 4% formaldehyde for at least 48 hours. Before staining, the sternum was decalcified with Entkalker soft (Roth) for at least 72 hours and tissue specimens were fixed in paraffin blocks. Paraffin-embedded tissue sections of 2 µm were subjected to deparaffinization and rehydration prior to introduction in a hematoxylin bath for 15 min. Next, tissue sections were rinsed in tap water for 15 minutes, followed by a wash in de-stilled water, and counterstained with eosin for 3 min. Subsequently, sections were dehydrated by passing through graded ethanol, cleared with xylol and mounted on glass slides. Images were obtained with a Leica DM6000B microscope.

2.7.2. Reticulum staining

For histological demonstration of reticular fibers, the Reticulum Stain Kit (Modified Gomori’s) (ab236473) was used according to manufacturer’s instructions.

2.8. Flow cytometry

Flow cytometry data were analyzed on FlowJo v10.7.1.

2.8.1. Measurement of β integrin and PSGL-1 expression

After neutrophil isolation with negative MACS, isolated cells were stained with allophycocyanin (APC) anti-CD29 (β_1 integrin, Biolegend, Clone: HMβ1-1) and Brilliant Violet (BV) 421 anti-CD18 (β_2 integrin, BD Biosciences, Clone: C71/16) or BV421 anti-CD162 (PSGL-1, BD Biosciences, Clone: 2PH1) in 1:100 dilution and analyzed on a fluorescence-activated cell sorting (FACS) Canto flow cytometer. In Catchup mice, mean fluorescence intensities (MFIs) for CD29 and CD18 were calculated on tdTomato$^+$ cells. In CALR$^{+/+}$ and CALR$^{del/+}$ mice, neutrophil purity was determined with BV510 anti-Ly6g (Biolegend, Clone: 1A8, 1:100) and MFIs were measured on Ly6g$^+$ cells. Dead cells were excluded with SYTOX Green (Thermo Fischer Scientific). To account for non-specific antibody binding, all MFIs were corrected by subtracting the MFI of the isotype control (MSFI). Antibodies used as isotype controls were APC mouse IgG1, κ Isotype for CD29 (Biolegend, Clone: H7K888), BV421 Rat IgG2α, κ Isotype (Biolegend, Clone: R35-95) for CD18 and BV421 Mouse IgG1, κ Isotype (Biolegend, Clone: X40) for CD162. Normalization of MSFIs was carried out by dividing the MSFI of each mouse with the mean MSFI of all WT mice included in the experiment.

2.8.2. Soluble ligand binding

After neutrophil isolation with negative MACS, isolated cells were resuspended in RPMI-1640 and were incubated with 10µg/ml recombinant Fc chimera VCAM-1/CD106, ICAM-1/CD54, P-selectin/CD62P and E-selectin/CD62E (R&D Systems) in 37 ℃ and 5% CO_2 for 45 minutes. Cells were then washed with Hank's balanced salt solution (HBSS) and stained with anti-human allophycocyanin-conjugated AffiniPure F(ab')2 fragment goat anti-human IgG, Fc-gamma fragment specific (Dianova). For non-Catchup mice, cells were additionally stained with BV510-Ly6g (1:200, 45 minutes, 4 ℃) to determine neutrophil purity. The MFI of the APC-labeled Ly6g$^+$ or tdTomato$^+$ cells was measured with a FACS Canto flow cytometer after exclusion of dead cells with SYTOX Green. MFI values were corrected by subtracting the MFI of the samples stained with secondary antibody only and were normalized as previously mentioned.

2.8.3. Hematopoietic stem and progenitor cell measurement

For hematopoietic stem and progenitor cell measurement, murine BM or spleen cells were labeled with the lineage biotin-conjugated antibodies anti-Gr-1 (BioLegend, Clone: RB6-8C5), anti-Mac-1 (BioLegend, Clone: M1/70), anti-Ter119 (BioLegend, Clone: TER-119) and anti-CD45R/B220 (BioLegend, Clone: RA3-

6B2) in 1:100 dilution and with anti-CD3 (BioLegend, Clone: 17A2), anti-CD4 (BioLegend, Clone: GK1.5), anti-CD8α (BioLegend, Clone: 53-6.7), anti-CD19 (BioLegend, Clone: 6D5) and anti-IL7Ra (CD127, BioLegend, Clone: A7R34) in 1:200 dilution and were incubated in 4 ℃ for 30 minutes. Subsequently, cells were washed with ice-cold PBS/1% FBS and stained with FITC anti-CD34 (BD Pharmingen, Clone: RAM34), PerCP anti-c-kit (CD117, BioLegend, Clone: 2B8), BV510 anti-CD16/32 (BioLegend, Clone: 93), PE/Cy7 anti-Sca-1 (BioLegend, Clone: D7) and APC anti-Flk2 (CD135, BioLegend, Clone: A2F10) in 1:100 dilution (4 ℃ for 30 minutes). APC/Cy7-Streptavidin (BioLegend) was used in 1:100 dilution for labelling of the primary biotin-conjugated antibodies. Exclusion of dead cells was performed with SYTOX Blue dead cell stain (Thermo Fischer Scientific). For erythroblast measurement, cells were first labeled with biotinylated anti-Ter119 (BioLegend, Clone: TER-119, 1:100, 30 minutes, 4 ℃) and then stained with APC/Cy7-Streptavidin and APC-CD71 (1:100, 30 minutes, 4 ℃). Dead cell exclusion was performed with SYTOX Blue. To determine the number of megakaryocyte progenitors (MkPs), anti-Sca-1 (1:100, BioLegend, Clone: D7) was added to the same biotin antibody panel that was used for hematopoietic stem and progenitor cells as mentioned above. Afterwards, cells were washed and stained with BV421-CD41 (BioLegend, Clone: MWReg30), APC-CD9 (BioLegend, Clone: MZ3), PerCP-ckit (BioLegend, Clone: 2B8) and BV510-CD16/32 (BioLegends, Clone: 93). Dead cells were excluded with SYTOX Green. Measurements were conducted on a FACS Canto Flow Cytometer.

2.8.4. Measurement of MPL expression

After neutrophil isolation with negative MACS, 1 x 10^6 isolated neutrophils were pretreated with mouse FcR Blocking Reagent (Miltenyi Biotec, 10 minutes, 4 ℃) and subsequently incubated with a primary biotin-conjugated anti-mouse c-MPL/TPOR monoclonal antibody (Immuno-Biological Laboratories, Clone: AMM2, 1:50, 30 minutes, 4 ℃). In parallel, 1 x 10^6 granulocytes were left untreated after Fc Block and were used as negative control. Next, cells were washed and incubated with APC/Cy7-Streptavidin (BioLegend, 1:100, 30 minutes, 4 ℃). Dead cells were excluded with SYTOX Blue. Determination of MFI values for c-MPL on tdTomato$^+$ cells was conducted on a Cytek Aurora Spectral Flow Cytometer. To account for non-specific antibody binding, MFIs of tdTomato$^+$ cells were corrected by subtracting the MFI of the negative control.

2.8.5. Measurement of intracellular phosphorylated STAT1, STAT3 and STAT5

After neutrophil isolation with negative MACS, 1 x 10^6 isolated neutrophils were resuspended in RPMI/0.5% FBS medium and were either left untreated or stimulated with 10 ng/ml murine TPO (Peprotech), 10 ng/ml recombinant mouse IL-3 (BioLegend) or both in 37 ℃ and 5% CO_2 for 15 minutes. Subsequently, cells were centrifuged and fixed with pre-warmed BD Phosflow Fix Buffer I (BD Biosciences) in 37 ℃ for 10 minutes. After a washing step with PBS only, cells were centrifuged, pellets were resuspended and cell membranes were permeabilized with pre-cooled BD Phosflow Perm Buffer III (BD Biosciences) in 4 ℃ for 30 minutes. Next, cells were washed twice with sodium azide-containing PBS (PBA) and were pre-treated with mouse FcR Blocking Reagent (Miltenyi Biotec, 10 minutes, 4 ℃). Finally, neutrophils were stained with Alexa Fluor 488 mouse anti-phospho-Stat1 (BD Biosciences, Clone: pY701, 5:100, 30 minutes, 4 ℃), BV421 mouse anti-phospho-Stat3 (BD Biosciences, Clone: pS727, 5:100, 30 minutes, 4 ℃) and Alexa Fluor 647 mouse anti-phospho-Stat5 (BD Biosciences, Clone: pY694, 5:100, 30 minutes, 4 ℃). Determination of MFI values for pSTAT1, pSTAT3 and pSTAT5 on tdTomato$^+$ cells was conducted on a Cytek Aurora Spectral Flow Cytometer.

2.9. Static adhesion assay

0.15 µg of recombinant Fc-free murine VCAM-1/CD106, ICAM-1/CD54, P-selectin/CD62P and E-selectin/CD62E (Leinco Technologies) were added to the appropriate wells of a 96-well black/clear bottom microplate, centrifuged briefly and were left in 4 ℃ for 24-72 hours to immobilize. Wells pre-coated with 1% BSA were additionally included as a negative control. Murine granulocytes were quantified with Trypan Blue, stained with calcein AM (Thermo Fischer) in 1µg/ml concentration and 100,000 cells per mouse were introduced into the appropriate wells. After brief centrifugation, cells were incubated in 37 ℃ and 5% CO_2 for 30 minutes and the fluorescence of each sample was immediately measured on a Synergy HT spectrophotometer. The respective wells were successively washed three times with HBSS and measurements were repeated after each wash. The percent adherence was calculated by dividing the optical density measured after the third wash with the pre-wash value and the mean percent adherence of all WT mice included in the experiment served as the control value for normalization.

2.10. Time lapse assay

For *in vitro* time-lapse imaging, we precoated two wells of a 15-well angiogenesis µ-slide (Ibidi) for 24 hours with 5 µg/mL recombinant mouce ICAM-1/CD54 and VCAM-1/CD106 Fc chimera (R&D Systems). Two wells precoated with 1% BSA were also included as a negative control. Next, we isolated tdTomato$^+$ cells from BM MACS-enriched neutrophils of 14-16 weeks old CALR$^{+/+}$ Catchup (n=3) or CALR$^{del/+}$ Catchup (n=3) mice by using a BD FACS Aria III cell sorter. TdTomato$^+$ cells were then resuspended in Ca^{2+} and Mg^{2+} containing HBSS with 0.2% fatty acid-free BSA (Roth) and 1 mM HEPES (Life Technologies) and 50,000 cells per well were introduced into the appropriate wells of the µ-slide. Immediately thereafter, time lapse recording was performed under a Leica DMI6000 microscope in 5% CO_2 at 37 °C (40x magnification, Leica Microsystems). Images in brightfield and tdTomato fluorescence protocols were captured every 32 sec over a period of three hours in four wells at a time. ImageJ and the MTrackJ plugin were used for manual tracking of 50 cells per mouse for one hour. Analysis of time-lapse data was conducted as already established in the work of Haage et al; a diagrammatic illustration of the employed parameters is available in Suppl. Figure 2.

2.11. Cytokine measurement

Determination of plasma cytokine levels was carried out by Eve Technologies (Calgary, Canada) using the Mouse Cytokine Array/Chemokine Array 31-Plex kit. Heparin plasma samples were stored at -80 °C before measurement.

2.12. Quantitative reverse transcription PCR (qRT-PCR)

Experiments were performed by Harit Kunjan from the research group of Dr. Gopala Krishna Nishanth (Hannover Medical School). qRT-PCR was conducted on neutrophils isolated with negative immune-enrichment from the BM of CALR$^{+/+}$ Catchup and CALR$^{del/+}$ Catchup mice. 1 x 10^6 isolated granulocytes were centrifuged, resuspended in RLT buffer and homogenized with the QIAshredder kit (Qiagen Hilden, Germany). The RNeasy Mini Kit (Qiagen Hilden, Germany) was employed to isolate RNA. RNA purity and concentration were determined with a NanoDrop ND-1000 spectrophotometer (Thermo Fisher Scientific, Waltham, USA). First strand complementary DNA was produced from 1 µg of isolated RNA with the Superscript Reverse Transcriptase Kit (Thermo Fisher Scientific, Waltham, USA). Before conducting qRT-PCR, DNA was excluded by performing PCR for the housekeeping gene hypoxanthine

phosphoribosyltransferase (HPRT) with the 5'-GCTGGTGAAAAGGAC-3' sequence as a primer according to the following protocol: initial denaturation (95 ℃ for 15 minutes) and then 38 cycles of cyclic denaturation (94 ℃ for 38 sec), cyclic annealing (53 ℃ for 38 sec) and cyclic elongation (72 ℃ for 38 sec) followed by final elongation (72 ℃ for 7 minutes). The KAPA PROBE FAST qPCR Master Mix (2X) Kit (KAPA Biosystems, Wilmington, USA) as well as the following TaqMan Assay probes (Thermo Fisher Scientific, Waltham, USA) were employed for qRT-PCR: CXCL10 (Assay ID: Mm01345163_g1), CXCL12 (Assay ID: Mm00445552_m1), HPRT (Assay ID: Mm01545399_m1), IL-1β (Assay ID: Mm00434228_m1), IL-4 (Mm01288596_m1), IL-6 (Mm00446190_m1), IL-10 (Assay ID: Mm01288386_m1) and TNF-α (Assay ID: Mm00443258_m1). Measurements were conducted on a LightCycler 480 II (Roche Diagnostics, Mannheim, Germany). Relative gene expression was determined by normalizing to the HPRT gene with the $2^{-\Delta\Delta CT}$ method.(173)

2.13. Data analysis, representation, and statistical methodology

Statistical tests were conducted on GraphPad 9.0.2. The unpaired Student's t-test was used for statistical significance, unless violations of the assumption of normality or presence of extreme outliers (defined as observations lying more than three standard deviations of the mean) were detected, in which case the non-parametric Mann-Whitney U test was performed. The assumption of normality was assessed individually for each data set by visual inspection of the data distribution on quantile-quantile plots and by conducting the Shapiro-Wilk test of normality.(174, 175) For all tests, a two-tailed p-value of less than 0.05 was considered significant. P-values for each depicted comparison are given in figure legends as P. The standard error of the mean (SEM) was used as a measure of variability.

2.14. Study approval

Animal experiments were approved by the regional government authority of Saxony-Anhalt, Germany (registration numbers: 42502-2-1496 and 42502-2-1726). Mice were maintained under standardized specific-pathogen-free conditions in the animal facility of the Otto-von-Guericke University Magdeburg, Medical Faculty.

3. Results

3.1. Negative immunomagnetic isolation of murine WT BM neutrophils yields a cell population with high neutrophil purity

To unravel the role of CALR mutations in neutrophil adhesive properties, we employed a magnetic-bead based negative cell-separation method to isolate "untouched" neutrophils from whole BM cells (See Methods Section 2.5b).(172) By flow cytometric evaluation after staining with the neutrophil-specific anti-Ly6g and monocyte-specific anti-Ly6c antibodies, Ly6g^{bright} (neutrophils), Ly6c^{bright} (monocytes) and Ly6c$^{negative\ to\ low}$ Ly6g^{negative} (lymphocytes) cells comprised 70.1% ± 1.1%, 8.2% ± 0.4% and 4.4% ± 0.6% (n = 6) of the whole cell population respectively (Figure 4A). Cells that did not fall under these gates (mostly immature granulocytes) were intermediately positive for Ly6c and negative to intermediately positive for Ly6g (Ly6c^{med} Ly6g$^{negative\ to\ med}$, 17.0% ± 0.6%, n = 6) (Figure 4A).

By mere morphological assessment of isolated cells in cytospins, about 83% were compatible with mature neutrophils or neutrophil precursors (62.2% ± 2.6% and 20.6% ± 1.9%, n = 6, respectively). Mature neutrophils were defined by the typical segmented ring-shaped nucleus or "figure-8" appearance, while neutrophil precursors either by a smooth ring-shaped (neutrophil bands or metamyelocytes) or kidney-like nucleus (myelocytes) (Figure 4B).(176)Morphology of the remaining cells was compatible with monocytes and lymphocytes (13.5% ± 2.2% and 3.7% ± 0.9%, n = 6, respectively). Taken together, the percentages observed in cytospins generally correlated well with the ones that were observed in flow cytometry.

To further characterize cell populations, Ly6g^{bright}, Ly6c^{med} Ly6g$^{negative\ to\ med}$, Ly6c^{bright} and Ly6c$^{negative\ to\ low}$ Ly6g^{negative} cells were isolated with FACS and examined on cytospins. In the Ly6g^{bright} group, the majority of cells were compatible with segmented neutrophils (70%). Most of the remaining Ly6g^{bright} cells exhibited neutrophil precursor features (29%), while < 2% were monocytes (Figure 4C). The majority of Ly6c^{med} Ly6g$^{negative\ to\ med}$ cells were identified as neutrophil precursors (87%); segmented neutrophils represented a minority in this population (11%) (Figure 4D). The significant percentage of immature neutrophils in the Ly6g^{intermediate} population is in accordance with previous studies demonstrating a positive correlation of Ly6g surface expression with neutrophil maturation.(150, 177) As expected, Ly6c^{bright} cells were mostly monocytes (91%) (Figure 4E), whereas more than half of Ly6c$^{negative\ to\ low}$

Ly6g^{negative} cells appeared morphologically as lymphocytes (59%) (Figure 4F). Interestingly, segmented neutrophils comprised a significant proportion of Ly6c$^{negative\ to\ low}$ Ly6g^{negative} cells (26%) (Figure 4F).

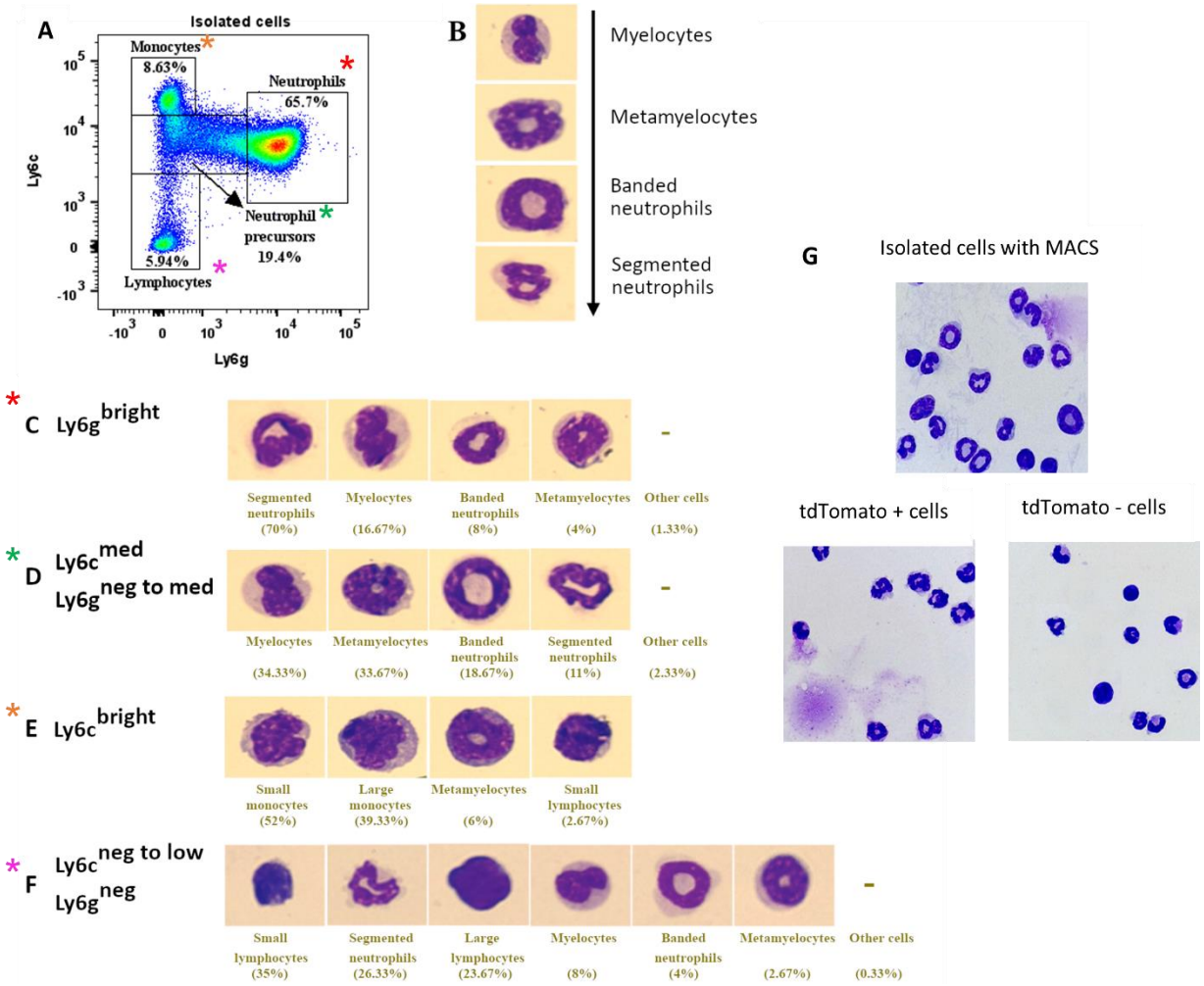

Figure 4. High neutrophil purity in isolated "granulocytes" from murine whole BM with magnetic cell sorting. (A) Representative pseudo color blot of isolated cells with MACS from the BM of a 12-week-old wild-type mouse after staining with PE/Cy7-Ly6c and BV510-Ly6g. An initial forward side scatter (FSC)/ side scatter (SSC) gate was used to exclude cellular debris followed by exclusion of doublets on FSC-A/FSC-H. (B) The normal differentiation stages of murine neutrophils. A segmented neutrophil exhibiting the typical figure-8 appearance is shown. (C-F) Morphology of sorted Ly6g^{bright}, Ly6c^{med} Ly6g$^{neg\ to\ med}$, Ly6c^{bright} and Ly6g$^{neg\ to\ low}$ Ly6g^{neg} cells on cytospins. (G) Cytospin of isolated cells after magnetic neutrophil sorting (up) and sorted tdTomato^{+} and tdTomato^{-} cells (down).

In Catchup mice, 59.0% ± 0.9% (n = 6) of isolated cells were tdTomato^{+} by flow cytometry. Among Ly6g^{+} cells, only 71.6% ± 0.6% (n = 6) were tdTomato^{+}, which indicates that not all neutrophils express tdTomato. On the contrary, practically all tdTomato^{+} cells (98.7% ± 0%, n = 6) were Ly6g^{+}. On cytospins, 90% of isolated tdTomato^{+} cells appeared as segmented neutrophils, whereas a minority of cells had

neutrophil precursor features (9%). The tdTomato$^-$ cell population was heterogeneous morphologically on cytospins and included segmented neutrophils (55.3%), neutrophil precursors (29.13%), monocytes (11.65%) and lymphocytes (3.88%) (Figure 4G).

3.2. PCR genotyping of VavCre CALR mice

We bred CALR$^{fl/+}$ mice with VavCre$^+$ mice to induce hematopoietic-specific expression of CALRdel52 (Figure 3A) and conducted PCR genotyping on DNA extracted from BM cells and ear punch tissues in the offspring. Effective recombination in the BM was confirmed with PCR in mice that were genotyped as VavCre$^+$ CALR$^{fl/+}$ in the ear punch (Suppl. Figure 1C). To our surprise, the CALRdel52 band was detected in ear punch tissue samples in some of the offspring, even in mice that did not exhibit expression of VavCre (Suppl. Figure 1C, mouse number 11). Ectopic Cre recombination, which leads to expression of the mutation of interest in unwanted tissues, is a well-known problem of Cre/lox systems and is attributed to unexpected Cre recombination in the germline of parent mice or during embryonic development of the offspring.(171) Expression of CALRdel52 in non-hematopoietic tissues was not anticipated given the hematological and endothelial specificity of VavCre recombinase in the VavCre CALR mouse model.(178) Moreover, blood contamination of ear punch tissues in VavCre$^+$ mutant mice was not deemed possible because it would correspond to a simultaneous presence of a CALR$^{fl/+}$ band (ear tissue) and of CALR$^{del/+}$ band (blood) in problematic mice, which solely exhibited a CALR$^{del/+}$ band (Suppl. Figure 1C, mouse number 3). Therefore, mice that were genotyped as CALR$^{del/+}$ in the ear punch were excluded from all experiments.

3.3. VavCre CALR$^{del/+}$ mice develop a phenotype resembling human ET

At 12-14 weeks of age VavCre CALR$^{del/+}$mice exhibited a 1.7-fold increase in PLT counts compared to VavCre CALR$^{+/+}$ mice (Figure 5A). RBCs were slightly but non-significantly increased in VavCre CALR$^{del/+}$ mice (CALR$^{del/+}$: 9.431 ± 0.1463 10^{12}/L; CALR$^{+/+}$: 9.120 ± 0.1074 10^{12}/L; P = 0.0904), whereas Hct and Hb levels were similar to VavCre CALR$^{+/+}$ mice (Figure 5A). VavCre CALR$^{del/+}$ mice did not demonstrate splenomegaly as assessed by similar spleen weight compared to WT control (CALR$^{del/+}$: 81.62 ± 2.541 mg; CALR$^{+/+}$: 83.95 ± 2.874 mg; P = 0.5448) (Figure 5B). VavCre CALR$^{del/+}$ mice developed mild leukocytosis (CALR$^{del/+}$: 7.755 ± 0.4850 10^9/L; CALR$^{+/+}$: 6.420 ± 0.4422 10^9/L; P = 0.0463) with a highly significant predominance of the lymphocytic population (CALR$^{del/+}$: 95.24 %; CALR$^{+/+}$: 89.53 %), while the percentage of peripheral blood neutrophils (CALR$^{del/+}$: 1.034 %; CALR$^{+/+}$: 5.333 %) and monocytes

(CALR$^{del/+}$: 0.5172 %; CALR$^{+/+}$: 1.7 %) was significantly reduced (Figure 5C). Evaluation of PLT indices revealed that PLTs of VavCre CALR$^{del/+}$mice displayed a significantly smaller distribution width (CALR$^{del/+}$: 45.06 %; CALR$^{+/+}$: 59.13 %; P = 0.0050) while remaining unchanged with respect to their volume. Finally, we observed significant changes regarding the erythrocyte parameters of VavCre CALR$^{del/+}$ mice, more specifically a significant decrease in mean corpuscular volume (MCV) (CALR$^{del/+}$: 54.47 fl; CALR$^{+/+}$: 56.33 fl; P = 0.0201) and a significant elevation in mean cell haemoglobin concentration mean (MCHC) (CALR$^{del/+}$: 15.53 g/dl; CALR$^{+/+}$: 14.67 g/dl; P = 0.0238) (Figure 5D).

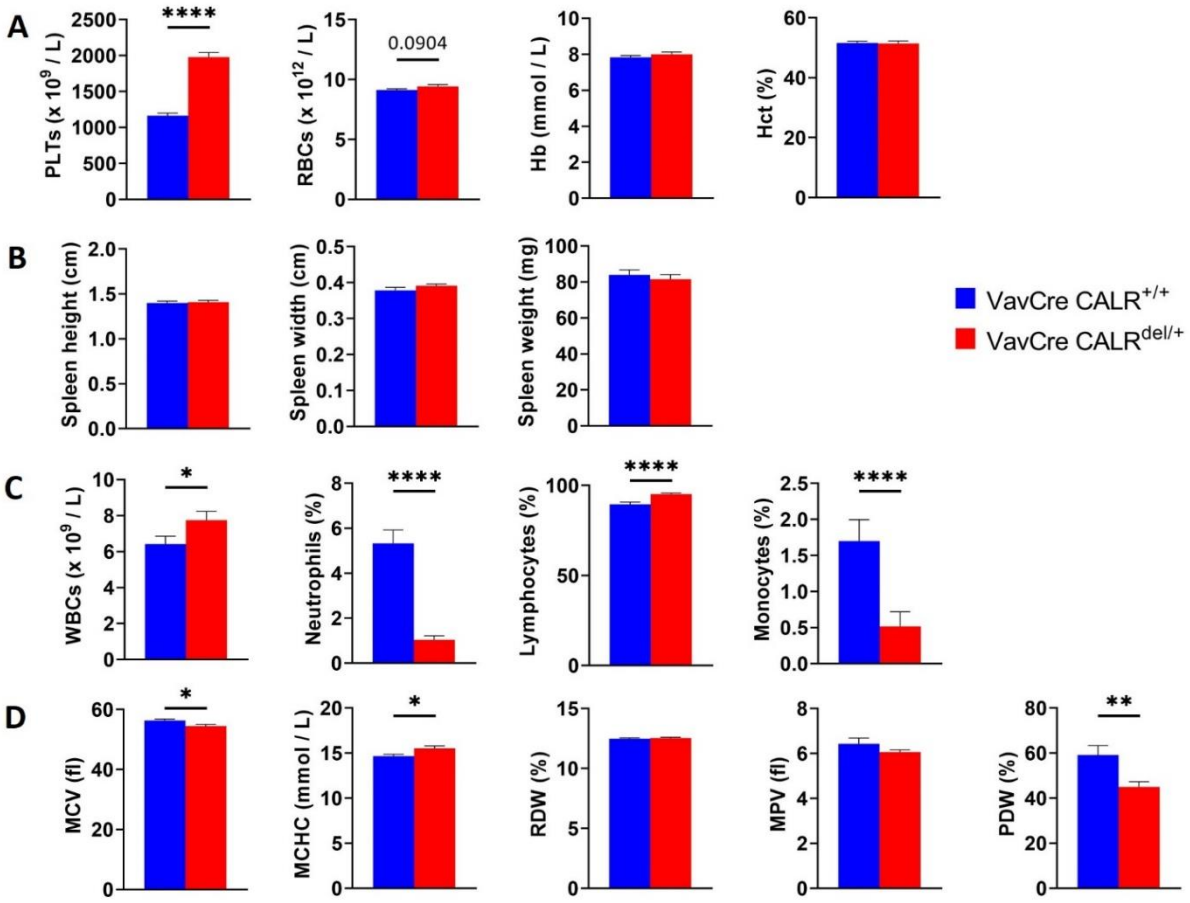

Figure 5. VavCre CALR$^{del/+}$ mice develop a chronic myeloproliferative phenotype resembling human ET. (A) PLT counts (P < 0.0001), RBC counts (P = 0.0904), Hct (P = 0.8563) and Hb levels (P = 0.3052) of VavCre CALR$^{+/+}$ (n = 30) and VavCre CALR$^{del/+}$ (n = 29) mice. (B) Spleen height (P = 0.3273), width (P = 0.1520) and weight (P = 0.5448) of VavCre CALR$^{+/+}$ (n = 21) and VavCre CALR$^{del/+}$ (n = 26) mice. (C) WBC counts (P = 0.0463), percentage of peripheral blood neutrophils (P < 0.0001), lymphocytes (percentage: P < 0.0001) and monocytes (percentage: P < 0.0001) of VavCre CALR$^{+/+}$ (n = 30) and VavCre CALR$^{del/+}$ (n = 29) mice. (D) RBC and PLT indices of VavCre CALR$^{+/+}$ (n = 30) and VavCre CALR$^{del/+}$ (n = 28 for MCV and MCHC, n =29 for RDW, MPV and PDW) mice. (MCV: P = 0.0201, RDW: P = 0.5251, MCHC: P = 0.0238, MPV: P = 0.6674, PDW: P = 0.0050). Data are shown as mean ± SEM. *P ≤ 0.05, **P ≤ 0.01, ***P ≤ 0.001, ****P ≤ 0.0001.

3.4. Granulocytes isolated from VavCre CALR$^{del/+}$ mice do not demonstrate increased integrin-mediated adhesion

The process of leukocyte rolling, firm adhesion and transmigration involves ligand binding to a receptor protein located on the leukocyte membrane.(135) To dissect the impact of CALRdel mutations on neutrophil adhesion, we employed magnetic cell sorting to isolate granulocytes from whole BM cells of VavCre CALR$^{+/+}$ and VavCre CALR$^{del/+}$ mice. Cell membrane expression of receptors for endothelial adhesion molecules on Ly6g^{bright} cells was determined with flow cytometry and a static adhesion as well as a soluble binding assay were employed to evaluate binding affinity of neutrophils to adhesion molecules normally expressed on the vascular endothelium.

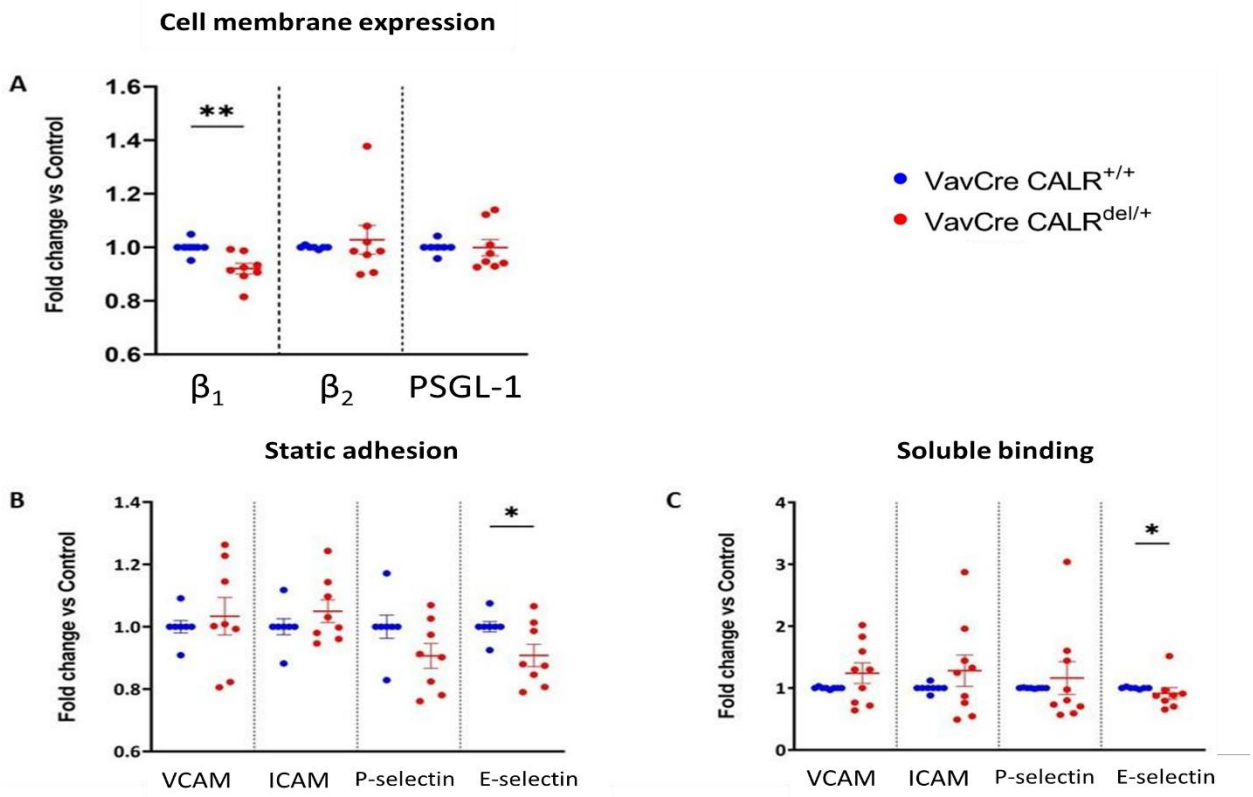

Figure 6. Granulocytes isolated from VavCre CALR$^{del/+}$ mice demonstrate downregulation of surface β_1 integrin, unaltered integrin-mediated adhesion and decreased binding to E-selectin. (A) β_1 integrin ($P \leq 0.01$), β_2 integrin ($P = 0.4569$) and PSGL-1 expression ($P = 0.4569$) on granulocytes isolated from 12- to 14-week-old VavCre CALR$^{+/+}$ (n = 7) and VavCre CALR$^{del/+}$ (n = 8) mice. (B) Static adhesion of VavCre CALR$^{+/+}$ (n = 7) and VavCre CALR$^{del/+}$ (n = 8) granulocytes on Fc-free VCAM-1 ($P = 0.6274$), ICAM-1 ($P = 0.2984$), P-selectin ($P = 0.1131$) and E-selectin ($P = 0.0443$). (C) Soluble binding of VavCre CALR$^{+/+}$ (n = 7 for VCAM, ICAM and P-selecin, n = 8 for E-selectin) and VavCre CALR$^{del/+}$ (n = 9 for VCAM-1, ICAM-1 and P-selectin, n = 8 for E-selectin) granulocytes to VCAM-1 ($P = 0.4658$), ICAM-1 ($P = 0.7204$), P-selectin ($P = 0.2553$) and E-selectin ($P = 0.0121$). Data are shown as mean ± SEM. *$P \leq 0.05$, **$P \leq 0.01$, ***$P \leq 0.001$, ****$P \leq 0.0001$.

Contrary to neutrophils isolated from VavCre JAK2$^{VF/+}$ mice, which were shown to display increased expression of β_2 integrin,(59) VavCre CALR$^{del/+}$ granulocytes did not exhibit upregulation of membrane β_1 and β_2 integrins compared to their WT counterparts (Figure 6A). Interestingly, β_1 integrin levels were significantly downregulated on the surface of VavCre CALR$^{del/+}$ neutrophils (fold decrease: 0.9209 ± 0.01974; CALR$^{+/+}$: 1 ± 0.01068; $P \leq 0.01$; n = 8) (Figure 6A). Expression of the selectin receptor PSGL-1 remained unaltered on neutrophils isolated from VavCre CALR$^{del/+}$ mice (Figure 6A).

As opposed to the stronger integrin-regulated neutrophil adhesion previously demonstrated in VavCre JAK2$^{VF/+}$ mice,(59) adhesion to VCAM-1 and ICAM-1 was not affected in VavCre CALR$^{del/+}$ neutrophils (Figure 6B). Static adhesion to P-selectin was decreased in VavCre CALR$^{del/+}$ neutrophils, but this reduction was not significant (fold decrease: 0.9062 ± 0.03994; CALR$^{+/+}$: 1 ± 0.03734; P = 0.1131; n = 8) (Figure 6B). Notably, granulocytes isolated from VavCre CALR$^{del/+}$ mice showed significantly reduced static adhesion to E-selectin (fold decrease: 0.9078 ± 0.03586; CALR$^{+/+}$: 1 ± 0.01639; P = 0.0443; n = 8) (Figure 6B).

In the soluble binding assay, the binding affinity of VavCre CALR$^{del/+}$ granulocytes to VCAM-1, ICAM-1 and P-selectin remained unaltered (Figure 6C). In line with reduced adhesion to E-selectin coated surface, binding to soluble E-selectin was found decreased in VavCre CALR$^{del/+}$ mice (fold decrease: 0.9131 ± 0.09409; CALR$^{+/+}$: 1 ± 0.00503; P = 0.0121; n = 8) (Figure 6C).

3.5. PCR genotyping of CALR Catchup mice

We bred CALR$^{del/+}$ mice with Catchup mice to induce neutrophil-specific expression of CALRdel52 (Figure 3B) and conducted PCR genotyping on DNA extracted from BM cells and ear punch tissues in the offspring. Interestingly, the CALRdel52 band was not detectable in whole BM samples, but only appeared when PCR genotyping was performed on isolated tdTomato$^+$ cells. Thus, CALRdel52 expression was effectively restricted in the neutrophil population of CALR$^{del/+}$ Catchup mice (Suppl. Figure 1D). Heterozygosity for the knock-in allele in the Ly6g locus was demonstrated with two separate PCRs, as previously described.(153) More specifically, a WT-PCR (PCR1) and a Ki-PCR (PCR2) were used for detection of the wild-type exon 1 of Ly6g and the knock-in Cre-tdTomato allele respectively (Suppl. Figure 1D). All Catchup mice that carried the mutated CALR allele were genotyped as CALR$^{fl/+}$ in the ear punch, which indicated that restricted expression of Cre recombinase in Ly6g$^+$ cells was not associated with any unwanted germline Cre recombination.

3.6. Neutrophil-specific expression of CALRdel52 is not sufficient to induce a chronic myeloproliferative disease

To elucidate whether restricted expression of CALR mutations in granulocytes is able to induce a chronic myeloproliferative phenotype, we generated a novel Catchup mouse model harboring neutrophil-specific expression of CALRdel52 and examined the phenotypic characteristics and blood counts of affected animals. To exclude an effect of zygosity to the tdTomato allele in the Rosa26 locus in the phenotype of resulting mice, mice were stratified in heterozygous ($Rosa^{het}$) and homozygous ($Rosa^{homo}$) groups.

Mean body weight of 14-week-old $CALR^{del/+}$ Catchup mice was similar to their WT counterparts (24.25 mg and 24.33 mg respectively) (Figure 7A). Moreover, $CALR^{del/+}$ Catchup mice did not develop splenomegaly as shown by unaltered spleen length and weight (Figure 7B, C). Phenotypically, $CALR^{del/+}$ Catchup mice exhibited the normal appearance of a healthy C57BL/6 mouse (Figure 7D, E) and demonstrated normal home-cage activity. Absolute leukocyte counts and Hct levels of $CALR^{del/+}$ Catchup mice did not differ significantly from their corresponding WT controls (Figure 8A, B).

Contrary to the previously described thrombocytosis in $JAK2^{VF/+}$ Catchup mice,(160) $CALR^{del/+}$ Catchup mice did not demonstrate elevated PLT counts compared to their $CALR^{+/+}$ counterparts (for $Rosa^{het}$: $CALR^{del/+}$: 1143 ± 35.86 10^9/L; $CALR^{+/+}$: 1092 ± 57.21 10^9/L; P = 0.45, for $Rosa^{homo}$: $CALR^{del/+}$: 1398 ± 48.67 10^9/L; $CALR^{+/+}$: 1343 ± 50.95 10^9/L; P = 0.4915) (Figure 8C). Despite neutrophil-restricted expression of CALRdel mutation, neutrophil counts of $CALR^{del/+}$ Catchup mice remained unchanged (Figure 8D). In addition, there was no lymphocytic or monocytic predominance (Figure 8E, F).

In contrast to the well-known megakaryocytic proliferation of CALR-mutant mouse models (Suppl. Table S2), $CALR^{del/+}$ Catchup mice demonstrated non-significantly altered mean number of BM MKs compared to $CALR^{+/+}$ Catchup mice in the $Rosa^{het}$ group ($CALR^{del/+}$: 17.67 ± 0.9851; $CALR^{+/+}$: 16.39 ± 1.492; P = 0.4911) (Figure 8G). Although the small number of $CALR^{+/+}$ Catchup mice in the $Rosa^{hom}$ group did not allow significance testing, there were less BM MKs in $CALR^{del/+}$ than $CALR^{+/+}$ $Rosa^{hom}$ mice ($CALR^{del/+}$: 19.25; $CALR^{+/+}$: 20.33) (Figure 8G).

BM tissue architecture was preserved in H&E stained tissue sections of $CALR^{del/+}$ Catchup mice (Figure 9). In spleen biopsies, CALR-mutant mice had normal spleen lymphoid follicles with no apparent alterations in white and red pulp (Figure 10). Moreover, we did not observe any signs of megakaryocytic dysplasia

such as hypolobulated forms, micromegakaryocytes, widely separated nuclear lobes, cytoplasmic vacuoles or emperipolesis in CALR$^{del/+}$ Catchup mice (Suppl. Figure 3).

Finally, modified Gomori's staining of BM and spleen samples was unremarkable for reticulin fiber thickening or increased reticulin deposits in CALR$^{del/+}$ Catchup animals (Suppl. Figure 5 & 6).

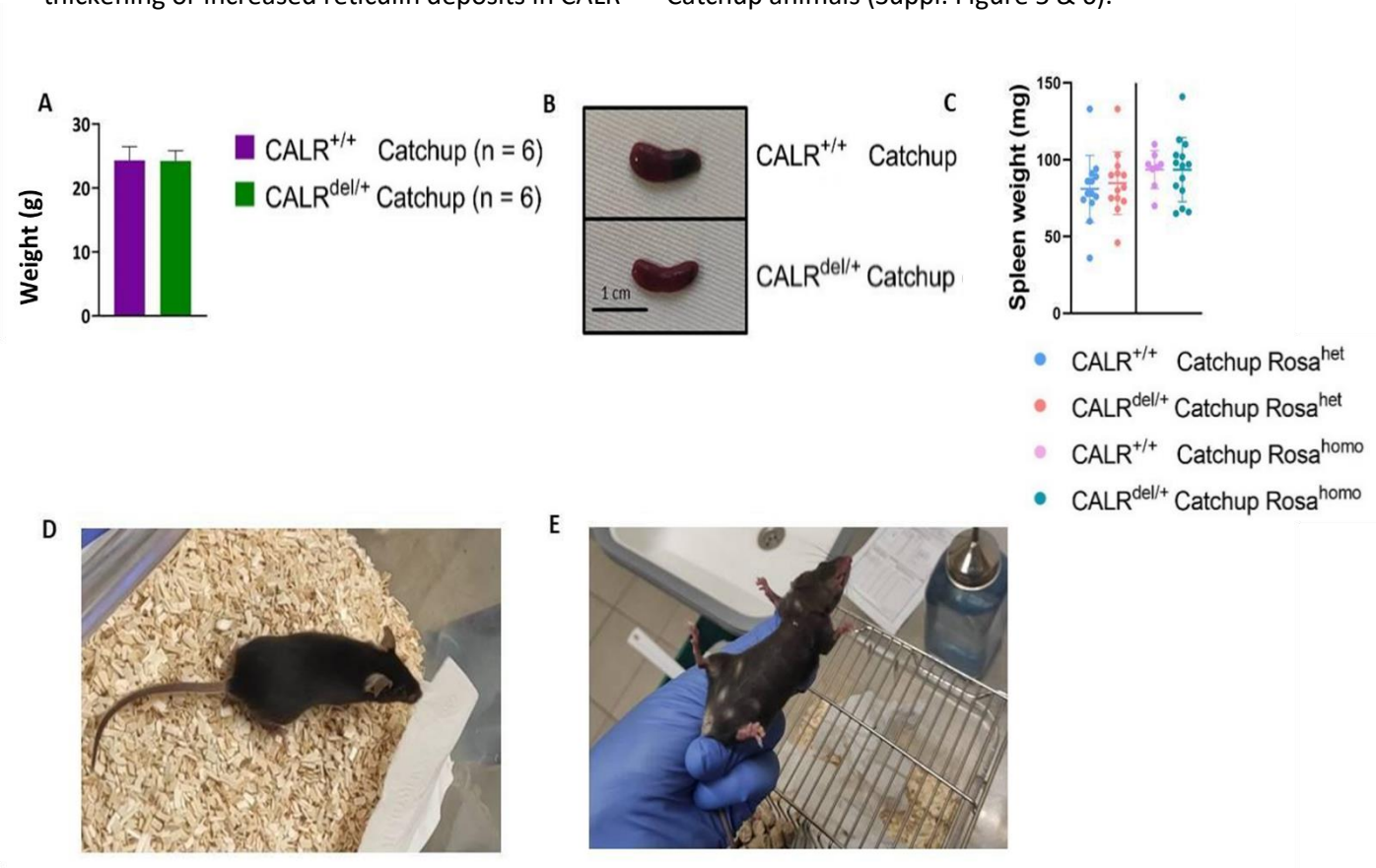

Figure 7. Gross appearance and spleen size of CALR$^{del/+}$ Catchup mice corresponded to their WT counterparts. (A) Weight comparison of 14-weeks-old CALR$^{+/+}$ Catchup (n = 6) and CALR$^{del/+}$ Catchup (n = 6) mice (P = 0.9758). Three male and three female mice were included in each group. (B) Representative photograph of spleens from a CALR$^{+/+}$ Catchup and a CALR$^{del/+}$ Catchup mouse. (C) Comparison of spleen weight between 12-16 week-old CALR$^{+/+}$ Catchup Rosa$^{tdTomato/+}$ (n = 13) vs CALR$^{del/+}$ Catchup Rosa$^{tdTomato/+}$ (n = 13) (P = 0.6538) and CALR$^{+/+}$ Catchup Rosa$^{tdTomato/tdTomato}$ (n = 8) vs CALR$^{del/+}$ Catchup Rosa$^{tdTomato/tdTomato}$ (n = 14) mice (P = 0.9948). (D) Dorsal view of a CALR$^{del/+}$ Catchup mouse demonstrating exploratory behavior in the cage. (E) Ventral view of a CALR$^{del/+}$ Catchup mouse. Data are shown as mean ± SEM.

Flow cytometric measurement of BM and spleen hematopoietic and progenitor cells did not reveal expansion of HSCs (defined as Lineage^{-} Sca-1^{+} c-kit^{+}) in CALR$^{del/+}$ Catchup mice (Figure 11A, B). In addition, CALR$^{del/+}$ Catchup mice did not exhibit significant changes in the composition of HSC subtypes [long term HSCs (LT-HSCs), short term HSCs (ST-HSCs) and multipotent progenitors (MPPs)] among total BM and spleen HSCs (Figure 11C, D).

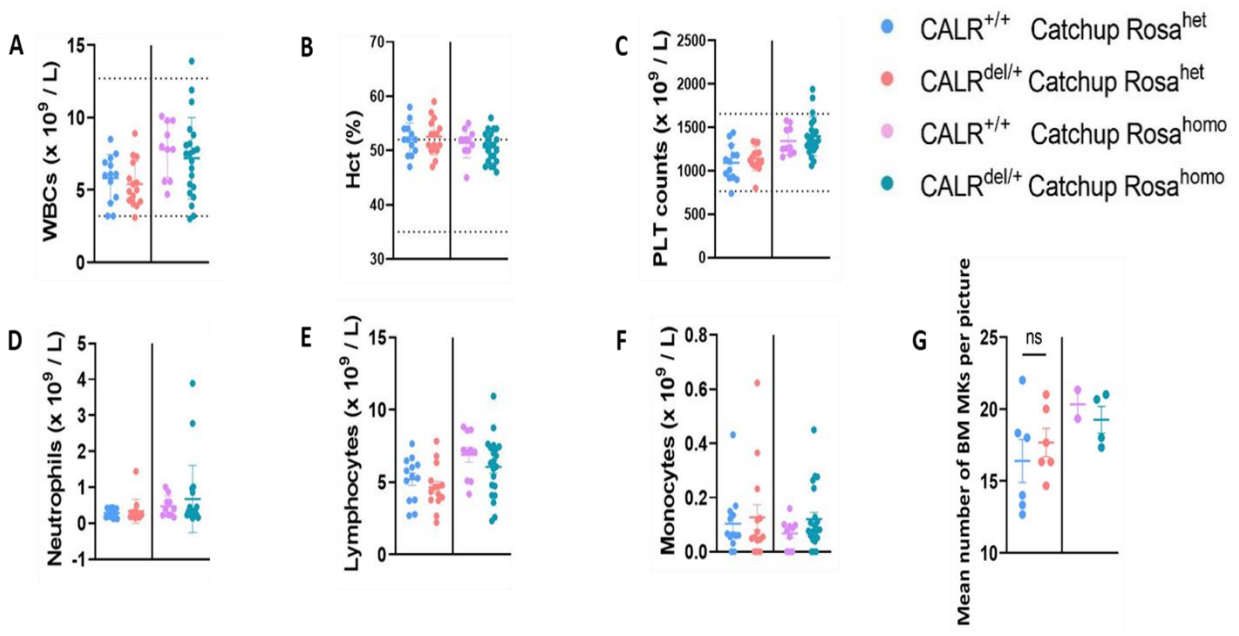

Figure 8. 12-16 week-old CALR$^{del/+}$ Catchup mice did not display significant alterations in complete blood counts or increased BM megakaryopoiesis regardless of heterozygosity or homozygosity to Rosa. Comparisons were conducted between CALR$^{+/+}$ Catchup Rosa$^{tdTomato/+}$ (n = 13) vs CALR$^{del/+}$ Catchup Rosa$^{tdTomato/+}$ (n = 15) and CALR$^{+/+}$ Catchup Rosa$^{tdTomato/tdTomato}$ (n = 10) vs CALR$^{del/+}$ Catchup Rosa$^{tdTomato/tdTomato}$ (n = 21) mice. (A) WBC counts (Rosa$^{tdTomato/+}$: P = 0.5236, Rosa$^{tdTomato/tdTomato}$: P = 0.5484). (B) Hct levels (Rosa$^{tdTomato/+}$: P = 0.7078, Rosa$^{tdTomato/tdTomato}$: P = 0.4476). (C) PLT counts (Rosa$^{tdTomato/+}$: P = 0.4500, Rosa$^{tdTomato/tdTomato}$: P = 0.4915). (D) Neutrophil counts (Rosa$^{tdTomato/+}$: P = 0.8953, Rosa$^{tdTomato/tdTomato}$: P = 0.8436) (E) Lymphocyte counts (Rosa$^{tdTomato/+}$: P = 0.3628, Rosa$^{tdTomato/tdTomato}$: P = 0.2727) (F) Monocyte counts (Rosa$^{tdTomato/+}$: P = 0.6147, Rosa$^{tdTomato/tdTomato}$: P = 0.4455) (G) Mean number of MKs per high-power field (Rosa$^{tdTomato/+}$: P = 0.4911). Data are shown as mean ± SEM. *P ≤ 0.05, **P ≤ 0.01, ***P ≤ 0.001, ****P ≤ 0.0001. Horizontal dotted lines indicate the normal reference range for a C57BL/6 mouse given by ADVIA 2120 blood analyzer.

Interestingly, there was a slight non-significant decrease in the relative number of spleen MPPs among total HSCs in CALR$^{del/+}$ Catchup mice (CALR$^{del/+}$: 818.9 ± 83.8 cells / 10^4 HSCs; CALR$^{+/+}$: 1081 ± 113.3 cells / 10^4 HSCs; P = 0.088) (Figure 11D). Absolute numbers of BM and spleen MPs (defined as Lineage$^-$ Sca-1$^+$ c-kit$^-$) was also found unchanged in CALR$^{del/+}$ Catchup mice (Figure 12A, B). There was a slight but non-significant expansion of common myeloid progenitors (CMPs) in the spleen of CALR$^{del/+}$ Catchup mice (CALR$^{del/+}$: 824.3 ± 83 cells / 10^6 spleen cells; CALR$^{+/+}$: 608.6 ± 70.83 cells / 10^6 spleen cells; P = 0.0715) (Figure 12B). Relative numbers of MP subtypes [GMPs, CMPs and Megakaryocyte-erythroid progenitors (MEPs)] among total BM and spleen MPs, remained unaltered in CALR$^{del/+}$ Catchup mice (Figure 12C, D).

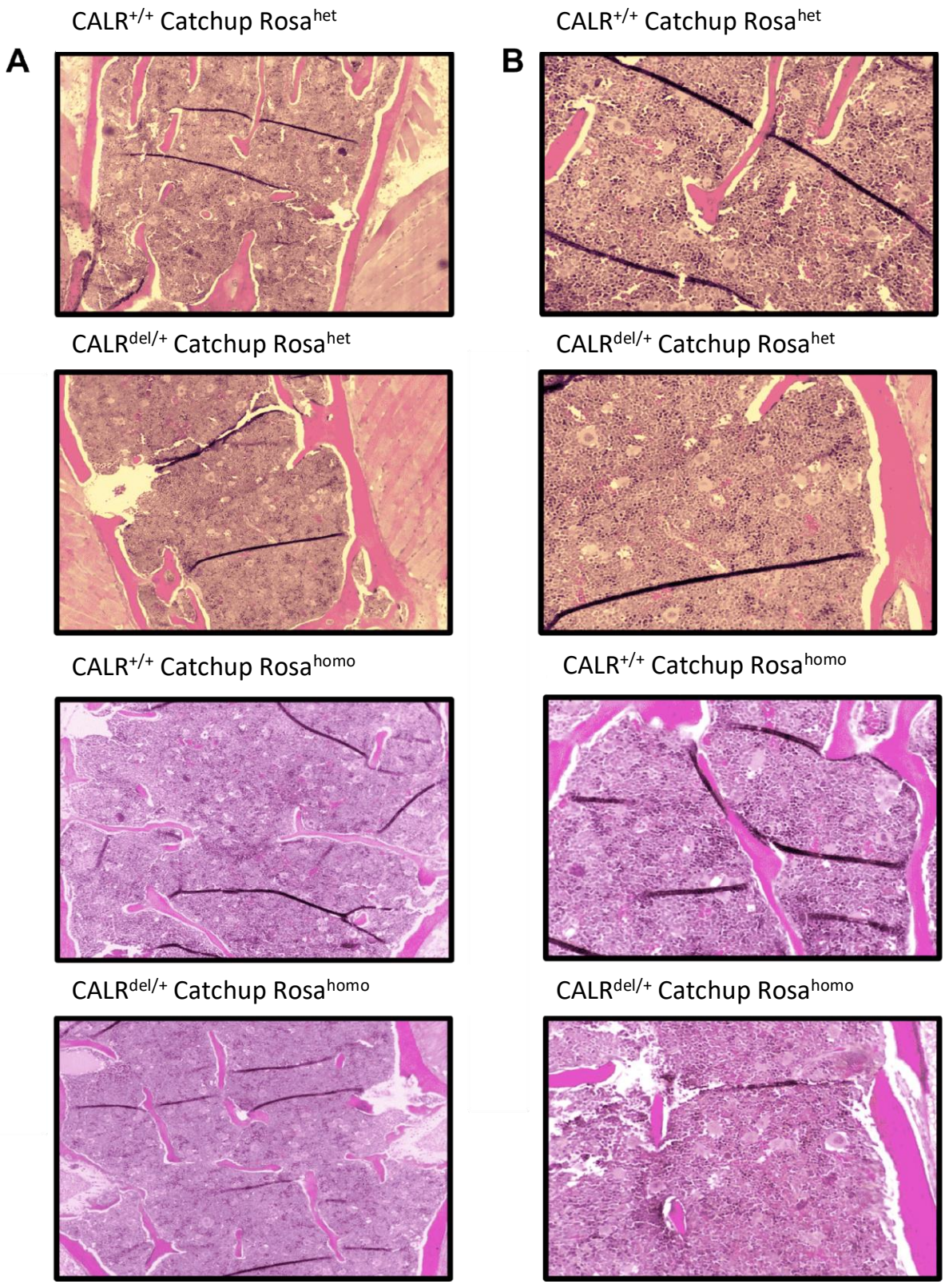

Figure 9. No notable differences in BM architecture were detected in BM sections of 12-16 weeks-old $CALR^{+/+}$ Catchup and $CALR^{del/+}$ Catchup mice regardless of heterozygosity or homozygosity to Rosa. Representative pictures of BM sections from $CALR^{+/+}$ Catchup $Rosa^{tdTomato/+}$ (n = 6), $CALR^{del/+}$ Catchup $Rosa^{tdTomato/+}$ (n = 6), $CALR^{+/+}$ Catchup $Rosa^{tdTomato/tdTomato}$ (n = 2) and $CALR^{del/+}$ Catchup $Rosa^{tdTomato/tdTomato}$ (n = 4) mice; original magnification x10 (A) and x20 (B).

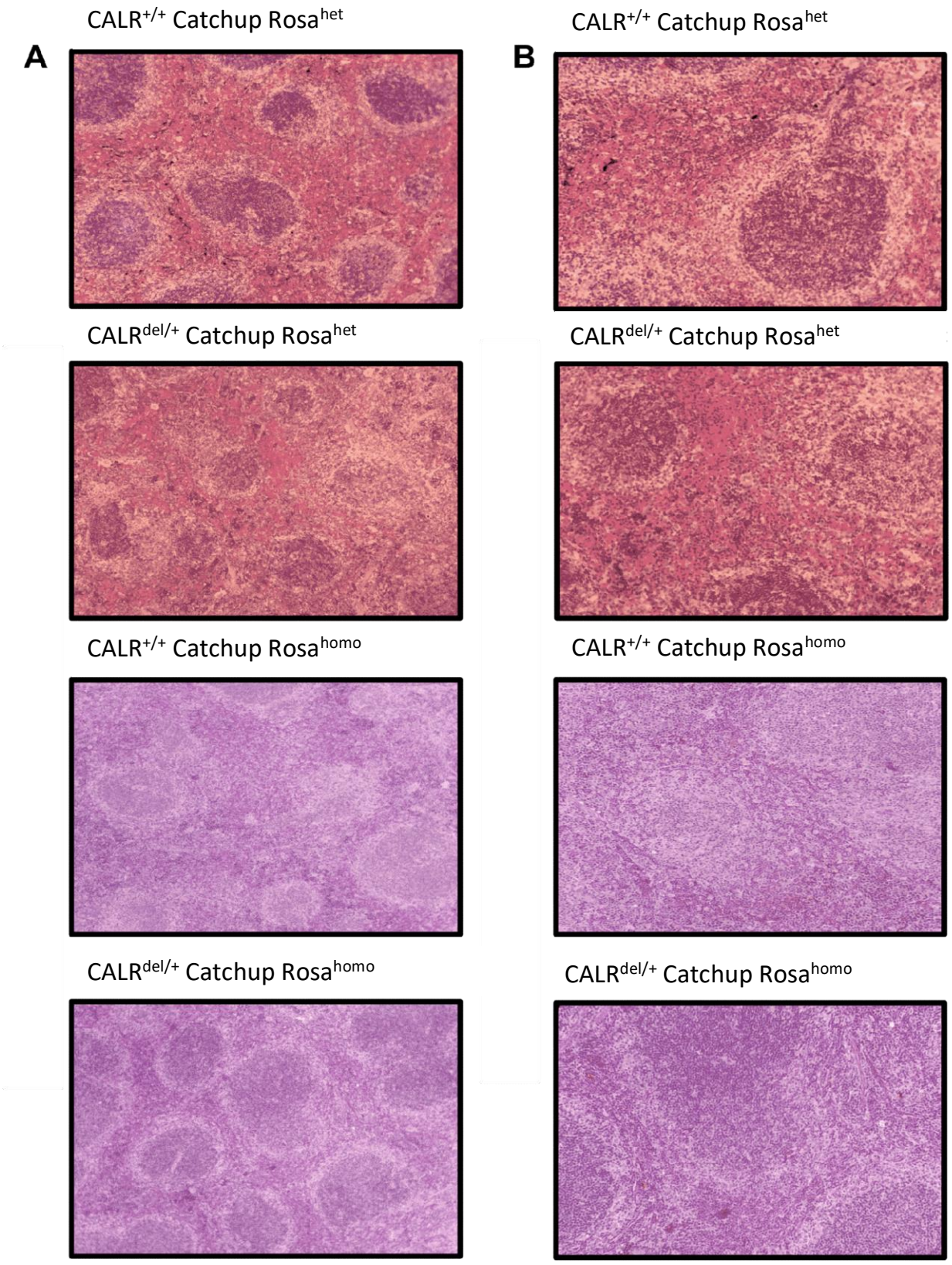

Figure 10. Architecture of splenic follicules was preserved in spleen sections of 12-16 weeks-old $CALR^{del/+}$ Catchup mice and was similar to $CALR^{+/+}$ Catchup mice regardless of heterozygosity or homozygosity to Rosa. Representative pictures of spleen sections from $CALR^{+/+}$ Catchup $Rosa^{tdTomato/+}$ (n = 7), $CALR^{del/+}$ Catchup $Rosa^{tdTomato/+}$ (n = 6), $CALR^{+/+}$ Catchup $Rosa^{tdTomato/tdTomato}$ (n = 2) and $CALR^{del/+}$ Catchup $Rosa^{tdTomato/tdTomato}$ (n = 4) mice; original magnification x10 (A) and x20 (B).

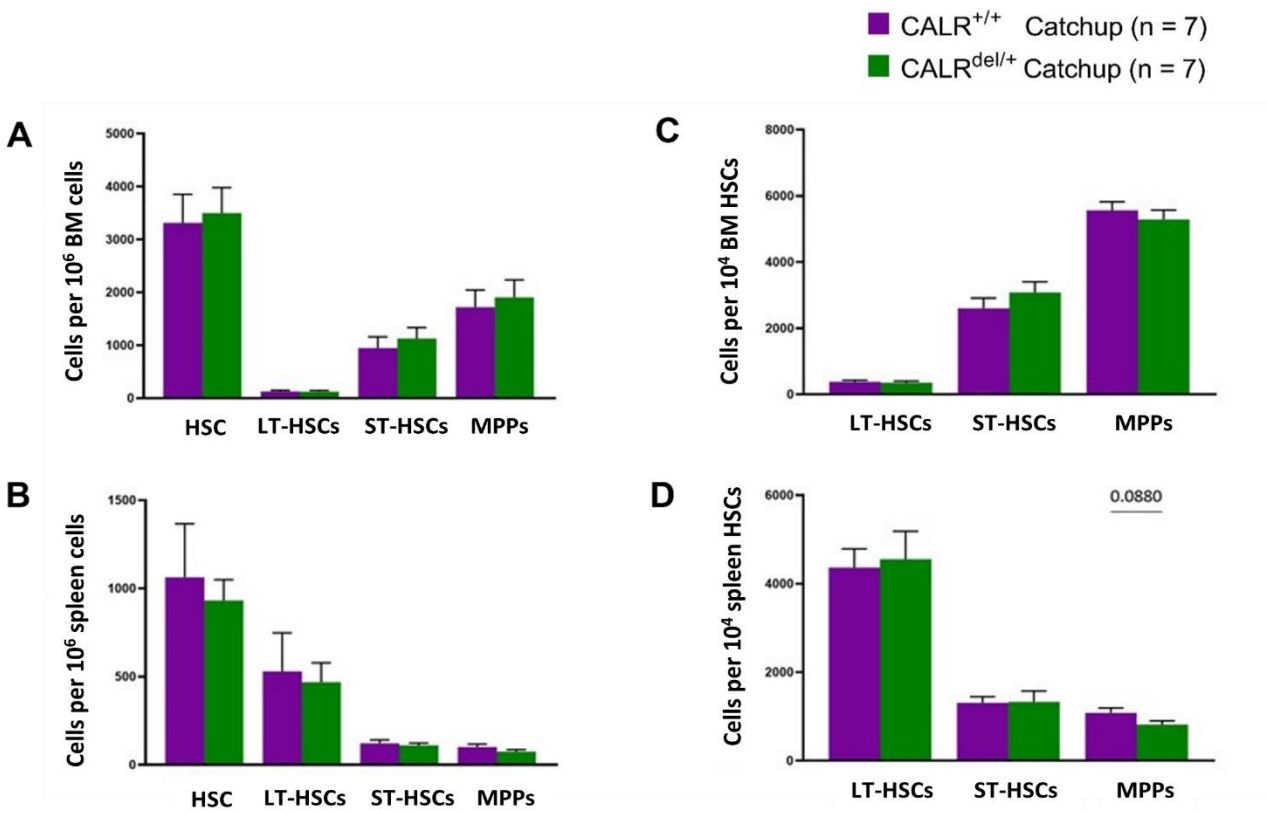

Figure 11. Numbers of HSCs, LT-HSCs, ST-HSCs and MPPs in the BM and spleen of $CALR^{+/+}$ Catchup (n = 7) and $CALR^{del/+}$ Catchup (n = 7) mice were comparable. Determination of HSCs (BM: P = 0.8015, Spleen: P = 0.6200), LT-HSCs (BM: P = 0.9762, Spleen: P = 0.7815), ST-HSCs (BM: P = 0.5582, Spleen: P = 0.6512) and MPPs (BM: P = 0.6946, Spleen: P = 0.2243) in total BM (A) and spleen cells (B). Determination of LT-HSCs (BM: P = 0.6957, Spleen: P = 0.8075), ST-HSCs (BM: P = 0.3047, Spleen: P = 0.9467) and MPPs (BM: P = 0.4801, Spleen: P = 0.0880) in total BM (C) and spleen HSCs (D). Data are shown as mean ± SEM.

Finally, BM and spleen $CD71^+$ $Ter119^+$ erythroid precursors and MkPs (defined as $Lineage^-$ $Sca\text{-}1^-$ $c\text{-}kit^+$ $FcγR^{low}$ $CD9^+$ $CD41^+$) were unaffected, indicating that $CALR^{del/+}$ Catchup mice do not exhibit alterations in hematopoiesis or thrombopoiesis (Suppl. Figure 4). The gating strategies used for flow cytometric identification of hematopoietic stem and progenitor cells (179-183), erythroblasts (171) and MkPs (184) are available in Suppl. Figure 7 and 8.

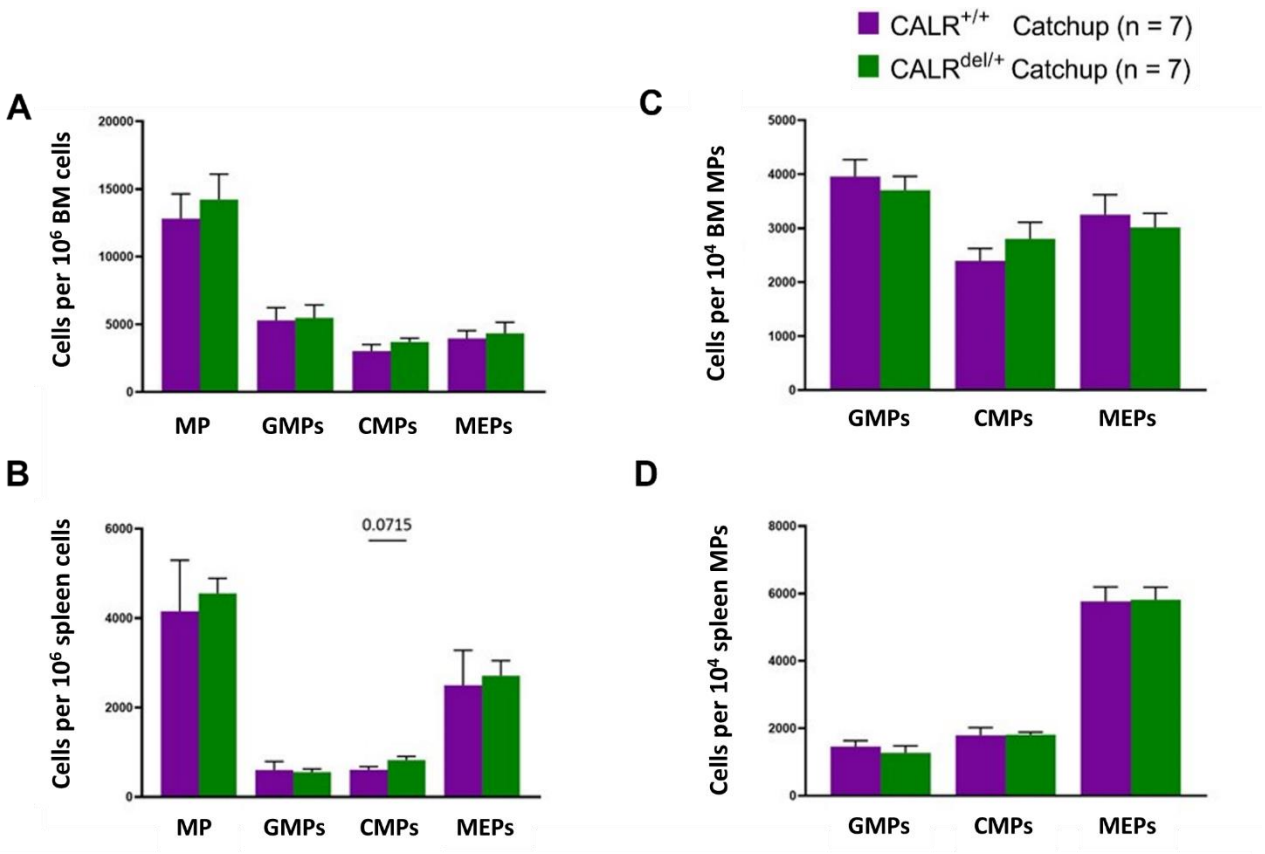

Figure 12. Numbers of MPs, GMPs, CMPs and MEPs in the BM and spleen of $CALR^{+/+}$ Catchup (n = 7) and $CALR^{del/+}$ Catchup (n = 7) mice did not differ significantly. Determination of MPs (BM: P = 0.5985, Spleen: P = 0.1177), GMPs (BM: P = 0.9002, Spleen: P = 0.5350), CMPs (BM: P = 0.2548, Spleen: P = 0.0715) and MEPs (BM: P = 0.7048, Spleen: P = 0.2226) in total BM (A) and spleen cells (B). Determination of GMPs (BM: P = 0.5392, Spleen: P = 0.5103), CMPs (BM: P = 0.3054, Spleen: P = 0.9484) and MEPs (BM: P = 0.6103, Spleen: P = 0.9311) in total BM (C) and spleen MPs (D). Data are shown as mean ± SEM.

3.7. $CALR^{del/+}$ Catchup mice do not show increased expression of inflammatory mediators in serum

To determine whether expression of the CALRdel52 mutation in murine neutrophils is associated with increased inflammation, the serum concentration of various cytokines und growth factors was measured in $CALR^{del/+}$ Catchup mice and compared to their WT counterparts by employing a Mouse Cytokine/Chemokine 31-Plex Discovery Assay (Eve Technologies, Calgary, Canada). In serum of $CALR^{del/+}$ Catchup mice, we did not find any significant upregulation of mean inflammatory mediator concentrations (Figure 13A-C). Interestingly, CALR-mutants exhibited slight upregulation of IL-5 ($CALR^{del/+}$: 28.97 pg/ml; $CALR^{+/+}$: 19.04 pg/ml; P = 0.0867) and slight downregulation of IL-1β ($CALR^{del/+}$:

14.63 pg/ml; CALR$^{+/+}$: 19.6 pg/ml; P = 0.0664). In the heat map representation, the top three upregulated inflammatory biomarkers in serum of CALR$^{del/+}$ Catchup mice (in percent change of 150-200% but again non-significantly) were the neutrophil-chemoattractant LIX (or CXCL5),(185) IL-5 and IL-4, which have a role in adaptive immunity rather than inflammation (Figure 13D).(186) Fold change values and P-values are summarized in Suppl. Table S1.

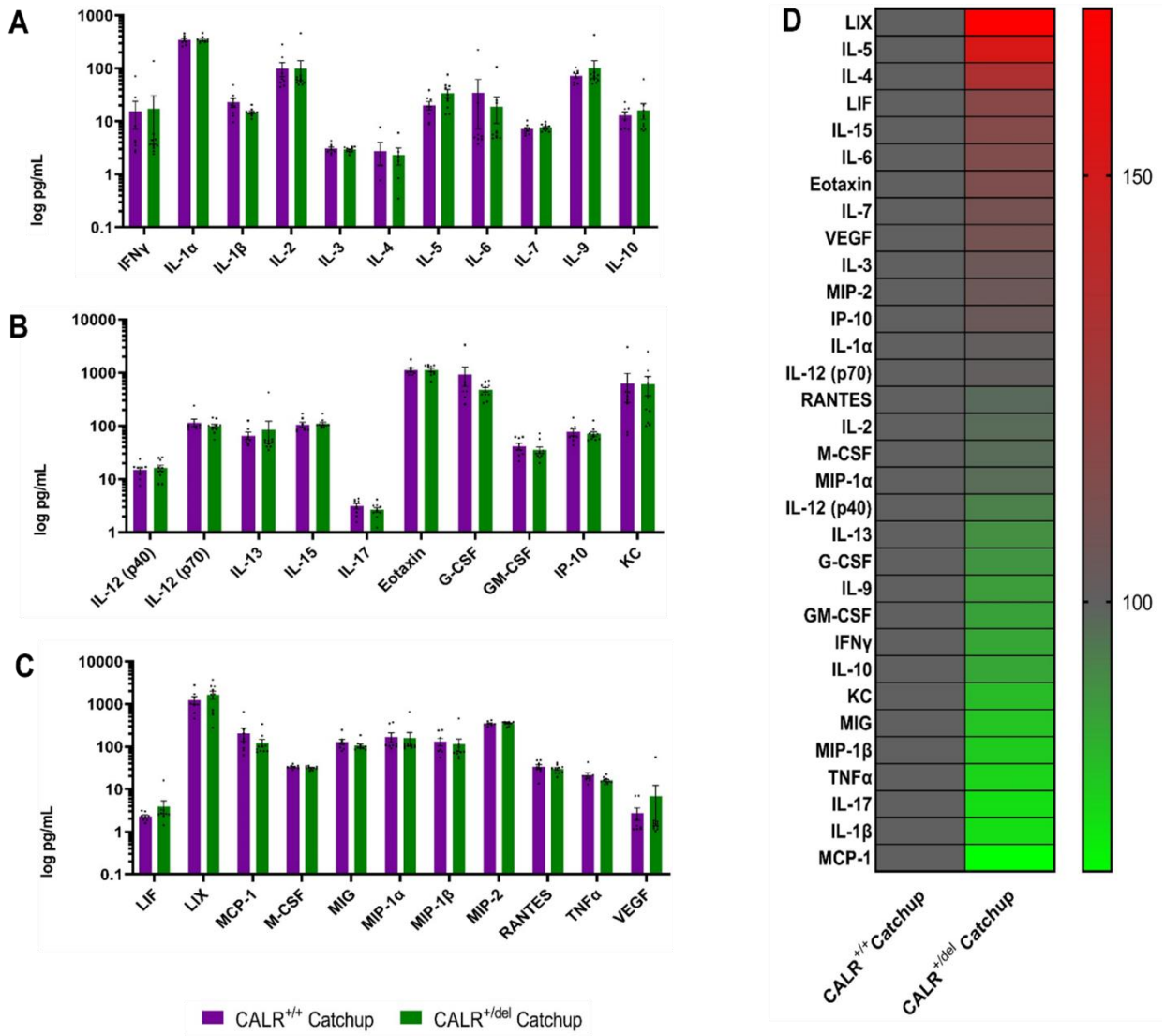

Figure 13. CALR$^{del/+}$ Catchup mice did not show increased inflammation as assessed by unaltered serum inflammatory biomarker concentrations compared to CALR$^{+/+}$ Catchup mice. (A-C) Bar plots of plasma inflammatory biomarker concentrations in CALR$^{+/+}$ Catchup (n = 8, n = 5 for IL-4) and CALR$^{del/+}$ Catchup mice (n = 10, n = 6 for IL-4, n = 9 for IL-17) expressed in log pg/mL. Plasma concentrations of (A) IFNγ – IL-10, (B) IL-12 (p40) – KC and (C) LIF – VEGF. Data are shown as mean ± SEM. (D) Graphical representation of cytokine concentrations with a heat map. Median concentrations of CALR$^{del/+}$ Catchup mice were expressed as fold change after scaling CALR$^{+/+}$ Catchup mice to 100%. No significant alterations were observed between the two groups (unpaired two-sample t-test).

To evaluate cytokine mRNA expression in murine CALR-mutated neutrophils, mRNA from 1 x 10^6 granulocytes was extracted by using RLT buffer and expression levels of key inflammatory biomarkers, namely IL-1β, IL-4, IL-6, IL-10, TNF-α, IP-10 and CXCL12 were measured with qRT-PCR. After normalizing with the HPRT gene using the $2^{-\Delta\Delta ct}$ method, cytokine mRNA levels of neutrophils isolated from $CALR^{del/+}$ Catchup mice were comparable to $CALR^{+/+}$ mice (Figure 14). Experiments were performed by Harit Kunjan from the research group of Dr. Gopala Krishna Nishanth (Hannover Medical School).

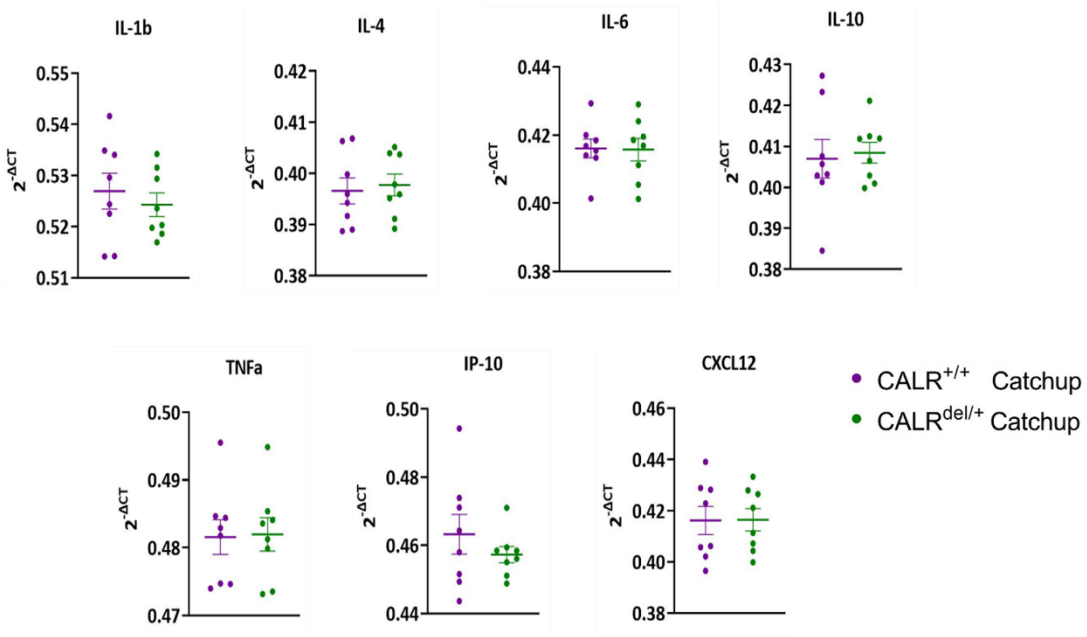

Figure 14. Neutrophils isolated from $CALR^{+/+}$ Catchup (n = 8) and $CALR^{del/+}$ Catchup mice (n = 8) demonstrate comparable mRNA expression of various cytokines. Cytokine concentrations were determined after mRNA isolation from 1 x 10^6 murine neutrophils with qRT-PCR and data were normalized with the $2^{-\Delta ct}$ method by using the HPRT gene as housekeeping gene. Data are shown as mean ± SEM.

3.8 Neutrophils isolated from $CALR^{del/+}$ Catchup mice express MPL and exhibit increased TPO-induced STAT5 phosphorylation

The major disease-driving mechanism of CALR mutations lies in constitutive activation of JAK2-STAT5 signaling downstream of MPL (Figure 1B).(112) Previously, Brizzi et al demonstrated that human neutrophils express MPL and that TPO stimulation induces STAT1 phosphorylation.(187) Further studies showed that TPO drives differentiation and expansion of immature but not mature granulocytes.(188) However, other authors failed to identify a functional response of polymorphonuclear cells upon incubation with TPO.(168)

To evaluate MPL expression on neutrophils isolated from Catchup mice, we sought to determine surface expression levels of MPL on tdTomato^{+} granulocytes with flow cytometry. A modest positive shift of MSFIs in most of the examined mice was compatible with presence of MPL yet in relatively low expression levels due to near-zero values in some cases (Figure 15A). Interestingly, there was a slightly increased (1.95-fold) MPL surface expression in granulocytes isolated from CALR$^{del/+}$ Catchup mice in comparison to their wild-type counterparts (Figure 15A).

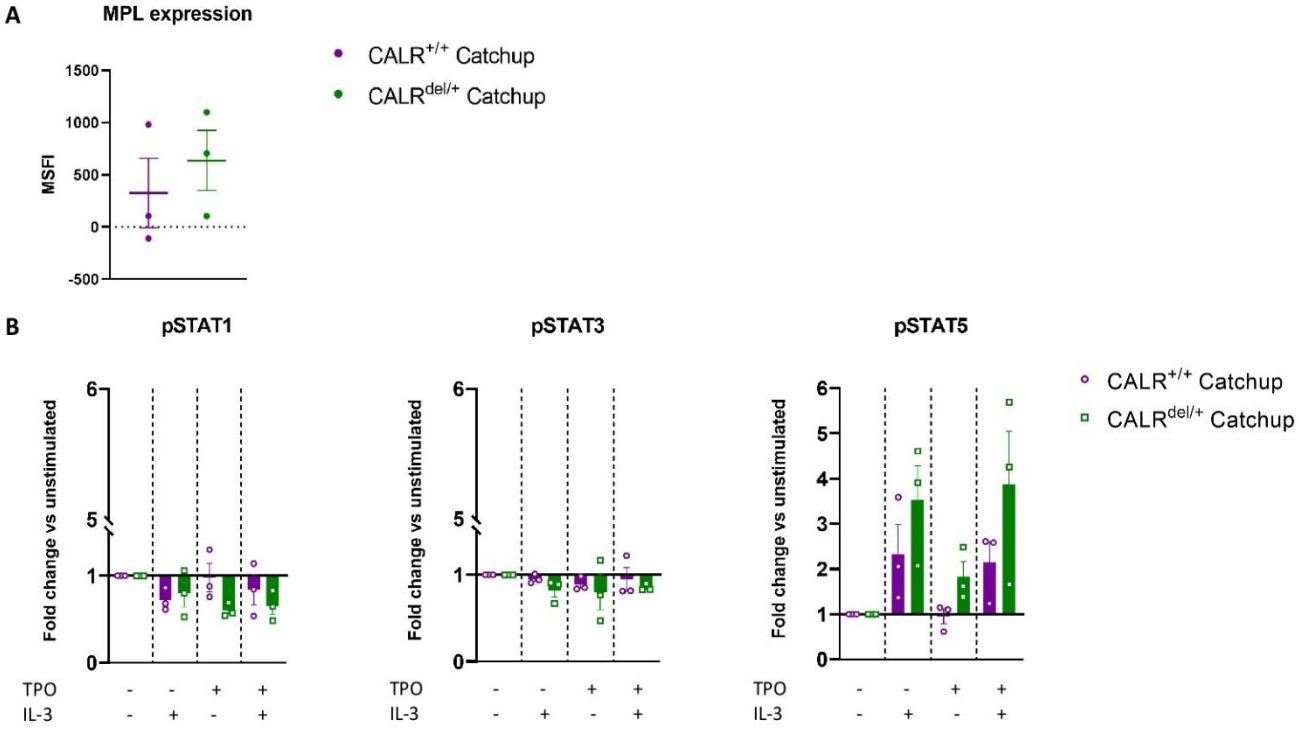

Figure 15: Granulocytes isolated from 23-week-old CALR$^{+/+}$ and CALR$^{del/+}$ Catchup mice express MPL and show TPO- and IL-3 induced alterations in STAT1, STAT3 and STAT5 phosphorylation. (A) MPL expression on granulocytes isolated from CALR$^{+/+}$ Catchup (n = 3) and CALR$^{del/+}$ Catchup (n = 3) mice. (B) pSTAT1, pSTAT3 and pSTAT5 expression in tdTomato^{+} neutrophils isolated from CALR$^{+/+}$ Catchup and CALR$^{del/+}$ Catchup mice in the unstimulated state and upon stimulation with TPO alone, IL-3 alone or both. Data are shown as mean ± SEM. Statistical testing was not conducted due to small sample size.

An assessment of MPL-associated JAK2-STAT5 activation upon TPO stimulation in tdTomato^{+} neutrophils showed higher STAT5 phosphorylation in CALR$^{del/+}$ Catchup mice (fold-increase 1.829 ± 0.3351; CALR$^{+/+}$: 0.9531 ± 0.1697), which is compatible with a pre-activated state of MPL in animals harboring CALRdel mutations (Figure 15B). On the contrary, pSTAT1 and pSTAT3 in neutrophils were found decreased upon TPO stimulation, while TPO led to 18.7-fold and 1.8-fold larger decreases in pSTAT1 and pSTAT3 in mutant mice as opposed to wild-type mice respectively (Figure 15B). TPO-induced alterations in STAT

phosphorylation balance could represent a manifestation of the so called “ying-yang” effect during competitive STAT complex activation, which was previously shown to regulate phenotypic features of T-cells.(189) Thus, MPL expression and JAK-STAT responsiveness of neutrophils upon TPO stimulation indicates that granulocytes are vulnerable to the MPL-related pathogenetic mechanism of CALR mutations.

Further evaluation of JAK-STAT activation in isolated granulocytes upon incubation with the pleiotropic hematopoietic cytokine IL-3 alone demonstrated noticeably more increased pSTAT5 expression in mutant mice ($CALR^{+/+}$: 2.336 ± 0.6560; $CALR^{del/+}$: 3.525 ± 0.7564) which might point towards a more generalized sensitivity of CALRdel granulocytes to STAT5 phosphorylation besides MPL-related JAK2-STAT5 activation (Figure 15B). Interestingly, IL-3 led to a 3.8-fold higher decrease in STAT3 phosphorylation in mutant animals as opposed to wild-type animals and modest decreases in pSTAT1 expression ($CALR^{+/+}$: 0.7194 ± 0.0747; $CALR^{del/+}$: 0.7947 ± 0.1537) (Figure 15B). Finally, a synergistic effect of simultaneous stimulation of TPO and IL-3 on STAT5 phosphorylation could not be demonstrated as shown by similar pSTAT5 expression levels to stimulation with IL-3 alone (for IL-3 alone, $CALR^{+/+}$: 2.336 ± 0.6560; $CALR^{del/+}$: 3.525 ± 0.7574; for IL-3 and TPO, $CALR^{+/+}$: 2.143 ± 0.4537; $CALR^{del/+}$: 3.871 ± 1.180) (Figure 15B).

3.9. Granulocytes isolated from $CALR^{del/+}$ Catchup mice do not demonstrate increased integrin-mediated adhesion

Measurement of β_1, β_2 integrin and PSGL-1 membrane levels on $tdTomato^+$ cells isolated from whole BM of $CALR^{+/+}$ Catchup and $CALR^{del/+}$ Catchup mice showed no significant differences between $CALR^{+/+}$ and $CALR^{del/+}$ $tdTomato^+$ granulocytes (Figure 16A). Contrary to the previously demonstrated significantly reduced β_1 integrin levels in VavCre $CALR^{del/+}$ mice (see Section 3.4), reduction of β_1 integrin levels did not reach statistical significance in $CALR^{del/+}$ Catchup mice (fold decrease 0.8497 ± 0.105; $CALR^{+/+}$: 1 ± 0.1141; P = 0.4881; n = 8) (Figure 16A).

In the static adhesion assay, FACS sorted $tdTomato^+$ cells isolated from $CALR^{+/+}$ Catchup and $CALR^{del/+}$ Catchup mice demonstrated similar percent adherence to VCAM-1, ICAM-1, P-selectin and E-selectin (Figure 16B). Binding of $CALR^{del/+}$ $tdTomato^+$ neutrophils to soluble VCAM-1 also remained unchanged (Figure 16C). Soluble binding to ICAM-1 was not evaluated, due to similar fluorescence intensities of cells incubated with ICAM-1 and the negative control samples in both WT and mutant animals. In line

with the previously demonstrated impaired binding of neutrophils isolated from VavCre CALR$^{del/+}$ mice to soluble E-selectin (see Section 3.4), there was a highly significant 0.77-fold reduction in the binding affinity of CALR$^{del/+}$ tdTomato^{+} neutrophils to soluble E-selectin (Figure 16C).

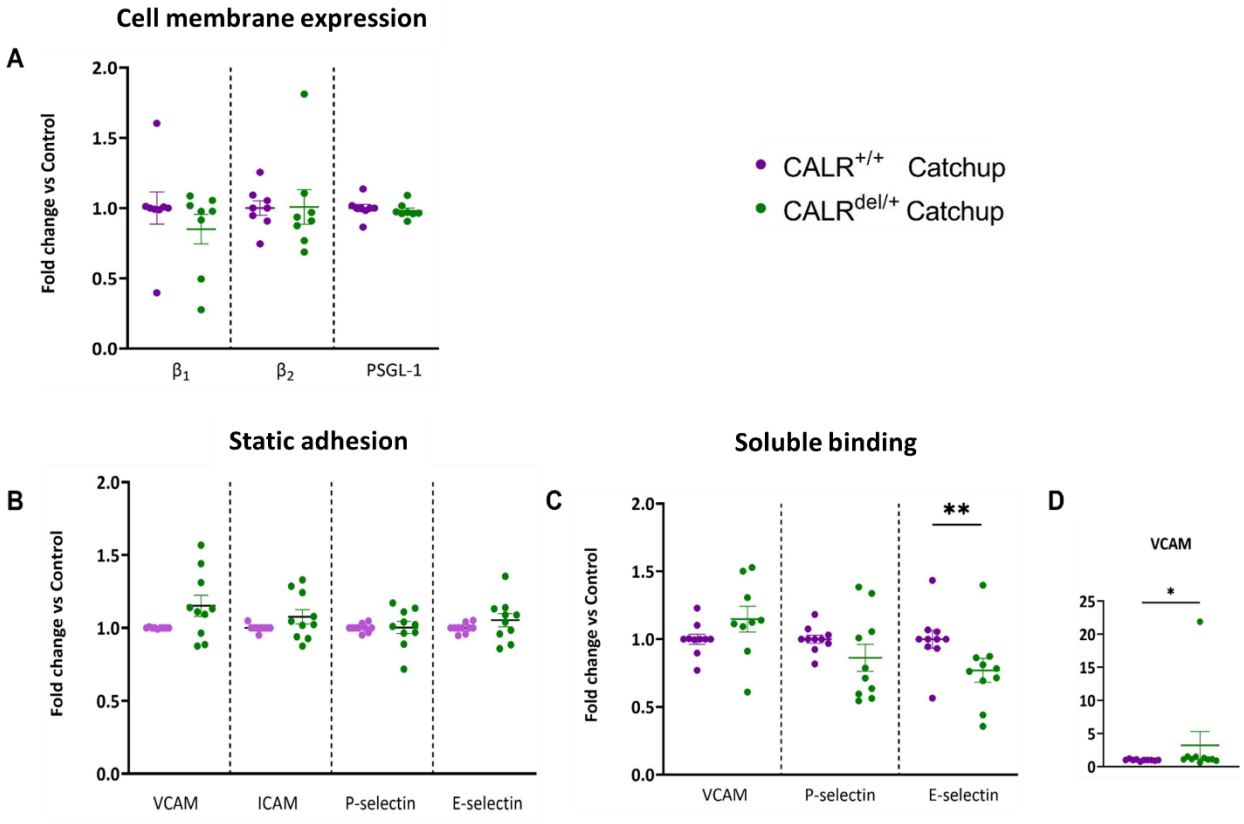

Figure 16. Neutrophils isolated from 12-16 week-old CALR$^{del/+}$ Catchup mice show unaltered integrin-mediated adhesion and decreased binding to E-selectin under flow conditions. (A) β_1 integrin (P = 0.4881), β_2 integrin (P = 0.4252) and PSGL-1 expression (P = 0.1852) on CALR$^{+/+}$ Catchup (n = 8) and CALR$^{del/+}$ Catchup (n = 8) granulocytes. (B) Static adhesion of CALR$^{+/+}$ Catchup (n = 9 for P-selectin, n = 10 for VCAM-1, ICAM-1 and E-selectin) and CALR$^{del/+}$ Catchup (n = 10) granulocytes on Fc-free VCAM-1 (P = 0.1463), ICAM-1 (P = 0.1681), P-selectin (P = 0.9443) and E-selectin (P = 0.2694). (C) Soluble binding of CALR$^{+/+}$ Catchup (n = 9 for VCAM-1, n = 10 for P-selectin and E-selectin) and CALR$^{del/+}$ Catchup (n = 9 for VCAM-1, n = 10 for P-selectin and E-selectin) granulocytes to VCAM-1 (P = 0.1493), P-selectin (P = 0.2052) and E-selectin (P = 0.0081). (D) Soluble binding to VCAM-1 is shown including an outlier corresponding to a 21.9-fold-change in a CALR$^{del/+}$ Catchup mouse. This extreme value was removed due to possible measurement error. Data are shown as mean ± SEM. *P ≤ 0.05, **P ≤ 0.01, ***P ≤ 0.001, ****P ≤ 0.0001

3.10. Migration of CALR$^{del/+}$ tdTomato^{+} granulocytes

Leukocyte migration is a multistep process which requires integrin activation, integrin-mediated adhesive leukocyte-endothelial interactions and cytoskeletal reorganization of migrating cells.(190) To

dissect the effect of CALR mutations in the migratory behavior of neutrophils on VCAM-1 and ICAM-1 expressing surfaces, tdTomato^{+} cells isolated from CALR$^{+/+}$ Catchup and CALR$^{del/+}$ Catchup mice were sorted using flow cytometry and were left to migrate into VCAM-1 and ICAM-1 pre-coated wells of an angiogenesis slide.

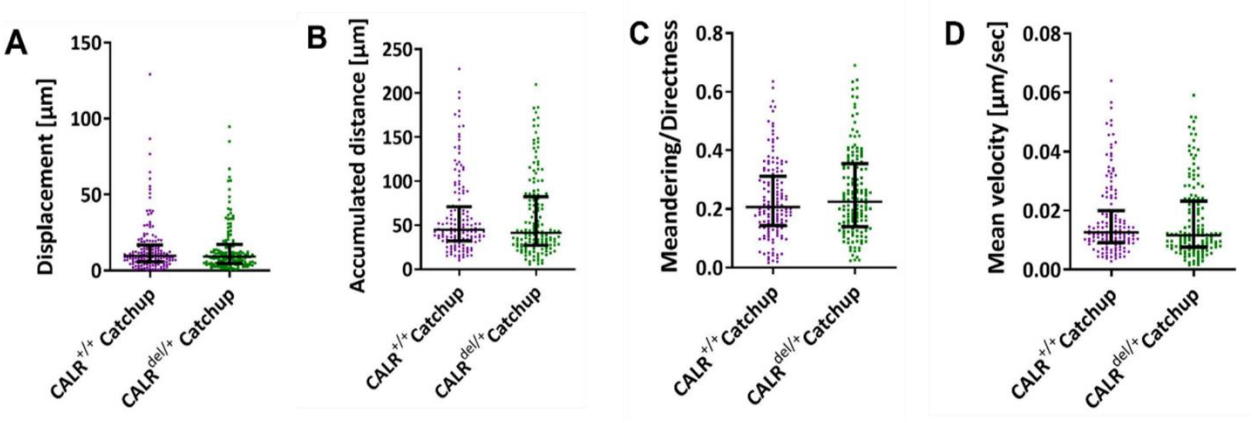

Figure 17. On a VCAM-1 and ICAM-1 pre-coated angiogenesis slide, the migratory movement properties of tdTomato^{+} cells isolated from 12-16 week-old CALR$^{del/+}$ Catchup mice were similar to WT tdTomato^{+} cells. Images of 50 cells per mouse were captured for one hour in three independent experiments (n = 3). (A) Displacement (in µm) of CALR$^{+/+}$ and CALR$^{del/+}$ tdTomato^{+} cells (P = 0.6167) (B) Accumulated distance (in µm) of CALR$^{+/+}$ and CALR$^{del/+}$ tdTomato^{+} cells (P = 0.2235) (C) Meandering/Directness of CALR$^{+/+}$ and CALR$^{del/+}$ tdTomato^{+} cells (P = 0.4134) (D) Mean velocity (in µm/sec) of CALR$^{+/+}$ and CALR$^{del/+}$ tdTomato^{+} cells (P = 0.2235).

Using *in vitro* time-lapse live cell imaging, we tracked isolated neutrophils (Suppl. Figure 9) and evaluated their migratory movement by means of displacement, accumulated distance, mean velocity and meandering/directness index (Suppl. Figure 2). There was no significant difference in the displacement from origin (14.51 µm) and the accumulated distance (58.92 µm) of neutrophils isolated from CALR$^{del/+}$ Catchup mice in comparison to the corresponding WT controls (15 and 60.8 µm, respectively) (Figure 17A, B). The meandering/directness index of CALRdel52 positive neutrophils was similar to their WT controls (CALR$^{del/+}$: 0.2525; CALR$^{+/+}$: 0.2337) (Figure 17C). Finally, the mean velocity was determined as 0.01657 µm/sec in the group of CALRdel52 positive neutrophils and did not differ significantly from the mean velocity of WT neutrophils (0.0171 µm/sec) (Figure 17D). In conclusion, *in vitro* tracking of migrating neutrophils harboring CALRdel52 mutations did not demonstrate alterations in VLA-4-VCAM-1 and LFA-1-ICAM-1 interactions.

4. Discussion

4.1. Hematopoietic expression of CALRdel52 affects primarily but not exclusively the megakaryocytic lineage

Marked thrombocytosis in VavCre CALR$^{del/+}$ mice is compatible with an ET phenotype, as already described.(170) A literature review of relevant studies of CALRdel52 mutations in mouse models shows that thrombocytosis with BM megakaryocytic hyperplasia in CALR-mutated mice is a universal finding (Suppl. Table 2).(170, 191-196) Hyperproliferation preferentially of the megakaryocytic lineage is in accordance with the central role of MPL in the oncogenic mechanism of CALR mutations. As mentioned previously, constitutive MPL activation is induced by CALR mutations through firm binding of mutant CALR to immature MPL forms followed by ER exit and cell membrane trafficking of the MPL-CALR complex (Figure 1B).(124) Indeed, homozygous animals showed extreme increases in PLT counts and pronounced BM and spleen megakaryopoiesis, along with BM reticulin fiber deposition and effacement of BM and splenic architecture reported by some authors, which points towards a MF phenotype.(170, 191, 193, 195) Apart from increases in MK number, CALR-mutant mice exhibited expansion of BM and spleen HSCs, including MkPs, and decreased hematopoiesis as determined by reductions of BM erythroblasts.(170, 191-196) Thus, the oncogenic potential of CALR mutations goes beyond the megakaryocytic lineage, which can be explained by the presence of the MPL receptor on the surface of early HSCs.(197)

An analysis of peripheral blood leukocyte subtypes of mice under study showed that VavCre CALR$^{del/+}$ animals developed lymphocytosis, neutropenia and monocytopenia. Overall, leukocytes were slightly but significantly increased in CALR-mutants (Figure 5C). In homozygous CALRdel52 and CALRins5 mice, Benlabiod et al showed increases in all leukocyte types, including T-, B- and NK cells, but leukocytosis in heterozygous animals was not further characterized.(193) It is worth mentioning that VavCre JAK2$^{VF/+}$ mice homed in our facility showed elevated neutrophil, lymphocyte and monocyte counts in accordance with JAK2-V617F-induced diffuse myeloproliferation (data not shown). Low neutrophil and high lymphocyte counts in VavCre CALR$^{del/+}$ mice point towards a reduced neutrophil-to-lymphocyte (NTL) ratio, an index that is widely used to reflect the balance between systemic inflammation and immunity.(198) In MF, elevation of NTL represents a dismal prognostic factor and is correlated particularly with presence of JAK2 mutations.(199) Different NTL ratios in VavCre CALR$^{del/+}$ and VavCre

JAK2$^{VF/+}$ mice might point towards a differential impact of CALRdel52 and JAK2-V617F in the inflammation-immunity balance. Elevations of lymphocyte counts in VavCre CALR$^{del/+}$ mice might be attributed to a reactive process possibly driven by immune changes, although a direct effect of CALRdel52 on lymphoid expansion is also possible. In MF, JAK2 and CALR mutations induce numerical changes in innate lymphoid cells, T-regulatory cells and dendritic cells in a pattern specific for each mutation.(96) In this regard, CALR mutations have been identified in circulating B- and T-lymphocytes of CALR-mutated MPN patients.(200)

4.2. Absence of increased integrin-mediated adhesion in neutrophils isolated from VavCre CALR$^{del/+}$ mice

During thrombus development, granulocytes adhere to the endothelial surface in a multistep process, which can be roughly divided into an initial deceleration phase mediated by weak selectin-mediated interactions between neutrophils and endothelial cells (leukocyte rolling) and a subsequent firm integrin-mediated adhesion to VCAM-1 and ICAM-1 (leukocyte arrest).(143) Integrin activation involves transition of integrins from the closed inactive to the open high affinity conformation and is triggered during the adhesion cascade by the initial binding of neutrophils to selectins as well as chemokine signals (inside-out signaling).(138) Firmly adherent neutrophils form DNA-based web-like structures, termed as NETs, which facilitate thrombus formation through engagement of PLTs, erythrocytes and coagulation factors (see Section 1.2.1).(144) The MPN-associated JAK-V617F mutation propagates thrombosis by activating the small GTPase Rap1, thus resulting in integrin activation and strengthening of neutrophil adhesion to VCAM-1 and ICAM-1 (see Section 1.2.2., Figure 2).(59) The impact of CALR mutations on integrin function in neutrophils however remains unknown.

The pivotal role of WT CALR in integrin-mediated adhesion has been demonstrated in multiple cell types. In Jurkat T-lymphoblastoid cells, CALR interacts with the α-subunit of $\alpha_2\beta_1$ integrin upon introduction of an activating signal (either phorbol-myristate-acetate or anti-integrin antibodies).(201) Moreover, downregulation of CALR expression with antisense oligonucleotides leads to inhibition of α_2 and β_1 integrin-mediated cell attachment of Jurkat cells on extracellular matrix.(202) The binding site of CALR to the α integrin subunit is a KXGFFKR motif in the amino acid sequence of the α chain, whose presence is important for adhesion of neutrophils and T-cells on VCAM-1 and ICAM-1.(203) In this respect, inhibition of CALR-KXGFFKR interaction has been shown to decrease leukocyte infiltration in inflammatory bowel disease.(204) Embryonic stem cells lacking CALR expression are unable to bind to

$\alpha_5\beta_1$ integrin antibodies as well as extracellular matrix substrates and CALR knock-out fibroblasts show impairments in integrin-mediated binding to vitronectin and fibronectin without alterations on $\alpha_5\beta_1$ and $\alpha_v\beta_3$ surface integrin levels.(205) Importantly, CALR participates in Ca^{2+}-influx regulation after integrin occupation.(205, 206) In B16 mouse melanoma cells, cytosolic CALR (endocalreticulin) associates with the KXGFFKR motif of the α integrin subunit and extracellular CALR (ectocalreticulin) interacts directly with both α_6 and β_1 subunits.(207) In human bladder cancer cells, CALR stabilizes fucosyltransferase mRNA, which in turn leads to activation of β_1 integrin via increased fucosylation.(208) Finally, CALR influences β_1 integrin function through regulation of glycosyltransferase expression and synthesis of N-glycan residues in trophoblasts.(209)

As an initial approach to examine the effect of CALRdel52 on neutrophil integrin-related adhesiveness, measurement of β integrin expression was conducted on the surface of neutrophils isolated from VavCre CALR mice. Interestingly, β_1 integrin levels were significantly reduced on VavCre $CALR^{del/+}$ neutrophils (Figure 6A). After taking into consideration the multiple mechanisms of CALR-mediated regulation of integrin function mentioned above, we propose the following pathways through which CALRdel52 might induce reductions of neutrophil β_1 integrin levels: (A) Defective protein quality control of β_1 integrin in the ER (B) destabilization of β_1 integrin mRNA (C) altered expression of enzymes that perform post-translational modifications on β_1 integrin (eg glycosyltransferase or fucosyltransferase) (D) dysregulated direct interaction of CALRdel52 with β_1 integrin.

Despite reduced surface β_1 integrin levels, an impaired adhesion of VavCre $CALR^{del/+}$ granulocytes on a VCAM-1 coated surface as well as binding to soluble VCAM-1 could not be demonstrated, which points towards an overall preserved functionality of the VLA-4 complex ($\alpha_4\beta_1$) in the presence of CALRdel52 (Figure 6B, C). Moreover, we did not find any altered surface β_2 integrin levels or dysregulated LFA-1-ICAM-1 interactions in neutrophils isolated from VavCre $CALR^{del/+}$ mice (Figures 6A-C). This represents a notable difference to the previously demonstrated upregulation of β_2 integrin and significantly stronger adhesion to VCAM-1 and ICAM-1 coated surfaces under static conditions in neutrophils isolated from VavCre $JAK2^{VF/+}$ mice.(59) Upregulated VLA-4-VCAM-1 and LFA-1-ICAM-1 interactions in JAK2-V617F mutant neutrophils has previously been shown to propagate thrombus formation,(59, 60) and it is well established that JAK2 mutations are associated with a significantly higher rate of thrombotic complications in MPN patients compared to CALR mutations.(126) In view of the findings of the present study, it is tempting to hypothesize that the more favorable thrombotic risk of CALR-mutant patients is attributed to the inability of CALRdel52 as opposed to JAK2-V617F to strengthen integrin-mediated

adhesion of neutrophils to the vascular endothelium. In this regard, a relatively minor impact of CALRdel mutations in neutrophil biology is supported by only weak activation of the G-CSF receptor, which plays a key role in neutrophil mobilization and adhesion,(210, 211) by CALR mutations (Figure 1B).(124) On the contrary, JAK2 mutations hyperactivate JAK-STAT signaling downstream all three primary myeloid growth factor receptors, including G-CSF receptor (see Section 1.1.5., Figure 1A).(124) A differential activation pattern of growth factor receptors between JAK2 and CALR mutations could therefore form the basis for the aforementioned different effect in neutrophil adhesion. In this respect, the small GTPase Rap1, which was found to mediate JAK2-V617F induced integrin activation,(60) has been shown to be activated by multiple signals involved in neutrophil stimulation, including activation of the GM-CSF receptor.(212)

4.3. Impaired adhesion of neutrophils isolated from VavCre CALR$^{del/+}$ mice to E-selectin

An interesting finding of our study was the significantly decreased static adhesion of neutrophils to E-selectin and reduced binding to soluble E-selectin in VavCre CALR$^{del/+}$ mice (Figures 6B, C). Although a large emphasis has been placed in the literature on the role of neutrophil integrin-mediated adhesion for the thrombotic risk of MPN patients, the importance of the initial selectin-mediated leukocyte rolling on the vascular endothelium during thrombogenesis should not be underestimated.(144) In an IVC ligation model, P- and E-selectin double knock-out mice displayed smaller thrombus size and reduced neutrophil and monocyte accumulation in the vein wall.(213) Moreover, E-selectin inhibition with the E-selectin antagonist GMI-1271 led to decreased thrombus development in rodent and primate venous thrombosis models.(214, 215) A first-in human phase I study of GMI-1271 administration in healthy volunteers and two DVT patients showed that E-selectin inhibition was effective in decreasing thrombus size and showed good tolerability without elevated risk of hemorrhage. Thus, inhibition of E-selectin represents a very promising treatment method for venous thrombosis and as opposed to traditional anticoagulation provides the additional advantage of non-significantly elevated bleeding risk.(216)

Given the non-significant alterations of surface PSGL-1 on neutrophils isolated from VavCre CALR$^{del/+}$ mice, the reductions in E-selectin binding cannot be attributed to quantitative alterations in PSGL-1 levels (Figures 6A). Due to its central role in quality control of many glycoproteins, it is tempting to hypothesize that PSGL-1 is also subjected to post-translational modifications by CALR. In this regard, the rare congenital disease leukocyte adhesion deficiency II serves as a paradigm for the impact of defective

post-translational modifications on PSGL-1 function.(217) Since both P- and E-selectin bind to PSGL-1, and given that neutrophil adhesiveness to P-selectin was left unchanged by CALRdel52 in the present study, amino acids of the PSGL-1 peptide that are particularly important for E-selectin binding might be affected by CALRdel52. Indeed, a different pattern of post-translational modifications is essential for P- and E-selectin binding to PSGL-1, for example sulfation of specific tyrosine residues is necessary for binding to P-selectin but does not influence E-selectin binding.(218) A possible implication of CALR in synthesis regulation of additional E-selectin receptors, namely CD44 or ESL-1, might also be responsible for the reduced affinity for E-selectin as opposed to the unaltered P-selectin adhesion by CALR-mutated neutrophils. For instance, CALR mutations could result in different glycosylation patterns of CD44, whose function has been shown to be dependent in a variety of post-translational modifications resulting in multiple glycoisoforms.(219) It should be noted, however, that there is currently to our knowledge no study demonstrating a role of CALR in selectin function or synthesis of selectin receptors.

Impaired adhesion of neutrophils to E-selectin in VavCre CALR$^{del/+}$ mice could provide insight into novel pathophysiological mechanisms of only moderately increased risk of thrombus formation in CALR-mutant patients. A few studies indicate that overactivation of the initial selectin-mediated leukocyte rolling on the endothelial surface contributes to thrombus development in MPN. In this regard, a role of E-selectin in the pathogenesis of MPN has been demonstrated by increased soluble E-selectin serum levels as a marker of endothelial activation in ET patients.(220) Moreover, thrombus formation in JAK2-mutant MPN is enhanced by increased P-selectin-mediated initial attachment of leukocytes on the endothelium due to upregulated P-selectin exposure by endothelial cells harboring JAK2-V617F mutations.(221, 222) In view of the above findings, it cannot be excluded that along with absence of elevated integrin-mediated adhesion (see Section 4.2), defective adhesion of CALR-mutated neutrophils to endothelial-expressed E-selectin during initial rolling of neutrophils on the vascular endothelium might also weaken an overall pronounced thrombotic risk in patients harboring the CALRdel52 mutation as compared with JAK2-V617F-mutated patients. However, after taking into consideration the importance of PSGL-1-selectin interactions in immune defence,(217) it should be noted that impaired adhesion to E-selectin during the initial leukocyte rolling should theoretically be associated with increased infection risk in CALR-mutant patients, which could not be demonstrated by a prospective study of infection frequency in MPN patients.(223)

4.4. Different phenotypes of JAK2$^{VF/+}$ Catchup and CALR$^{del/+}$ Catchup models indicate a differential role of CALRdel52 and JAK2-V617F in neutrophil biology

To elucidate the effect of CALRdel52 in neutrophils we generated a mouse model with neutrophil-restricted expression of CALRdel52 (CALR Catchup) and characterized resulting mice. CALR$^{del/+}$ Catchup mice were similar to their CALR$^{+/+}$ counterparts in terms of phenotype, spleen size (Figure 7), blood counts (Figure 8) as well as BM and spleen tissue architecture (Figure 9, 10) and numerical composition of BM and spleen hematopoietic progenitor cells (Figure 11-12). Thus, the present study does not support a contribution of neutrophils to chronic myeloproliferation of CALR-mutated MPNs. Neutrophil-specific expression of CALRdel52 was not associated with any changes in the megakaryocytic lineage as shown by non-significantly altered numbers of BM MKs (Figure 8G), MEPs (Figure 12) and MkPs (Suppl. Figure 4B, D) in CALR$^{del/+}$ Catchup mice. In the work of Haage and colleagues, JAK2$^{VF/+}$ Catchup mice developed thrombocytosis and increased BM megakaryopoiesis (See section 1.3.2.).(160) This difference is noteworthy, because it points towards a differential role of CALR-mutated and JAK2-mutated neutrophils in megakaryopoiesis and PLT production. According to Haage et al, neutrophil-mediated secondary signals, possibly aberrant cytokine production, might drive thrombocytosis development and megakaryocytic hyperplasia in JAK2$^{VF/+}$ Catchup animals, given the absence of JAK2-V617F in hematopoietic progenitor cells of JAK2$^{VF/+}$ Catchup mice. Plasma concentration of IL-1α, which is known to enhance PLT release through MK rupture,(162) was found elevated in JAK2$^{VF/+}$ Catchup mice and might therefore be responsible for thrombocytosis development. Interestingly, IL-1α was not significantly upregulated in CALR$^{del/+}$ Catchup mice, which is in line with the normal PLT counts and unaltered BM MK number in these animals (Figure 12). A role of IL-1α in the pathophysiology of MPN has been demonstrated by increased serum IL-1α levels in a small cohort of MPN patients (224) as well as mice harboring MPL-W515L mutations.(225)

In the JAK2 Catchup mouse model, Haage and colleagues observed increased concentrations of the p40 subunit of IL-12 in JAK2$^{VF/+}$ Catchup mice, which was found non-significantly altered in CALR$^{del/+}$ Catchup mice. Elevated IL-12 concentrations were found in PMF and were predictive of inferior survival and transfusion need.(85) Moreover, Jain and colleagues demonstrated that the common p40 subunit of IL-12/23 was raised in the serum of PV patients.(226) Recently, our group showed a 46.5-fold increase in IL-12(p40) after TNFR2 inhibition in VavCre JAK2$^{VF/+}$ mice.(227) Interestingly, IL-12 has been shown to be implicated in the differentiation of CD34+ Th1 cells.(228) Given the increment of serum IL-12(p40) in

JAK2$^{VF/+}$ Catchup but not in CALR$^{del/+}$ Catchup mice, it remains to be further elucidated whether there exists a different role of JAK2$^{VF/+}$ and CALR$^{del/+}$ neutrophils in guiding T-cell differentiation via IL-12 in MPNs.

Non-significant alterations in plasma levels of multiple inflammatory mediators in CALR$^{del/+}$ Catchup mice point towards a milder inflammatory phenotype than JAK2$^{VF/+}$ Catchup mice (Figure 13). According to a study involving 467 and 136 JAK2- and CALR-mutated MF patients respectively, constitutional symptoms were more frequent in JAK2-V617F positive patients, which is consistent with the hypothesis that JAK2-V617F confers larger elevations in cytokine levels than CALR mutations.(111) Nevertheless, other studies could not demonstrate significant differences regarding the frequency of constitutional symptom appearance between JAK2-mutated and CALR-mutated patients.(122, 229) Moreover, high-sensitivity CRP values have been proven to be independent of driver mutation.(77) Therefore, although JAK2 and CALR mutations might be associated with a different pattern of cytokine expression (See Section 1.1.3), there is currently no convincing data that JAK2-V617F leads to higher serum levels of inflammatory cytokines as compared to CALR mutations in MPN patients.

In a qRT-PCR assessment of neutrophil mRNA, expression of key pro-inflammatory cytokines in granulocytes isolated from CALR$^{del/+}$ Catchup mice were found unchanged (Figure 14). According to Haage et al, granulocytes isolated from JAK2$^{VF/+}$ Catchup mice exhibited a distinctive inflammatory mediator overexpression signature as assessed by elevated mRNA levels of the TNF-α, IP-10 and IL-1β. In the pathophysiology of MPN, TNF-α promotes clonal expansion of JAK2-V617F cells,(230) IL-1β is implicated in neuropathy of HSC niche (231) and IP-10 is predictive of inferior survival in PMF.(93) Significantly elevated expression of TNF-α, IP-10 and IL-1β in neutrophils isolated from JAK2$^{VF/+}$ Catchup but not CALR$^{del/+}$ Catchup mice indicates that JAK2-V617F but not CALRdel expression in neutrophils is linked to chronic non-resolving inflammation in MPN.

4.5. Absence of increased integrin-mediated adhesion in neutrophils isolated from CALR$^{del/+}$ Catchup mice

Granulocytes isolated from CALR$^{del/+}$ Catchup mice showed unaltered cell membrane expression of β_1 and β_2 integrins (Figure 16A) as well as non-significant changes in adhesion to VCAM-1 and ICAM-1 coated surfaces and binding to soluble VCAM-1 and ICAM-1 (Figure 16B, C). These findings point towards non-augmented adhesion in CALR-mutated neutrophils. Previously, Haage et al showed that

granulocytes isolated from JAK2$^{VF/+}$ Catchup mice adhered significantly stronger to VCAM-1 under flow and static conditions (see Section 1.3.2., data not yet published). This difference in adhesion state activation between granulocytes isolated from CALR$^{del/+}$ Catchup and JAK2$^{VF/+}$ Catchup mice is intriguing as it strongly indicates normal adhesion properties of VLA-4 and of LFA-1 in CALRdel mutated granulocytes as opposed to a pro-adhesive phenotype of JAK2-V617F mutated granulocytes and confirms previous observations regarding augmented neutrophil adhesion in VavCre JAK2$^{VF/+}$ contrary to VavCre CALR$^{del/+}$ mice (see Section 4.2.). Taken together, these data support absence of a pro-adhesive phenotype in CALRdel expressing granulocytes contrary to the previously demonstrated hyperactive adhesive state in JAK2-V617F mutated neutrophils which is compatible with the decreased thrombotic risk of CALR-mutated compared to JAK2-mutated MPN patients (see Section 4.2).

As opposed to neutrophils isolated from VavCre CALR$^{del/+}$ mice (see Section 4.2), cell membrane β_1 integrin levels were not found reduced in neutrophils isolated from CALR$^{del/+}$ Catchup mice, which indicates that neutrophil-specific expression of CALRdel52 is not sufficient to decrease surface β_1 integrin levels (Figure 16A). Therefore, reduced β_1 integrin particularly in VavCre CALR$^{del/+}$ mice might be related to paracrine signals from adjacent CALRdel52 mutant hematopoietic cells, expression of CALRdel52 in hematopoietic precursor cells, including GMPs, and the method of neutrophil purity determination, as in VavCre CALR mice an anti-Ly6g antibody was used to define neutrophils in flow cytometry, whereas in CALR Catchup mice the natural autofluorescence of tdTomato was employed for neutrophil gating. In this regard, β_1 integrin shedding in VavCre CALR$^{del/+}$ granulocytes after incubation with the anti-Ly6g antibody used to identify murine neutrophils during integrin measurement cannot be excluded; a similar mechanism has been described for L-selectin upon neutrophil activation.(232)

4.6. Impaired binding of neutrophils isolated from CALR$^{del/+}$ Catchup mice to soluble E-selectin but not immobilized E-selectin

In line with the decreased affinity to soluble E-selectin in granulocytes isolated from VavCre CALR$^{del/+}$ mice (see Section 4.3), we also observed reduced neutrophil binding to soluble E-selectin in CALR$^{del/+}$ Catchup mice (Figure 16C). Impaired binding affinity to soluble E-selectin in both VavCre CALR$^{del/+}$ and CALR$^{del/+}$ Catchup mice is intriguing and further supports an implication of CALR in E-selectin signaling. Similarly to VavCre CALR$^{del/+}$ mice, cell membrane expression of PSGL-1 remained unaltered on neutrophils isolated from CALR$^{del/+}$ Catchup mice (Figure 16A), which is as discussed in Section 4.3 compatible with a possible involvement of CALRdel in functional dysregulation of PSGL-1. Moreover, we

considered previously a possible role of dysregulated adhesion of CALRdel expressing neutrophils to E-selectin normally expressed on the injured vascular endothelium during leukocyte recruitment at the initial stages of thrombus development as contributing factor of only modest elevated thrombotic risk in CALR-mutated in contrast to JAK2-mutated patients (see Section 4.3). In line with this hypothesis, Haage and colleagues from our research group did not observe any increased binding of $JAK2^{VF/+}$ $tdTomato^{+}$ granulocytes to soluble E-selectin (data not shown), which indicates absence of dysregulated adhesion to E-selectin in JAK2-V617F expressing granulocytes. Taken together, diminished binding affinity of neutrophils to E-selectin in $CALR^{del/+}$ Catchup mice but not $JAK^{VF/+}$ Catchup mice further supports an implication of dysregulated E-selectin signaling specifically in the pathophysiology of CALR-mutant MPN.

However, contradictory to the decreased binding to soluble E-selectin, a reduced static adhesion of granulocytes isolated from $CALR^{del/+}$ Catchup mice to E-selectin coated surface could not be demonstrated. Interestingly, reduced binding affinity to immobilized as opposed to soluble E-selectin has been described in truncated E-selectin forms due to partial masking of cell binding epitopes during fixation of E-selectin molecules on the plate.(233) Inability of CALRdel expressing neutrophils to adhere to immobilized E-selectin in $CALR^{del/+}$ Catchup mice but not VavCre $CALR^{del/+}$ mice could be related to the inherent neutrophil-restricted expression of CALRdel in Catchup mice, which results in absence of CALRdel in immature myeloid cells. Because of the crucial role of CALR as an ER chaperone in maturation and folding of various glycoproteins,(100) post-translational modifications of E-selectin receptors, for example PSGL-1, could also be dysregulated in the presence of CALR mutations. PSGL-1 is expressed on myeloid cells and is subjected to a variety of post-translational modifications to acquire its functional form.(234) Specific cell types have been shown to perform distinct post-translational modifications of PSGL-1,(235) therefore distinct glycosylation patterns could take place by each myeloid progenitor subtype during myeloid differentiation. In line with this hypothesis, it has been shown that leukemic myeloid cells blocked at different stages of differentiation demonstrate a different patterns of cell surface glycoproteins.(236) From the above it could be speculated that VavCre $CALR^{del/+}$ mice possess a form of E-selectin receptor that differs from $CALR^{del/+}$ Catchup mice as a result of a different post-translational modification pattern during myeloid differentiation, thus reducing adhesion to immobilized E-selectin. An alternative explanation for the absence of impaired adhesion to E-selectin in $CALR^{del/+}$ Catchup but not VavCre $CALR^{del/+}$ mice could lie in the absence of indirect inflammatory signals of adjacent mutant blood cells due to expression of CALRdel solely by neutrophils in $CALR^{del/+}$ Catchup mice. In this regard, upregulation of PSGL-1 by inflammatory signals in leukocytes leading to stronger

PSGL-1-selectin interactions has been demonstrated in an uveitis model.(237) Finally, a negative impact of shear stress during FACS isolation of $CALR^{del/+}$ $tdTomato^{+}$ cells for the static adhesion assay on the ability of mutant neutrophils to adhere on immobilized E-selectin cannot be excluded, although it should be mentioned that solely autofluorescence-based flow cytometric isolation of neutrophils was not associated with changes in adhesive or migratory neutrophil properties.(238)

4.7. Neutrophil-specific expression of CALRdel52 does not alter migration of granulocytes in vitro

Cell migration involves a complex interplay between pro-inflammatory cytokines, integrin-regulated adhesion and cell locomotion through cytoskeletal changes (190) and represents an inherent part of thrombo-inflammation.(239) Integrins orchestrate the dynamic interplay between migrating cells and the extracellular environment through linking cytoskeletal actin with external adhesion sites and mediating intracellular signals.(240) We therefore sought to examine the integrin-mediated neutrophil migration of CALRdel expressing neutrophils *in vitro*. For this purpose, Catchup mice provide a useful model to explore the cell-intrinsic impact of MPN-associated mutations to the migratory behavior of neutrophils without the influence of indirect signals derived from other JAK2-V617F or CALRdel expressing myeloid cells. Haage et al demonstrated previously that neutrophils isolated from $JAK2^{VF/+}$ Catchup mice exhibited slower and shorter migratory movement on a pre-coated with VCAM-1 and ICAM-1 surface compared to their corresponding WT controls (see Section 1.3.2., data not yet published). These findings point towards a significant impact of the activated pro-adhesive state of JAK2-V617F expressing neutrophils to cell locomotion and corroborate previous studies associating stronger integrin-regulated adhesion with restricted cell movement.(241) In the present study, the integrin-regulated motility of neutrophils isolated from $CALR^{del/+}$ Catchup mice remained unaltered in comparison to their WT counterparts by means of accumulated distance, displacement, mean velocity and directness (Figure 17). The more restricted integrin-mediated locomotion demonstrated in neutrophils isolated from $JAK2^{VF/+}$ Catchup contrary to $CALR^{del/+}$ Catchup mice could translate into stronger VLA-4-VCAM-1 and LFA-1-ICAM-1 interactions during the initial stages of thrombus formation and thus easier aggregation of JAK2-V617F compared to CALRdel expressing neutrophils on the vascular endothelium.(143) Firmly adherent neutrophils on the endothelial surface increase thrombotic tendency by forming neutrophil-PLT aggregates,(31) inducing endothelial damage through ROS production,(54, 55) and releasing NETs.(62) In conclusion, unremarkable integrin-mediated migration of CALRdel

expressing neutrophils is compatible with the considerably decreased thrombotic risk of CALR- compared to JAK2-mutated MPN patients.

4.8. Limitations

An emphasis should be placed on the limitation of the soluble and static adhesion assays as well as the time-lapse migration assay employed in this study to reflect the sophisticated physiological process of neutrophil-endothelial interactions. As mentioned previously, integrin-mediated adhesion is highly regulated by the preceded weak selectin-mediated binding. Indeed, initial attachment of neutrophils to E-selectin on the endothelial surface is able to activate integrin-mediated adhesion by inducing a shift of the conformational status of ICAM-1 into the active state followed by firm adhesion and transmigration.(138, 139) A presumed CALR-mediated functional defect in selectin-mediated adhesion might also translate into decreased integrin-dependent binding *in vivo* as a result of alterations in the signal transduction cascade connecting selectin- and integrin-dependent adhesion. Assays that focus on examining neutrophil binding to solely a specific endothelial adhesion molecule lack the ability to reveal such an effect. Moreover, the time-lapse migration assay evaluates passive horizontal neutrophil movement on a surface pre-coated with VCAM-1 and ICAM-1 without examining the vertical transepithelial neutrophil motion. In addition, the influence of chemokine signals, which are well known to play a pivotal role in regulating integrin conformation during leukocyte rolling, firm adhesion and transmigration,(140) is not taken into account by the employed assays. Employment of assays that take into account the combined effect of integrin- and selectin-mediated adhesion as well as the role of inflammatory signals in the neutrophil transmigration process by future studies would be of outmost importance in unraveling the impact of CALR mutations on the complex neutrophil-endothelial cellular interactions.

Another limitation of the present study might be that inter-model differences of VavCre CALR and CALR Catchup animal models are discussed and attributed to a different effect of hematopoietic-specific as compared to neutrophil-specific expression of CALRdel52 without exclusion of a role of tdTomato or VavCre genes as modifier genes CALRdel52; presence of such an interaction might influence the outcomes of this study. However, in view of the multitude of studies applying these models which did not describe such an effect, this is not deemed as likely. Nevertheless, it is well known that the genetic background might unpredictably induce major modulations in the expression of several mutations.(242)

4.9. Implications for future research

Because of the role of CALR in many cellular functions, it is possible that the disease-driving mechanism of CALR-mutated MPN goes beyond a mere hyperactivation of the MPL receptor and involves a complex interplay between a variety and yet undiscovered pathophysiological mechanisms. In this regard, it is well known that CALR mutations are able to indirectly influence the function of many other proteins, as CALR regulates folding of many newly synthesized glycoproteins in collaboration with calnexin in the ER.(243) An impaired protein folding stress response fueled by ER calcium depletion by type 1 CALRdel52 mutations has recently been shown to promote cell survival through hyperactivation of the IRE1α/XBP1 pathway.(115) In addition, CALR is able to interact with some mRNAs and determine the fate of the resulting proteins.(244, 245) Thus, synthesis of a variety of proteins expressed in neutrophils might also be dysregulated by CALRdel52 either through defects in post-translational modifications or mRNA destabilization.

Although the primary focus of this doctoral thesis is neutrophil adhesion, the impact of CALRdel52 on additional aspects of neutrophil function remains to be elucidated by future studies. In neutrophil biology, CALR participates in several biological processes from the beginning to the end of a neutrophil's life cycle. In the ER of neutrophil precursor cells, CALR takes part in the biosynthesis of myeloperoxidase.(246) In this regard, Theocharides et al recently demonstrated myeloperoxidase deficiency in a MF patient harboring homozygous mutations of CALRdel52, which was induced by impaired folding of newly synthesized myeloperoxidase due to defective CALR-mediated ER quality control.(247) During the final stages of a neutrophil's life, CALR induces clearance of apoptotic neutrophils by tissue macrophages through activation of "eat me" signals on the cell surface.(248) It is therefore apparent that clarification of the multifaceted role of CALR in neutrophils function might pave the way towards unraveling the role of neutrophils in the pathophysiology CALR-mutated MPNs.

Recently, it was proposed that CALR type-1 mutations regulate surface expression levels of IL-6 receptor complexes by hindering membrane transport of IL-6R und gp130. CALRdel mutations conferred loss of the ability of normal CALR to bind to IL-6R and gp130, which led to increased levels of the aforementioned receptors on the cell surface, thus resulting in hyperproliferation due to hyperactivation of IL-6 signaling. For this reason, IL-6 inhibitors might be promising targets for CALR-specific therapies in MPNs. However, it is worth mentioning that animal data supporting this hypothesis are still lacking.(98)

In many human cancers, surface CALR is recognized by the immune system as a pro-phagocytic signal and is counterbalanced by the anti-phagocytic integrin-associated protein (CD47). In these cases, a positive correlation between surface CALR and CD47 has been well described.(249) Interestingly, in patients with MPN, there is a reverse relationship between CALR and CD47 surface levels. More specifically, CALR was found significantly downregulated and CD47 significantly upregulated, which points toward a role of CD47 in immune escape in the pathogenesis of MPNs. In view of this finding, it remains to be elucidated whether CD47 blockade might represent an effective treatment option in MPNs.(250)

5. Summary

To dissect the largely unknown impact of CALRdel on neutrophil pathophysiology, we generated a hematopoietic tissue-specific VavCre CALR-knock-in mouse model and a novel neutrophil-specific CALR Catchup mouse model. Comparisons were conducted between wild-type and mutant animals. An in-depth phenotypic characterization of CALR-mutants revealed that hematopoietic-specific expression of CALRdel induces an essential thrombocythemia phenotype, corroborating previous studies, whereas neutrophil-specific expression of CALRdel does not lead to development of a chronic myeloproliferative phenotype. Expression levels of the key adhesion receptors β_1 integrin, β_2 integrin and PSGL-1 were not elevated on the surface of neutrophils isolated from mutant mice. Static adhesion of isolated granulocytes on surfaces pre-coated with adhesion molecules normally expressed on the vascular endothelium, namely VCAM-1, ICAM-1, P-selectin and E-selectin as well as the binding affinity to soluble forms of the aforementioned ligands were determined and compared between wild-type and mutant mice. CALR mutant neutrophils did not exhibit increased integrin-mediated adhesion, which represents a noteworthy difference to the well-demonstrated elevated adhesion of JAK2 mutant neutrophils to VCAM-1 in previous studies. In accordance to these results, locomotion of CALR mutant tdTomato$^+$ neutrophils on a plate pre-coated with VCAM-1 and ICAM-1 remained unaffected. Interestingly, CALR mutations led to decreases in E-selectin dependent adhesion. In contrast to the elevated plasma concentrations of IL-1α and increased neutrophil mRNA expression levels of key inflammatory mediators in a previously described JAK2 Catchup mouse model, CALR Catchup mice did not exhibit overexpression of inflammatory mediators. Overall, our data point towards a differential impact of JAK2-V617F and CALRdel on neutrophil-associated adhesion and inflammation and pave the way towards elucidating the contribution of neutrophils for the mutation specific pathogenesis of MPNs.

German summary

Um den weitgehend unbekannten Einfluss von CALRdel auf die Pathophysiologie von Neutrophilen zu untersuchen, haben wir ein hämatopoetisch gewebespezifisches VavCre CALR-Knock-in-Mausmodell und ein neuartiges Neutrophilen-spezifisches CALR Catchup-Mausmodell eingesetzt. Es wurden Vergleiche zwischen Mäusen mit Wildtyp-Genotyp und Trägern der CALR-Mutation durchgeführt. Eine eingehende phänotypische Charakterisierung der CALR-Mutanten ergab, dass die Hämatopoese-spezifische Expression von CALRdel einen essentiellen Thrombozythämie-Phänotyp induziert, was frühere Studien bestätigt, während die Neutrophilen-spezifische Expression von CALRdel nicht zur Entwicklung eines MPN-ähnlichen Phänotyps führt. Das Expressionsniveau der Schlüssel-Adhäsionsrezeptoren β1-Integrin, β2-Integrin und PSGL-1 zeigten sich auf der Oberfläche von Neutrophilen, die aus Mutantenmäusen isoliert wurden, nicht erhöht. Die Adhäsion von isolierten Granulozyten zu Oberflächen, die mit Adhäsionsmolekülen vorbeschichtet worden sind, die normalerweise auf dem vaskulären Endothel exprimiert werden, nämlich VCAM-1, ICAM-1, P-Selektin und E-Selektin, sowie die Bindungsaffinität zu löslichen Formen der oben genannten Liganden wurden bestimmt und zwischen Wildtyp- und Mutantenmäusen verglichen. CALR-mutierte Neutrophile zeigten keine erhöhte Integrin-vermittelte Adhäsion, was einen bemerkenswerten Unterschied zu der gut nachgewiesenen erhöhten Bindung an VCAM- 1 von JAK2-mutierten Neutrophilen in früheren Studien darstellt. In Übereinstimmung mit diesen Ergebnissen blieb die Migration von CALR-mutierten tdTomato^{+} Neutrophilen auf einer mit VCAM-1 und ICAM-1 vorbeschichteten Platte unbeeinflusst. Interessanterweise führten CALR-Mutationen zu einer Verringerung der E-Selektin-abhängigen Adhäsion. Im Gegensatz zu den erhöhten Plasmakonzentrationen von IL-1α und den erhöhten mRNA-Expressionsspiegeln von Schlüsselentzündungsmediatoren in Neutrophilen im Rahmen des zuvor beschriebenen JAK2V617F-Catchup-Mausmodells zeigten CALRdel-Catchup-Mäuse keine Überexpression von Entzündungsmediatoren. Insgesamt deuten unsere Daten auf einen unterschiedlichen Einfluss von JAK2-V617F und CALRdel auf Neutrophilen-assoziierte Adhäsion und Entzündung hin und ebnen den Weg zur Abklärung des Beitrags der Neutrophilen in der mutationsspezifischen Pathogenese von MPNs.

References

1. Campbell PJ, Green AR. The myeloproliferative disorders. N Engl J Med. 2006;355(23):2452-66.
2. Barbui T, Thiele J, Gisslinger H, Kvasnicka HM, Vannucchi AM, Guglielmelli P, et al. The 2016 WHO classification and diagnostic criteria for myeloproliferative neoplasms: document summary and in-depth discussion. Blood Cancer J. 2018;8(2):15.
3. Skoda RC, Duek A, Grisouard J. Pathogenesis of myeloproliferative neoplasms. Exp Hematol. 2015;43(8):599-608.
4. Elliott MA, Tefferi A. Thrombosis and haemorrhage in polycythaemia vera and essential thrombocythaemia. Br J Haematol. 2005;128(3):275-90.
5. Tefferi A, Guglielmelli P, Larson DR, Finke C, Wassie EA, Pieri L, et al. Long-term survival and blast transformation in molecularly annotated essential thrombocythemia, polycythemia vera, and myelofibrosis. Blood. 2014;124(16):2507-13; quiz 615.
6. Barosi G, Mesa RA, Thiele J, Cervantes F, Campbell PJ, Verstovsek S, et al. Proposed criteria for the diagnosis of post-polycythemia vera and post-essential thrombocythemia myelofibrosis: a consensus statement from the International Working Group for Myelofibrosis Research and Treatment. Leukemia. 2008;22(2):437-8.
7. Titmarsh GJ, Duncombe AS, McMullin MF, O'Rorke M, Mesa R, De Vocht F, et al. How common are myeloproliferative neoplasms? A systematic review and meta-analysis. Am J Hematol. 2014;89(6):581-7.
8. Finazzi G, Barbui T. How I treat patients with polycythemia vera. Blood. 2007;109(12):5104-11.
9. Fowlkes S, Murray C, Fulford A, De Gelder T, Siddiq N. Myeloproliferative neoplasms (MPNs) - Part 1: An overview of the diagnosis and treatment of the "classical" MPNs. Can Oncol Nurs J. 2018;28(4):262-8.
10. Tefferi A, Rumi E, Finazzi G, Gisslinger H, Vannucchi AM, Rodeghiero F, et al. Survival and prognosis among 1545 patients with contemporary polycythemia vera: an international study. Leukemia. 2013;27(9):1874-81.
11. Wolanskyj AP, Schwager SM, McClure RF, Larson DR, Tefferi A. Essential thrombocythemia beyond the first decade: life expectancy, long-term complication rates, and prognostic factors. Mayo Clin Proc. 2006;81(2):159-66.
12. Geyer HL, Mesa RA. Therapy for myeloproliferative neoplasms: when, which agent, and how? Hematology Am Soc Hematol Educ Program. 2014;2014(1):277-86.
13. Cervantes F, Dupriez B, Pereira A, Passamonti F, Reilly JT, Morra E, et al. New prognostic scoring system for primary myelofibrosis based on a study of the International Working Group for Myelofibrosis Research and Treatment. Blood. 2009;113(13):2895-901.
14. Barbui T, Carobbio A, Cervantes F, Vannucchi AM, Guglielmelli P, Antonioli E, et al. Thrombosis in primary myelofibrosis: incidence and risk factors. Blood. 2010;115(4):778-82.
15. Levine RL, Gilliland DG. Myeloproliferative disorders. Blood. 2008;112(6):2190-8.
16. James C, Ugo V, Le Couedic JP, Staerk J, Delhommeau F, Lacout C, et al. A unique clonal JAK2 mutation leading to constitutive signalling causes polycythaemia vera. Nature. 2005;434(7037):1144-8.
17. Levine RL, Wadleigh M, Cools J, Ebert BL, Wernig G, Huntly BJ, et al. Activating mutation in the tyrosine kinase JAK2 in polycythemia vera, essential thrombocythemia, and myeloid metaplasia with myelofibrosis. Cancer Cell. 2005;7(4):387-97.
18. Kralovics R, Passamonti F, Buser AS, Teo SS, Tiedt R, Passweg JR, et al. A gain-of-function mutation of JAK2 in myeloproliferative disorders. N Engl J Med. 2005;352(17):1779-90.
19. Baxter EJ, Scott LM, Campbell PJ, East C, Fourouclas N, Swanton S, et al. Acquired mutation of the tyrosine kinase JAK2 in human myeloproliferative disorders. Lancet. 2005;365(9464):1054-61.

20. Jones AV, Kreil S, Zoi K, Waghorn K, Curtis C, Zhang L, et al. Widespread occurrence of the JAK2 V617F mutation in chronic myeloproliferative disorders. Blood. 2005;106(6):2162-8.
21. Scott LM, Tong W, Levine RL, Scott MA, Beer PA, Stratton MR, et al. JAK2 exon 12 mutations in polycythemia vera and idiopathic erythrocytosis. N Engl J Med. 2007;356(5):459-68.
22. Pikman Y, Lee BH, Mercher T, McDowell E, Ebert BL, Gozo M, et al. MPLW515L is a novel somatic activating mutation in myelofibrosis with myeloid metaplasia. PLoS Med. 2006;3(7):e270.
23. Nangalia J, Massie CE, Baxter EJ, Nice FL, Gundem G, Wedge DC, et al. Somatic CALR mutations in myeloproliferative neoplasms with nonmutated JAK2. N Engl J Med. 2013;369(25):2391-405.
24. Klampfl T, Gisslinger H, Harutyunyan AS, Nivarthi H, Rumi E, Milosevic JD, et al. Somatic mutations of calreticulin in myeloproliferative neoplasms. N Engl J Med. 2013;369(25):2379-90.
25. Spivak JL. Polycythemia vera: myths, mechanisms, and management. Blood. 2002;100(13):4272-90.
26. Cortelazzo S, Finazzi G, Ruggeri M, Vestri O, Galli M, Rodeghiero F, et al. Hydroxyurea for patients with essential thrombocythemia and a high risk of thrombosis. N Engl J Med. 1995;332(17):1132-6.
27. Birgegård G. The Use of Anagrelide in Myeloproliferative Neoplasms, with Focus on Essential Thrombocythemia. Curr Hematol Malig Rep. 2016 Oct;11(5):348-55.
28. Santos FP, Verstovsek S. JAK2 inhibitors for myelofibrosis: why are they effective in patients with and without JAK2V617F mutation? Anticancer Agents Med Chem. 2012;12(9):1098-109.
29. Rampal R, Al-Shahrour F, Abdel-Wahab O, Patel JP, Brunel JP, Mermel CH, et al. Integrated genomic analysis illustrates the central role of JAK-STAT pathway activation in myeloproliferative neoplasm pathogenesis. Blood. 2014;123(22):e123-33.
30. Rungjirajittranon T, Owattanapanich W, Ungprasert P, Siritanaratkul N, Ruchutrakool T. A systematic review and meta-analysis of the prevalence of thrombosis and bleeding at diagnosis of Philadelphia-negative myeloproliferative neoplasms. BMC Cancer. 2019;19(1):184.
31. Barbui T, Finazzi G, Falanga A. Myeloproliferative neoplasms and thrombosis. Blood. 2013;122(13):2176-84.
32. Falanga A, Marchetti M. Thrombosis in myeloproliferative neoplasms. Semin Thromb Hemost. 2014;40(3):348-58.
33. Barbui T, Carobbio A, Rambaldi A, Finazzi G. Perspectives on thrombosis in essential thrombocythemia and polycythemia vera: is leukocytosis a causative factor? Blood. 2009;114(4):759-63.
34. Carobbio A, Finazzi G, Guerini V, Spinelli O, Delaini F, Marchioli R, et al. Leukocytosis is a risk factor for thrombosis in essential thrombocythemia: interaction with treatment, standard risk factors, and Jak2 mutation status. Blood. 2007;109(6):2310-3.
35. Palandri F, Polverelli N, Catani L, Ottaviani E, Baccarani M, Vianelli N. Impact of leukocytosis on thrombotic risk and survival in 532 patients with essential thrombocythemia: a retrospective study. Ann Hematol. 2011;90(8):933-8.
36. Marchioli R, Finazzi G, Specchia G, Cacciola R, Cavazzina R, Cilloni D, et al. Cardiovascular events and intensity of treatment in polycythemia vera. N Engl J Med. 2013;368(1):22-33.
37. Gangat N, Strand J, Li CY, Wu W, Pardanani A, Tefferi A. Leucocytosis in polycythaemia vera predicts both inferior survival and leukaemic transformation. Br J Haematol. 2007;138(3):354-8.
38. Caramazza D, Caracciolo C, Barone R, Malato A, Saccullo G, Cigna V, et al. Correlation between leukocytosis and thrombosis in Philadelphia-negative chronic myeloproliferative neoplasms. Ann Hematol. 2009;88(10):967-71.
39. Di Nisio M, Barbui T, Di Gennaro L, Borrelli G, Finazzi G, Landolfi R, et al. The haematocrit and platelet target in polycythemia vera. Br J Haematol. 2007;136(2):249-59.
40. Adams BD, Baker R, Lopez JA, Spencer S. Myeloproliferative disorders and the hyperviscosity syndrome. Hematol Oncol Clin North Am. 2010;24(3):585-602.
41. Turitto VT, Weiss HJ. Red blood cells: their dual role in thrombus formation. Science. 1980;207(4430):541-3.

42. Carobbio A, Finazzi G, Antonioli E, Guglielmelli P, Vannucchi AM, Delaini F, et al. Thrombocytosis and leukocytosis interaction in vascular complications of essential thrombocythemia. Blood. 2008;112(8):3135-7.
43. Marin Oyarzun CP, Heller PG. Platelets as Mediators of Thromboinflammation in Chronic Myeloproliferative Neoplasms. Front Immunol. 2019;10:1373.
44. Arellano-Rodrigo E, Alvarez-Larran A, Reverter JC, Villamor N, Colomer D, Cervantes F. Increased platelet and leukocyte activation as contributing mechanisms for thrombosis in essential thrombocythemia and correlation with the JAK2 mutational status. Haematologica. 2006;91(2):169-75.
45. Maugeri N, Malato S, Femia EA, Pugliano M, Campana L, Lunghi F, et al. Clearance of circulating activated platelets in polycythemia vera and essential thrombocythemia. Blood. 2011;118(12):3359-66.
46. Rodriguez-Linares B, Watson SP. Thrombopoietin potentiates activation of human platelets in association with JAK2 and TYK2 phosphorylation. Biochem J. 1996;316 (Pt 1):93-8.
47. Laguna MS, Kornblihtt LI, Marta RF, Molinas FC. [Thromboxane B2 and platelet derived growth factor in essential thrombocythemia treated with anagrelide]. Medicina (B Aires). 2000;60(4):448-52.
48. Lev PR, Marta RF, Vassallu P, Molinas FC. Variation of PDGF, TGFbeta, and bFGF levels in essential thrombocythemia patients treated with anagrelide. Am J Hematol. 2002;70(2):85-91.
49. van Genderen PJ, Lucas IS, van Strik R, Vuzevski VD, Prins FJ, van Vliet HH, et al. Erythromelalgia in essential thrombocythemia is characterized by platelet activation and endothelial cell damage but not by thrombin generation. Thromb Haemost. 1996;76(3):333-8.
50. De Grandis M, Cambot M, Wautier MP, Cassinat B, Chomienne C, Colin Y, et al. JAK2V617F activates Lu/BCAM-mediated red cell adhesion in polycythemia vera through an EpoR-independent Rap1/Akt pathway. Blood. 2013;121(4):658-65.
51. Falanga A, Marchetti M, Evangelista V, Vignoli A, Licini M, Balicco M, et al. Polymorphonuclear leukocyte activation and hemostasis in patients with essential thrombocythemia and polycythemia vera. Blood. 2000;96(13):4261-6.
52. Marchetti M, Falanga A. Leukocytosis, JAK2V617F mutation, and hemostasis in myeloproliferative disorders. Pathophysiol Haemost Thromb. 2008;36(3-4):148-59.
53. Simon DI, Chen Z, Xu H, Li CQ, Dong J, McIntire LV, et al. Platelet glycoprotein ibalpha is a counterreceptor for the leukocyte integrin Mac-1 (CD11b/CD18). J Exp Med. 2000;192(2):193-204.
54. Afshar-Kharghan V, Thiagarajan P. Leukocyte adhesion and thrombosis. Curr Opin Hematol. 2006;13(1):34-9.
55. Friedenberg WR, Roberts RC, David DE. Relationship of thrombohemorrhagic complications to endothelial cell function in patients with chronic myeloproliferative disorders. Am J Hematol. 1992;40(4):283-9.
56. Falanga A, Marchetti M, Vignoli A, Balducci D, Russo L, Guerini V, et al. V617F JAK-2 mutation in patients with essential thrombocythemia: relation to platelet, granulocyte, and plasma hemostatic and inflammatory molecules. Exp Hematol. 2007;35(5):702-11.
57. Cella G, Marchetti M, Vianello F, Panova-Noeva M, Vignoli A, Russo L, et al. Nitric oxide derivatives and soluble plasma selectins in patients with myeloproliferative neoplasms. Thromb Haemost. 2010;104(1):151-6.
58. Wang GR, Zhu Y, Halushka PV, Lincoln TM, Mendelsohn ME. Mechanism of platelet inhibition by nitric oxide: in vivo phosphorylation of thromboxane receptor by cyclic GMP-dependent protein kinase. Proc Natl Acad Sci U S A. 1998;95(9):4888-93.
59. Edelmann B, Gupta N, Schnoeder TM, Oelschlegel AM, Shahzad K, Goldschmidt J, et al. JAK2-V617F promotes venous thrombosis through beta1/beta2 integrin activation. J Clin Invest. 2018;128(10):4359-71.

60. Gupta N, Edelmann B, Schnoeder TM, Saalfeld FC, Wolleschak D, Kliche S, et al. JAK2-V617F activates beta1-integrin-mediated adhesion of granulocytes to vascular cell adhesion molecule 1. Leukemia. 2017;31(5):1223-6.
61. Oh ST. Neutralize the neutrophils! Neutrophil beta1/beta2 integrin activation contributes to JAK2-V617F-driven thrombosis. J Clin Invest. 2018;128(10):4248-50.
62. Wolach O, Sellar RS, Martinod K, Cherpokova D, McConkey M, Chappell RJ, et al. Increased neutrophil extracellular trap formation promotes thrombosis in myeloproliferative neoplasms. Sci Transl Med. 2018;10(436).
63. Laridan E, Martinod K, De Meyer SF. Neutrophil Extracellular Traps in Arterial and Venous Thrombosis. Semin Thromb Hemost. 2019;45(1):86-93.
64. Fuchs TA, Abed U, Goosmann C, Hurwitz R, Schulze I, Wahn V, et al. Novel cell death program leads to neutrophil extracellular traps. J Cell Biol. 2007;176(2):231-41.
65. Wang Y, Li M, Stadler S, Correll S, Li P, Wang D, et al. Histone hypercitrullination mediates chromatin decondensation and neutrophil extracellular trap formation. J Cell Biol. 2009;184(2):205-13.
66. Papayannopoulos V, Metzler KD, Hakkim A, Zychlinsky A. Neutrophil elastase and myeloperoxidase regulate the formation of neutrophil extracellular traps. J Cell Biol. 2010;191(3):677-91.
67. Bottazzi B, Riboli E, Mantovani A. Aging, inflammation and cancer. Semin Immunol. 2018;40:74-82.
68. Landskron G, De la Fuente M, Thuwajit P, Thuwajit C, Hermoso MA. Chronic inflammation and cytokines in the tumor microenvironment. J Immunol Res. 2014;2014:149185.
69. Hua Y, Bergers G. Tumors vs. Chronic Wounds: An Immune Cell's Perspective. Front Immunol. 2019;10:2178.
70. Hasselbalch HC. Chronic inflammation as a promotor of mutagenesis in essential thrombocythemia, polycythemia vera and myelofibrosis. A human inflammation model for cancer development? Leuk Res. 2013;37(2):214-20.
71. Hasselbalch HC. The role of cytokines in the initiation and progression of myelofibrosis. Cytokine Growth Factor Rev. 2013;24(2):133-45.
72. Desterke C, Martinaud C, Ruzehaji N, Le Bousse-Kerdiles MC. Inflammation as a Keystone of Bone Marrow Stroma Alterations in Primary Myelofibrosis. Mediators Inflamm. 2015;2015:415024.
73. Mascarenhas J, Mughal TI, Verstovsek S. Biology and clinical management of myeloproliferative neoplasms and development of the JAK inhibitor ruxolitinib. Curr Med Chem. 2012;19(26):4399-413.
74. Sapre M, Tremblay D, Wilck E, James A, Leiter A, Coltoff A, et al. Metabolic Effects of JAK1/2 Inhibition in Patients with Myeloproliferative Neoplasms. Sci Rep. 2019;9(1):16609.
75. Barbui T, Carobbio A, Finazzi G, Guglielmelli P, Salmoiraghi S, Rosti V, et al. Elevated C-reactive protein is associated with shortened leukemia-free survival in patients with myelofibrosis. Leukemia. 2013;27(10):2084-6.
76. Barbui T, Carobbio A, Finazzi G, Vannucchi AM, Barosi G, Antonioli E, et al. Inflammation and thrombosis in essential thrombocythemia and polycythemia vera: different role of C-reactive protein and pentraxin 3. Haematologica. 2011;96(2):315-8.
77. Lussana F, Carobbio A, Salmoiraghi S, Guglielmelli P, Vannucchi AM, Bottazzi B, et al. Driver mutations (JAK2V617F, MPLW515L/K or CALR), pentraxin-3 and C-reactive protein in essential thrombocythemia and polycythemia vera. J Hematol Oncol. 2017;10(1):54.
78. Hsu HC, Lee YM, Tsai WH, Jiang ML, Ho CH, Ho CK, et al. Circulating levels of thrombopoietic and inflammatory cytokines in patients with acute myeloblastic leukemia and myelodysplastic syndrome. Oncology. 2002;63(1):64-9.
79. Bourantas KL, Hatzimichael EC, Makis AC, Chaidos A, Kapsali ED, Tsiara S, et al. Serum beta-2-microglobulin, TNF-alpha and interleukins in myeloproliferative disorders. Eur J Haematol. 1999;63(1):19-25.

80. Panteli KE, Hatzimichael EC, Bouranta PK, Katsaraki A, Seferiadis K, Stebbing J, et al. Serum interleukin (IL)-1, IL-2, sIL-2Ra, IL-6 and thrombopoietin levels in patients with chronic myeloproliferative diseases. Br J Haematol. 2005;130(5):709-15.
81. Boissinot M, Cleyrat C, Vilaine M, Jacques Y, Corre I, Hermouet S. Anti-inflammatory cytokines hepatocyte growth factor and interleukin-11 are over-expressed in Polycythemia vera and contribute to the growth of clonal erythroblasts independently of JAK2V617F. Oncogene. 2011;30(8):990-1001.
82. Hermouet S, Godard A, Pineau D, Corre I, Raher S, Lippert E, et al. Abnormal production of interleukin (IL)-11 and IL-8 in polycythaemia vera. Cytokine. 2002;20(4):178-83.
83. Gangemi S, Allegra A, Pace E, Alonci A, Ferraro M, Petrungaro A, et al. Evaluation of interleukin-23 plasma levels in patients with polycythemia vera and essential thrombocythemia. Cell Immunol. 2012;278(1-2):91-4.
84. Ho CL, Lasho TL, Butterfield JH, Tefferi A. Global cytokine analysis in myeloproliferative disorders. Leuk Res. 2007;31(10):1389-92.
85. Tefferi A, Vaidya R, Caramazza D, Finke C, Lasho T, Pardanani A. Circulating interleukin (IL)-8, IL-2R, IL-12, and IL-15 levels are independently prognostic in primary myelofibrosis: a comprehensive cytokine profiling study. J Clin Oncol. 2011;29(10):1356-63.
86. Vaidya R, Gangat N, Jimma T, Finke CM, Lasho TL, Pardanani A, et al. Plasma cytokines in polycythemia vera: phenotypic correlates, prognostic relevance, and comparison with myelofibrosis. Am J Hematol. 2012;87(11):1003-5.
87. Cacemiro MDC, Cominal JG, Tognon R, Nunes NS, Simoes BP, Figueiredo-Pontes LL, et al. Philadelphia-negative myeloproliferative neoplasms as disorders marked by cytokine modulation. Hematol Transfus Cell Ther. 2018;40(2):120-31.
88. Mambet C, Necula L, Mihai S, Matei L, Bleotu C, Chivu-Economescu M, et al. Increased Dkk-1 plasma levels may discriminate disease subtypes in myeloproliferative neoplasms. J Cell Mol Med. 2018.
89. Barosi G, Campanelli R, Catarsi P, De Amici M, Abba C, Viarengo G, et al. Plasma sIL-2Ralpha levels are associated with disease progression in myelofibrosis with JAK2(V617F) but not CALR mutation. Leuk Res. 2020;90:106319.
90. Obro NF, Grinfeld J, Belmonte M, Irvine M, Shepherd MS, Rao TN, et al. Longitudinal Cytokine Profiling Identifies GRO-alpha and EGF as Potential Biomarkers of Disease Progression in Essential Thrombocythemia. Hemasphere. 2020;4(3):e371.
91. Skov V, Larsen TS, Thomassen M, Riley CH, Jensen MK, Bjerrum OW, et al. Molecular profiling of peripheral blood cells from patients with polycythemia vera and related neoplasms: identification of deregulated genes of significance for inflammation and immune surveillance. Leuk Res. 2012;36(11):1387-92.
92. Wong KL, Tai JJ, Wong WC, Han H, Sem X, Yeap WH, et al. Gene expression profiling reveals the defining features of the classical, intermediate, and nonclassical human monocyte subsets. Blood. 2011;118(5):e16-31.
93. Masselli E, Pozzi G, Gobbi G, Merighi S, Gessi S, Vitale M, et al. Cytokine Profiling in Myeloproliferative Neoplasms: Overview on Phenotype Correlation, Outcome Prediction, and Role of Genetic Variants. Cells. 2020;9(9).
94. Pourcelot E, Trocme C, Mondet J, Bailly S, Toussaint B, Mossuz P. Cytokine profiles in polycythemia vera and essential thrombocythemia patients: clinical implications. Exp Hematol. 2014;42(5):360-8.
95. Verstovsek S, Kantarjian H, Mesa RA, Pardanani AD, Cortes-Franco J, Thomas DA, et al. Safety and efficacy of INCB018424, a JAK1 and JAK2 inhibitor, in myelofibrosis. N Engl J Med. 2010;363(12):1117-27.
96. Romano M, Sollazzo D, Trabanelli S, Barone M, Polverelli N, Perricone M, et al. Mutations in JAK2 and Calreticulin genes are associated with specific alterations of the immune system in myelofibrosis. Oncoimmunology. 2017;6(10):e1345402.

97. Sollazzo D, Forte D, Polverelli N, Perricone M, Romano M, Luatti S, et al. Circulating Calreticulin Is Increased in Myelofibrosis: Correlation with Interleukin-6 Plasma Levels, Bone Marrow Fibrosis, and Splenomegaly. Mediators Inflamm. 2016;2016:5860657.
98. Balliu M, Calabresi L, Bartalucci N, Romagnoli S, Maggi L, Manfredini R, et al. Activated IL-6 signaling contributes to the pathogenesis of, and is a novel therapeutic target for, CALR-mutated MPNs. Blood Adv. 2021;5(8):2184-95.
99. Hebert DN, Molinari M. In and out of the ER: protein folding, quality control, degradation, and related human diseases. Physiol Rev. 2007;87(4):1377-408.
100. Michalak M, Groenendyk J, Szabo E, Gold LI, Opas M. Calreticulin, a multi-process calcium-buffering chaperone of the endoplasmic reticulum. Biochem J. 2009;417(3):651-66.
101. Leach MR, Cohen-Doyle MF, Thomas DY, Williams DB. Localization of the lectin, ERp57 binding, and polypeptide binding sites of calnexin and calreticulin. J Biol Chem. 2002;277(33):29686-97.
102. Nakamura K, Zuppini A, Arnaudeau S, Lynch J, Ahsan I, Krause R, et al. Functional specialization of calreticulin domains. J Cell Biol. 2001;154(5):961-72.
103. Mesaeli N, Nakamura K, Zvaritch E, Dickie P, Dziak E, Krause KH, et al. Calreticulin is essential for cardiac development. J Cell Biol. 1999;144(5):857-68.
104. Rauch F, Prud'homme J, Arabian A, Dedhar S, St-Arnaud R. Heart, brain, and body wall defects in mice lacking calreticulin. Exp Cell Res. 2000;256(1):105-11.
105. How J, Hobbs GS, Mullally A. Mutant calreticulin in myeloproliferative neoplasms. Blood. 2019;134(25):2242-8.
106. Stengel A, Jeromin S, Haferlach T, Meggendorfer M, Kern W, Haferlach C. Detection and characterization of homozygosity of mutated CALR by copy neutral loss of heterozygosity in myeloproliferative neoplasms among cases with high CALR mutation loads or with progressive disease. Haematologica. 2019;104(5):e187-e90.
107. Pietra D, Rumi E, Ferretti VV, Di Buduo CA, Milanesi C, Cavalloni C, et al. Differential clinical effects of different mutation subtypes in CALR-mutant myeloproliferative neoplasms. Leukemia. 2016;30(2):431-8.
108. Cabagnols X, Defour JP, Ugo V, Ianotto JC, Mossuz P, Mondet J, et al. Differential association of calreticulin type 1 and type 2 mutations with myelofibrosis and essential thrombocytemia: relevance for disease evolution. Leukemia. 2015;29(1):249-52.
109. Tefferi A, Lasho TL, Finke C, Belachew AA, Wassie EA, Ketterling RP, et al. Type 1 vs type 2 calreticulin mutations in primary myelofibrosis: differences in phenotype and prognostic impact. Leukemia. 2014;28(7):1568-70.
110. Tefferi A, Lasho TL, Tischer A, Wassie EA, Finke CM, Belachew AA, et al. The prognostic advantage of calreticulin mutations in myelofibrosis might be confined to type 1 or type 1-like CALR variants. Blood. 2014;124(15):2465-6.
111. Tefferi A, Nicolosi M, Mudireddy M, Szuber N, Finke CM, Lasho TL, et al. Driver mutations and prognosis in primary myelofibrosis: Mayo-Careggi MPN alliance study of 1,095 patients. Am J Hematol. 2018;93(3):348-55.
112. Pecquet C, Chachoua I, Roy A, Balligand T, Vertenoeil G, Leroy E, et al. Calreticulin mutants as oncogenic rogue chaperones for TpoR and traffic-defective pathogenic TpoR mutants. Blood. 2019;133(25):2669-81.
113. Garbati MR, Welgan CA, Landefeld SH, Newell LF, Agarwal A, Dunlap JB, et al. Mutant calreticulin-expressing cells induce monocyte hyperreactivity through a paracrine mechanism. Am J Hematol. 2016;91(2):211-9.
114. Salati S, Genovese E, Carretta C, Zini R, Bartalucci N, Prudente Z, Pennucci V, Ruberti S, Rossi C, Rontauroli S, Enzo E, Calabresi L, Balliu M, Mannarelli C, Bianchi E, Guglielmelli P, Tagliafico E, Vannucchi

AM, Manfredini R. Calreticulin Ins5 and Del52 mutations impair unfolded protein and oxidative stress responses in K562 cells expressing CALR mutants. Sci Rep. 2019 Jul 22;9(1):10558.
115. Ibarra J, Elbanna YA, Kurylowicz K, Ciboddo M, Greenbaum HS, Arellano NS, Rodriguez D, Evers M, Bock-Hughes A, Liu C, Smith Q, Lutze J, Baumeister J, Kalmer M, Olschok K, Nicholson B, Silva D, Maxwell L, Dowgielewicz J, Rumi E, Pietra D, Casetti IC, Catricala S, Koschmieder S, Gurbuxani S, Schneider RK, Oakes SA, Elf SE. Type I but Not Type II Calreticulin Mutations Activate the IRE1α/XBP1 Pathway of the Unfolded Protein Response to Drive Myeloproliferative Neoplasms. Blood Cancer Discov. 2022 Jul 6;3(4):298-315.
116. Lau WW, Hannah R, Green AR, Göttgens B. The JAK-STAT signaling pathway is differentially activated in CALR-positive compared with JAK2V617F-positive ET patients. Blood. 2015 Mar 5;125(10):1679-81.
117. Di Buduo CA, Abbonante V, Marty C, Moccia F, Rumi E, Pietra D, Soprano PM, Lim D, Cattaneo D, Iurlo A, Gianelli U, Barosi G, Rosti V, Plo I, Cazzola M, Balduini A. Defective interaction of mutant calreticulin and SOCE in megakaryocytes from patients with myeloproliferative neoplasms. Blood. 2020 Jan 9;135(2):133-144.
118. Pronier E, Cifani P, Merlinsky TR, Berman KB, Somasundara AVH, Rampal RK, LaCava J, Wei KE, Pastore F, Maag JL, Park J, Koche R, Kentsis A, Levine RL. Targeting the CALR interactome in myeloproliferative neoplasms. JCI Insight. 2018 Nov 15;3(22):e122703.
119. Rumi E, Pietra D, Ferretti V, Klampfl T, Harutyunyan AS, Milosevic JD, et al. JAK2 or CALR mutation status defines subtypes of essential thrombocythemia with substantially different clinical course and outcomes. Blood. 2014;123(10):1544-51.
120. Rumi E, Pietra D, Pascutto C, Guglielmelli P, Martinez-Trillos A, Casetti I, et al. Clinical effect of driver mutations of JAK2, CALR, or MPL in primary myelofibrosis. Blood. 2014;124(7):1062-9.
121. Tefferi A, Lasho TL, Finke CM, Knudson RA, Ketterling R, Hanson CH, et al. CALR vs JAK2 vs MPL-mutated or triple-negative myelofibrosis: clinical, cytogenetic and molecular comparisons. Leukemia. 2014;28(7):1472-7.
122. Rotunno G, Mannarelli C, Guglielmelli P, Pacilli A, Pancrazzi A, Pieri L, et al. Impact of calreticulin mutations on clinical and hematological phenotype and outcome in essential thrombocythemia. Blood. 2014;123(10):1552-5.
123. Pei YQ, Wu Y, Wang F, Cui W. Prognostic value of CALR vs. JAK2V617F mutations on splenomegaly, leukemic transformation, thrombosis, and overall survival in patients with primary fibrosis: a meta-analysis. Ann Hematol. 2016;95(9):1391-8.
124. Vainchenker W, Kralovics R. Genetic basis and molecular pathophysiology of classical myeloproliferative neoplasms. Blood. 2017;129(6):667-79.
125. Guglielmelli P, Rotunno G, Bogani C, Mannarelli C, Giunti L, Provenzano A, et al. Ruxolitinib is an effective treatment for CALR-positive patients with myelofibrosis. Br J Haematol. 2016;173(6):938-40.
126. Saki N, Shirzad R, Rahim F, Saki Malehi A. Estimation of diagnosis and prognosis in ET by assessment of CALR and JAK2(V617F) mutations and laboratory findings: a meta-analysis. Clin Transl Oncol. 2017;19(7):874-83.
127. Andrikovics H, Krahling T, Balassa K, Halm G, Bors A, Koszarska M, et al. Distinct clinical characteristics of myeloproliferative neoplasms with calreticulin mutations. Haematologica. 2014;99(7):1184-90.
128. Elala YC, Lasho TL, Gangat N, Finke C, Barraco D, Haider M, et al. Calreticulin variant stratified driver mutational status and prognosis in essential thrombocythemia. Am J Hematol. 2016;91(5):503-6.
129. Binder FP, Ernst B. E- and P-selectin: differences, similarities and implications for the design of P-selectin antagonists. Chimia (Aarau). 2011;65(4):210-3.
130. McEver RP, Zhu C. Rolling cell adhesion. Annu Rev Cell Dev Biol. 2010;26:363-96.

131. Zarbock A, Ley K, McEver RP, Hidalgo A. Leukocyte ligands for endothelial selectins: specialized glycoconjugates that mediate rolling and signaling under flow. Blood. 2011;118(26):6743-51.
132. Bonfanti R, Furie BC, Furie B, Wagner DD. PADGEM (GMP140) is a component of Weibel-Palade bodies of human endothelial cells. Blood. 1989;73(5):1109-12.
133. Stenberg PE, McEver RP, Shuman MA, Jacques YV, Bainton DF. A platelet alpha-granule membrane protein (GMP-140) is expressed on the plasma membrane after activation. J Cell Biol. 1985;101(3):880-6.
134. Bevilacqua MP, Pober JS, Mendrick DL, Cotran RS, Gimbrone MA, Jr. Identification of an inducible endothelial-leukocyte adhesion molecule. Proc Natl Acad Sci U S A. 1987;84(24):9238-42.
135. McEver RP. Selectins: initiators of leucocyte adhesion and signalling at the vascular wall. Cardiovasc Res. 2015;107(3):331-9.
136. Kinashi T. Intracellular signalling controlling integrin activation in lymphocytes. Nat Rev Immunol. 2005;5(7):546-59.
137. Springer TA, Dustin ML. Integrin inside-out signaling and the immunological synapse. Curr Opin Cell Biol. 2012;24(1):107-15.
138. Kim C, Ye F, Ginsberg MH. Regulation of integrin activation. Annu Rev Cell Dev Biol. 2011;27:321-45.
139. Kuwano Y, Spelten O, Zhang H, Ley K, Zarbock A. Rolling on E- or P-selectin induces the extended but not high-affinity conformation of LFA-1 in neutrophils. Blood. 2010;116(4):617-24.
140. Jung U, Norman KE, Scharffetter-Kochanek K, Beaudet AL, Ley K. Transit time of leukocytes rolling through venules controls cytokine-induced inflammatory cell recruitment in vivo. J Clin Invest. 1998;102(8):1526-33.
141. Abram CL, Lowell CA. The ins and outs of leukocyte integrin signaling. Annu Rev Immunol. 2009;27:339-62.
142. Cook-Mills JM, Marchese ME, Abdala-Valencia H. Vascular cell adhesion molecule-1 expression and signaling during disease: regulation by reactive oxygen species and antioxidants. Antioxid Redox Signal. 2011 Sep 15;15(6):1607-38.
143. Swystun LL, Liaw PC. The role of leukocytes in thrombosis. Blood. 2016;128(6):753-62.
144. von Bruhl ML, Stark K, Steinhart A, Chandraratne S, Konrad I, Lorenz M, et al. Monocytes, neutrophils, and platelets cooperate to initiate and propagate venous thrombosis in mice in vivo. J Exp Med. 2012;209(4):819-35.
145. Ammollo CT, Semeraro F, Xu J, Esmon NL, Esmon CT. Extracellular histones increase plasma thrombin generation by impairing thrombomodulin-dependent protein C activation. J Thromb Haemost. 2011;9(9):1795-803.
146. Fuchs TA, Brill A, Duerschmied D, Schatzberg D, Monestier M, Myers DD, Jr., et al. Extracellular DNA traps promote thrombosis. Proc Natl Acad Sci U S A. 2010;107(36):15880-5.
147. Medeiros RB, Dickey DM, Chung H, Quale AC, Nagarajan LR, Billadeau DD, et al. Protein kinase D1 and the beta 1 integrin cytoplasmic domain control beta 1 integrin function via regulation of Rap1 activation. Immunity. 2005;23(2):213-26.
148. Arai A, Nosaka Y, Kanda E, Yamamoto K, Miyasaka N, Miura O. Rap1 is activated by erythropoietin or interleukin-3 and is involved in regulation of beta1 integrin-mediated hematopoietic cell adhesion. J Biol Chem. 2001;276(13):10453-62.
149. Heng TS, Painter MW, Immunological Genome Project C. The Immunological Genome Project: networks of gene expression in immune cells. Nat Immunol. 2008;9(10):1091-4.
150. Lee PY, Wang JX, Parisini E, Dascher CC, Nigrovic PA. Ly6 family proteins in neutrophil biology. J Leukoc Biol. 2013;94(4):585-94.
151. Rock KL, Reiser H, Bamezai A, McGrew J, Benacerraf B. The LY-6 locus: a multigene family encoding phosphatidylinositol-anchored membrane proteins concerned with T-cell activation. Immunol Rev. 1989;111:195-224.

152. Hestdal K, Ruscetti FW, Ihle JN, Jacobsen SE, Dubois CM, Kopp WC, et al. Characterization and regulation of RB6-8C5 antigen expression on murine bone marrow cells. J Immunol. 1991;147(1):22-8.
153. Hasenberg A, Hasenberg M, Mann L, Neumann F, Borkenstein L, Stecher M, et al. Catchup: a mouse model for imaging-based tracking and modulation of neutrophil granulocytes. Nat Methods. 2015;12(5):445-52.
154. Wang JX, Bair AM, King SL, Shnayder R, Huang YF, Shieh CC, et al. Ly6G ligation blocks recruitment of neutrophils via a beta2-integrin-dependent mechanism. Blood. 2012;120(7):1489-98.
155. Day RN, Davidson MW. The fluorescent protein palette: tools for cellular imaging. Chem Soc Rev. 2009;38(10):2887-921.
156. Muzumdar MD, Tasic B, Miyamichi K, Li L, Luo L. A global double-fluorescent Cre reporter mouse. Genesis. 2007;45(9):593-605.
157. Winnard PT, Jr., Kluth JB, Raman V. Noninvasive optical tracking of red fluorescent protein-expressing cancer cells in a model of metastatic breast cancer. Neoplasia. 2006;8(10):796-806.
158. Clausen BE, Burkhardt C, Reith W, Renkawitz R, Forster I. Conditional gene targeting in macrophages and granulocytes using LysMcre mice. Transgenic Res. 1999;8(4):265-77.
159. Faust N, Varas F, Kelly LM, Heck S, Graf T. Insertion of enhanced green fluorescent protein into the lysozyme gene creates mice with green fluorescent granulocytes and macrophages. Blood. 2000;96(2):719-26.
160. Haage TR, Müller AJ, Arunachalam P, Fischer T. Reveal the Neutrophil: Elucidating the Role of a Neutrophil-Specific JAK2-V617F Mutation. Blood. 2019;134.
161. Mullally A, Lane SW, Ball B, Megerdichian C, Okabe R, Al-Shahrour F, et al. Physiological Jak2V617F expression causes a lethal myeloproliferative neoplasm with differential effects on hematopoietic stem and progenitor cells. Cancer Cell. 2010;17(6):584-96.
162. Nishimura S, Nagasaki M, Kunishima S, Sawaguchi A, Sakata A, Sakaguchi H, et al. IL-1alpha induces thrombopoiesis through megakaryocyte rupture in response to acute platelet needs. J Cell Biol. 2015;209(3):453-66.
163. Mirenda M, Toffali L, Montresor A, Scardoni G, Sorio C, Laudanna C. Protein tyrosine phosphatase receptor type gamma is a JAK phosphatase and negatively regulates leukocyte integrin activation. J Immunol. 2015;194(5):2168-79.
164. Montresor A, Toffali L, Mirenda M, Rigo A, Vinante F, Laudanna C. JAK2 tyrosine kinase mediates integrin activation induced by CXCL12 in B-cell chronic lymphocytic leukemia. Oncotarget. 2015;6(33):34245-57.
165. Haan C, Kreis S, Margue C, Behrmann I. Jaks and cytokine receptors--an intimate relationship. Biochem Pharmacol. 2006;72(11):1538-46.
166. Futosi K, Fodor S, Mocsai A. Neutrophil cell surface receptors and their intracellular signal transduction pathways. Int Immunopharmacol. 2013;17(3):638-50.
167. Chachoua I, Pecquet C, El-Khoury M, Nivarthi H, Albu RI, Marty C, et al. Thrombopoietin receptor activation by myeloproliferative neoplasm associated calreticulin mutants. Blood. 2016;127(10):1325-35.
168. Schattner M, Pozner RG, Gorostizaga AB, Lazzari MA. Effect of thrombopoietin and granulocyte colony-stimulating factor on platelets and polymorphonuclear leukocytes. Thromb Res. 2000;99(2):147-154
169. Ferrer-Marin F, Cuenca-Zamora EJ, Guijarro-Carrillo PJ, Teruel-Montoya R. Emerging Role of Neutrophils in the Thrombosis of Chronic Myeloproliferative Neoplasms. Int J Mol Sci. 2021;22(3).
170. Li J, Prins D, Park HJ, Grinfeld J, Gonzalez-Arias C, Loughran S, et al. Mutant calreticulin knockin mice develop thrombocytosis and myelofibrosis without a stem cell self-renewal advantage. Blood. 2018;131(6):649-61.

171. Song AJ, Palmiter RD. Detecting and Avoiding Problems When Using the Cre-lox System. Trends Genet. 2018;34(5):333-40.
172. Hasenberg M, Kohler A, Bonifatius S, Borucki K, Riek-Burchardt M, Achilles J, et al. Rapid immunomagnetic negative enrichment of neutrophil granulocytes from murine bone marrow for functional studies in vitro and in vivo. PLoS One. 2011;6(2):e17314.
173. Livak KJ, Schmittgen TD. Analysis of relative gene expression data using real-time quantitative PCR and the 2(-Delta Delta C(T)) Method. Methods. 2001;25(4):402-8.
174. Rochon J, Gondan M, Kieser M. To test or not to test: Preliminary assessment of normality when comparing two independent samples. BMC Med Res Methodol. 2012;12:81.
175. Ghasemi A, Zahediasl S. Normality tests for statistical analysis: a guide for non-statisticians. Int J Endocrinol Metab. 2012;10(2):486-9.
176. O'Connell KE, Mikkola AM, Stepanek AM, Vernet A, Hall CD, Sun CC, et al. Practical murine hematopathology: a comparative review and implications for research. Comp Med. 2015;65(2):96-113.
177. Deniset JF, Surewaard BG, Lee WY, Kubes P. Splenic Ly6G(high) mature and Ly6G(int) immature neutrophils contribute to eradication of S. pneumoniae. J Exp Med. 2017;214(5):1333-50.
178. Georgiades P, Ogilvy S, Duval H, Licence DR, Charnock-Jones DS, Smith SK, et al. VavCre transgenic mice: a tool for mutagenesis in hematopoietic and endothelial lineages. Genesis. 2002;34(4):251-6.
179. Okada S, Nakauchi H, Nagayoshi K, Nishikawa S, Miura Y, Suda T. In vivo and in vitro stem cell function of c-kit- and Sca-1-positive murine hematopoietic cells. Blood. 1992;80(12):3044-50.
180. Adolfsson J, Borge OJ, Bryder D, Theilgaard-Monch K, Astrand-Grundstrom I, Sitnicka E, et al. Upregulation of Flt3 expression within the bone marrow Lin(-)Sca1(+)c-kit(+) stem cell compartment is accompanied by loss of self-renewal capacity. Immunity. 2001;15(4):659-69.
181. Yang L, Bryder D, Adolfsson J, Nygren J, Mansson R, Sigvardsson M, et al. Identification of Lin(-)Sca1(+)kit(+)CD34(+)Flt3- short-term hematopoietic stem cells capable of rapidly reconstituting and rescuing myeloablated transplant recipients. Blood. 2005;105(7):2717-23.
182. Akashi K, Traver D, Miyamoto T, Weissman IL. A clonogenic common myeloid progenitor that gives rise to all myeloid lineages. Nature. 2000;404(6774):193-7.
183. Challen GA, Boles N, Lin KK, Goodell MA. Mouse hematopoietic stem cell identification and analysis. Cytometry A. 2009;75(1):14-24.
184. Nakorn TN, Miyamoto T, Weissman IL. Characterization of mouse clonogenic megakaryocyte progenitors. Proc Natl Acad Sci U S A. 2003;100(1):205-10.
185. Rovai LE, Herschman HR, Smith JB. The murine neutrophil-chemoattractant chemokines LIX, KC, and MIP-2 have distinct induction kinetics, tissue distributions, and tissue-specific sensitivities to glucocorticoid regulation in endotoxemia. J Leukoc Biol. 1998 Oct;64(4):494-502.
186. Turner MD, Nedjai B, Hurst T, Pennington DJ. Cytokines and chemokines: At the crossroads of cell signalling and inflammatory disease. Biochim Biophys Acta. 2014 Nov;1843(11):2563-2582.
187. Brizzi MF, Battaglia E, Rosso A, Strippoli P, Montrucchio G, Camussi G, Pegoraro L. Regulation of polymorphonuclear cell activation by thrombopoietin. J Clin Invest. 1997 Apr 1;99(7):1576-84.
188. Terada Y, Hato F, Sakamoto C, Hasegawa T, Suzuki K, Nakamae H, Ohta K, Yamane T, Kitagawa S, Hino M. Thrombopoietin stimulates ex vivo expansion of mature neutrophils in the early stages of differentiation. Ann Hematol. 2003 Nov;82(11):671-6.
189. Sadreev, I.I., Chen, M.Z.Q., Umezawa, Y., Biktashev, V.N., Kemper, C., Salakhieva, D.V., Welsh, G.I. and Kotov, N.V. (2018), The competitive nature of signal transducer and activator of transcription complex formation drives phenotype switching of T cells. Immunology, 153: 488-501.
190. Nourshargh S, Alon R. Leukocyte migration into inflamed tissues. Immunity. 2014 Nov 20;41(5):694-707.

191. Achyutuni S, Nivarthi H, Majoros A, Hug E, Schueller C, Jia R, et al. Hematopoietic expression of a chimeric murine-human CALR oncoprotein allows the assessment of anti-CALR antibody immunotherapies in vivo. Am J Hematol. 2021;96(6):698-707.
192. Balligand T, Achouri Y, Pecquet C, Gaudray G, Colau D, Hug E, et al. Knock-in of murine Calr del52 induces essential thrombocythemia with slow-rising dominance in mice and reveals key role of Calr exon 9 in cardiac development. Leukemia. 2020;34(2):510-21.
193. Benlabiod C, Cacemiro MDC, Nedelec A, Edmond V, Muller D, Rameau P, et al. Calreticulin del52 and ins5 knock-in mice recapitulate different myeloproliferative phenotypes observed in patients with MPN. Nat Commun. 2020;11(1):4886.
194. Elf S, Abdelfattah NS, Chen E, Perales-Paton J, Rosen EA, Ko A, et al. Mutant Calreticulin Requires Both Its Mutant C-terminus and the Thrombopoietin Receptor for Oncogenic Transformation. Cancer Discov. 2016;6(4):368-81.
195. Marty C, Pecquet C, Nivarthi H, El-Khoury M, Chachoua I, Tulliez M, et al. Calreticulin mutants in mice induce an MPL-dependent thrombocytosis with frequent progression to myelofibrosis. Blood. 2016;127(10):1317-24.
196. Shide K, Kameda T, Yamaji T, Sekine M, Inada N, Kamiunten A, et al. Calreticulin mutant mice develop essential thrombocythemia that is ameliorated by the JAK inhibitor ruxolitinib. Leukemia. 2017;31(5):1136-44.
197. Alexander WS. Thrombopoietin and the c-Mpl receptor: insights from gene targeting. Int J Biochem Cell Biol. 1999;31(10):1027-35.
198. Song M, Graubard BI, Rabkin CS, Engels EA. Neutrophil-to-lymphocyte ratio and mortality in the United States general population. Sci Rep. 2021;11(1):464.
199. Lucijanic M, Cicic D, Stoos-Veic T, Pejsa V, Lucijanic J, Fazlic Dzankic A, et al. Elevated Neutrophil-to-Lymphocyte-ratio and Platelet-to-Lymphocyte Ratio in Myelofibrosis: Inflammatory Biomarkers or Representatives of Myeloproliferation Itself? Anticancer Res. 2018;38(5):3157-63.
200. Kjaer L, Holmstrom MO, Cordua S, Andersen MH, Svane IM, Thomassen M, et al. Sorted peripheral blood cells identify CALR mutations in B- and T-lymphocytes. Leuk Lymphoma. 2018;59(4):973-7.
201. Coppolino M, Leung-Hagesteijn C, Dedhar S, Wilkins J. Inducible interaction of integrin alpha 2 beta 1 with calreticulin. Dependence on the activation state of the integrin. J Biol Chem. 1995;270(39):23132-8.
202. Leung-Hagesteijn CY, Milankov K, Michalak M, Wilkins J, Dedhar S. Cell attachment to extracellular matrix substrates is inhibited upon downregulation of expression of calreticulin, an intracellular integrin alpha-subunit-binding protein. J Cell Sci. 1994;107 (Pt 3):589-600.
203. Ohkuro M, Hishinuma I. The alpha integrin cytoplasmic motif KXGFFKR is essential for integrin-mediated leukocyte adhesion. Int J Mol Med. 2010;25(3):439-44.
204. Ohkuro M, Kim JD, Kuboi Y, Hayashi Y, Mizukami H, Kobayashi-Kuramochi H, et al. Calreticulin and integrin alpha dissociation induces anti-inflammatory programming in animal models of inflammatory bowel disease. Nat Commun. 2018;9(1):1982.
205. Coppolino MG, Woodside MJ, Demaurex N, Grinstein S, St-Arnaud R, Dedhar S. Calreticulin is essential for integrin-mediated calcium signalling and cell adhesion. Nature. 1997;386(6627):843-7.
206. Kwon MS, Park CS, Choi K, Ahnn J, Kim JI, Eom SH, et al. Calreticulin couples calcium release and calcium influx in integrin-mediated calcium signaling. Mol Biol Cell. 2000;11(4):1433-43.
207. Zhu Q, Zelinka P, White T, Tanzer ML. Calreticulin-integrin bidirectional signaling complex. Biochem Biophys Res Commun. 1997;232(2):354-8.
208. Lu YC, Chen CN, Chu CY, Lu J, Wang BJ, Chen CH, et al. Calreticulin activates beta1 integrin via fucosylation by fucosyltransferase 1 in J82 human bladder cancer cells. Biochem J. 2014;460(1):69-78.

209. Yamamoto M, Ikezaki M, Toujima S, Iwahashi N, Mizoguchi M, Nanjo S, et al. Calreticulin Is Involved in Invasion of Human Extravillous Trophoblasts Through Functional Regulation of Integrin beta1. Endocrinology. 2017;158(11):3874-89.
210. Håkansson L, Höglund M, Jönsson UB, Torsteinsdottir I, Xu X, Venge P. Effects of in vivo administration of G-CSF on neutrophil and eosinophil adhesion. Br J Haematol. 1997 Sep;98(3):603-11.
211. Köhler A, De Filippo K, Hasenberg M, van den Brandt C, Nye E, Hosking MP, Lane TE, Männ L, Ransohoff RM, Hauser AE, Winter O, Schraven B, Geiger H, Hogg N, Gunzer M. G-CSF-mediated thrombopoietin release triggers neutrophil motility and mobilization from bone marrow via induction of Cxcr2 ligands. Blood. 2011 Apr 21;117(16):4349-57.
212. M'Rabet L, Coffer P, Zwartkruis F, Franke B, Segal AW, Koenderman L, Bos JL. Activation of the small GTPase rap1 in human neutrophils. Blood. 1998 Sep 15;92(6):2133-40.
213. Myers D, Jr., Farris D, Hawley A, Wrobleski S, Chapman A, Stoolman L, et al. Selectins influence thrombosis in a mouse model of experimental deep venous thrombosis. J Surg Res. 2002;108(2):212-21.
214. Culmer DL, Dunbar ML, Hawley AE, Sood S, Sigler RE, Henke PK, et al. E-selectin inhibition with GMI-1271 decreases venous thrombosis without profoundly affecting tail vein bleeding in a mouse model. Thromb Haemost. 2017;117(6):1171-81.
215. Myers D, Jr., Lester P, Adili R, Hawley A, Durham L, Dunivant V, et al. A new way to treat proximal deep venous thrombosis using E-selectin inhibition. J Vasc Surg Venous Lymphat Disord. 2020;8(2):268-78.
216. Devata S, Angelini DE, Blackburn S, Hawley A, Myers DD, Schaefer JK, et al. Use of GMI-1271, an E-selectin antagonist, in healthy subjects and in 2 patients with calf vein thrombosis. Res Pract Thromb Haemost. 2020;4(2):193-204.
217. Wild MK, Luhn K, Marquardt T, Vestweber D. Leukocyte adhesion deficiency II: therapy and genetic defect. Cells Tissues Organs. 2002;172(3):161-73.
218. Kanamori A, Kojima N, Uchimura K, Muramatsu T, Tamatani T, Berndt MC, et al. Distinct sulfation requirements of selectins disclosed using cells that support rolling mediated by all three selectins under shear flow. L-selectin prefers carbohydrate 6-sulfation totyrosine sulfation, whereas p-selectin does not. J Biol Chem. 2002;277(36):32578-86.
219. Azevedo, R., Gaiteiro, C., Peixoto, A. *et al.* CD44 glycoprotein in cancer: a molecular conundrum hampering clinical applications. *Clin Proteom* 15, 22 (2018).
220. Belotti A, Elli E, Speranza T, Lanzi E, Pioltelli P, Pogliani E. Circulating endothelial cells and endothelial activation in essential thrombocythemia: results from CD146+ immunomagnetic enrichment--flow cytometry and soluble E-selectin detection. Am J Hematol. 2012 Mar;87(3):319-20.
221. Guy A, Gourdou-Latyszenok V, Le Lay N, Peghaire C, Kilani B, Dias JV, Duplaa C, Renault MA, Denis C, Villeval JL, Boulaftali Y, Jandrot-Perrus M, Couffinhal T, James C. Vascular endothelial cell expression of JAK2^{V617F} is sufficient to promote a pro-thrombotic state due to increased P-selectin expression. Haematologica. 2019 Jan;104(1):70-81.
222. Guadall A, Lesteven E, Letort G, Awan Toor S, Delord M, Pognant D, Brusson M, Verger E, Maslah N, Giraudier S, Larghero J, Vanneaux V, Chomienne C, El Nemer W, Cassinat B, Kiladjian JJ. Endothelial Cells Harbouring the JAK2V617F Mutation Display Pro-Adherent and Pro-Thrombotic Features. Thromb Haemost. 2018 Sep;118(9):1586-1599.
223. Crodel, C.C., Jentsch-Ullrich, K., Koschmieder, S. *et al.* Frequency of infections in 948 MPN patients: a prospective multicenter patient-reported pilot study. *Leukemia* 34, 1949–1953 (2020).
224. Slezak S, Jin P, Caruccio L, Ren J, Bennett M, Zia N, Adams S, Wang E, Ascensao J, Schechter G, Stroncek D. Gene and microRNA analysis of neutrophils from patients with polycythemia vera and essential thrombocytosis: down-regulation of micro RNA-1 and -133a. J Transl Med. 2009 Jun 4;7:39.
225. Kleppe M, Koche R, Zou L, van Galen P, Hill CE, Dong L, De Groote S, Papalexi E, Hanasoge Somasundara AV, Cordner K, Keller M, Farnoud N, Medina J, McGovern E, Reyes J, Roberts J, Witkin M,

Rapaport F, Teruya-Feldstein J, Qi J, Rampal R, Bernstein BE, Bradner JE, Levine RL. Dual Targeting of Oncogenic Activation and Inflammatory Signaling Increases Therapeutic Efficacy in Myeloproliferative Neoplasms. Cancer Cell. 2018 Jan 8;33(1):29-43.e7
226. Jain A, Deo P, Sachdeva MUS, Bose P, Lad D, Prakash G, et al. Aberrant expression of cytokines in polycythemia vera correlate with the risk of thrombosis. Blood Cells Mol Dis. 2021;89:102565.
227. Muller P, Baldauf CK, Haage TR, Waldleben AM, Richter F, Pfizenmaier K, et al. Anti-inflammatory treatment in MPN: Targeting TNFalpha-receptor 1 (TNFR1) and TNFR2 in JAK2-V617F induced disease. Blood Adv. 2021.
228. Hsieh CS, Macatonia SE, Tripp CS, Wolf SF, O'Garra A, Murphy KM. Development of TH1 CD4+ T cells through IL-12 produced by Listeria-induced macrophages. Science. 1993;260(5107):547-9.
229. Zaidi U, Sufaida G, Rashid M, Kaleem B, Maqsood S, Mukry SN, et al. A distinct molecular mutational profile and its clinical impact in essential thrombocythemia and primary myelofibrosis patients. BMC Cancer. 2020;20(1):205.
230. Fleischman AG, Aichberger KJ, Luty SB, Bumm TG, Petersen CL, Doratotaj S, et al. TNFalpha facilitates clonal expansion of JAK2V617F positive cells in myeloproliferative neoplasms. Blood. 2011;118(24):6392-8.
231. Arranz L, Sanchez-Aguilera A, Martin-Perez D, Isern J, Langa X, Tzankov A, et al. Neuropathy of haematopoietic stem cell niche is essential for myeloproliferative neoplasms. Nature. 2014;512(7512):78-81.
232. Lee D, Schultz JB, Knauf PA, King MR. Mechanical shedding of L-selectin from the neutrophil surface during rolling on sialyl Lewis x under flow. J Biol Chem. 2007;282(7):4812-20.
233. Li SH, Burns DK, Rumberger JM, Presky DH, Wilkinson VL, Anostario M Jr, Wolitzky BA, Norton CR, Familletti PC, Kim KJ, et al. Consensus repeat domains of E-selectin enhance ligand binding. J Biol Chem. 1994 Feb 11;269(6):4431-7.
234. Yang J, Furie BC, Furie B. The biology of P-selectin glycoprotein ligand-1: its role as a selectin counterreceptor in leukocyte-endothelial and leukocyte-platelet interaction. Thromb Haemost. 1999 Jan;81(1):1-7.
235. Schäkel K, Kannagi R, Kniep B, Goto Y, Mitsuoka C, Zwirner J, Soruri A, von Kietzell M, Rieber E. 6-Sulfo LacNAc, a novel carbohydrate modification of PSGL-1, defines an inflammatory type of human dendritic cells. Immunity. 2002 Sep;17(3):289-301.
236. Fukuda M, Koeffler HP, Minowada J. Membrane differentiation in human myeloid cells: expression of unique profiles of cell surface glycoproteins in myeloid leukemic cell lines blocked at different stages of differentiation and maturation. Proc Natl Acad Sci U S A. 1981 Oct;78(10):6299-303.
237. Almulki L, Noda K, Amini R, Schering A, Garland RC, Nakao S, Nakazawa T, Hisatomi T, Thomas KL, Masli S, Hafezi-Moghadam A. Surprising up-regulation of P-selectin glycoprotein ligand-1 (PSGL-1) in endotoxin-induced uveitis. FASEB J. 2009 Mar;23(3):929-39.
238. Dorward DA, Lucas CD, Alessandri AL, Marwick JA, Rossi F, Dransfield I, Haslett C, Dhaliwal K, Rossi AG. Technical advance: autofluorescence-based sorting: rapid and nonperturbing isolation of ultrapure neutrophils to determine cytokine production. J Leukoc Biol. 2013 Jul;94(1):193-202.
239. Bhuria, V.; Baldauf, C.K.; Schraven, B.; Fischer, T. Thromboinflammation in Myeloproliferative Neoplasms (MPN)—A Puzzle Still to Be Solved. Int. J. Mol. Sci. 2022, 23, 3206
240. Huttenlocher A, Horwitz AR. Integrins in cell migration. Cold Spring Harb Perspect Biol. 2011 Sep 1;3(9):a005074. doi: 10.1101/cshperspect.a005074.
241. Huttenlocher A, Ginsberg MH, Horwitz AF. Modulation of cell migration by integrin-mediated cytoskeletal linkages and ligand-binding affinity. J Cell Biol. 1996 Sep;134(6):1551-62.
242. Montagutelli X. Effect of the genetic background on the phenotype of mouse mutations. J Am Soc Nephrol. 2000;11 Suppl 16:S101-5.

243. Kozlov G, Gehring K. Calnexin cycle - structural features of the ER chaperone system. FEBS J. 2020;287(20):4322-40.
244. Timchenko LT, Iakova P, Welm AL, Cai ZJ, Timchenko NA. Calreticulin interacts with C/EBPalpha and C/EBPbeta mRNAs and represses translation of C/EBP proteins. Mol Cell Biol. 2002;22(20):7242-57.
245. Lee PC, Chiang JC, Chen CY, Chien YC, Chen WM, Huang CW, et al. Calreticulin regulates vascular endothelial growth factor-A mRNA stability in gastric cancer cells. PLoS One. 2019;14(11):e0225107.
246. Nauseef WM. Myeloperoxidase in human neutrophil host defence. Cell Microbiol. 2014;16(8):1146-55.
247. Theocharides AP, Lundberg P, Lakkaraju AK, Lysenko V, Myburgh R, Aguzzi A, et al. Homozygous calreticulin mutations in patients with myelofibrosis lead to acquired myeloperoxidase deficiency. Blood. 2016;127(25):3253-9.
248. Gardai SJ, McPhillips KA, Frasch SC, Janssen WJ, Starefeldt A, Murphy-Ullrich JE, et al. Cell-surface calreticulin initiates clearance of viable or apoptotic cells through trans-activation of LRP on the phagocyte. Cell. 2005;123(2):321-34.
249. Chao MP, Jaiswal S, Weissman-Tsukamoto R, Alizadeh AA, Gentles AJ, Volkmer J, et al. Calreticulin is the dominant pro-phagocytic signal on multiple human cancers and is counterbalanced by CD47. Sci Transl Med. 2010;2(63):63ra94.
250. Rinaldi CR, Boasman K, Simmonds M. Expression of CD47 and CALR in myeloproliferative neoplasms: Potential new therapeutical targets. Journal of Clinical Oncology. 2022;40(16):e19075.

Acknowledgments

I would like to say a special thank you to my supervisor Prof. Dr. Thomas Fischer for his constant support throughout my research year in the lab, for his brilliant ideas and for giving me the opportunity to write this thesis and to start my career as a doctor in Germany. A dept of gratitude is also owed to Dr. Vikas Bhuria for helping me shape my research thinking and for his excellent advice and guidance. I would also like to thank Dr. Ronny Haage for sharing his knowledge and expertise in research and clinic. The completion of this thesis would not have been possible without the support of Stephanie Adam-Frey, who patiently taught me to hold the pipette and draw blood from mice and who took care of the preparation of bone marrow and spleen biopsies and the PCR genotyping. I would like to express the deepest appreciation to Corinna Fahldieck and Anja Sammt for helping me become familiar with the laboratory techniques and for sharing their technical knowledge in many experiments. Many thanks also goes to Dr. Peter Müller and to Conny Baldauf for their scientific advice. In addition, I would like to recognize the inestimable help of Dr. Mark Korthals for making the time-lapse cell migration experiments possible. Many thanks go to Dr. Roland Hartig for conducting the fluorescence-activated cell sorting and for the interesting discussions as we waited for the completion of cell isolation. I am deeply indepted to Dr. Gopala Krishna Nishanth and Harit Kunjan for conducting the qRT-PCR experiment of inflammatory cytokines in granulocytes. I am incredibly thankful to Prof. Dr. Mougiakakos for his unwavering support in clinic and research. Last but not least I would like to acknowledge the invaluable support received from my parents, my sister and my friends over the years.

Ehrenerklärung

Ich erkläre, dass ich die der Medizinischen Fakultät der Otto-von-Guericke-Universität zur Promotion eingereichte Dissertation mit dem Titel

A study on the effects of calreticulin del52 mutation on neutrophil adhesion: Results from CALRdel52 knock-in mice and characterization of a novel CALRdel52 Catchup mouse model

in der
Universitätsklinik für Hämatologie und Onkologie
Medizinische Fakultät der Otto-von-Guericke-Universität Magdeburg

mit Unterstützung durch
Herrn Prof. Dr. med. Thomas Fischer

ohne sonstige Hilfe durchgeführt und bei der Abfassung der Dissertation keine anderen als die dort aufgeführten Hilfsmittel benutzt habe.

Bei der Abfassung der Dissertation sind Rechte Dritter nicht verletzt worden.

Ich habe diese Dissertation bisher an keiner in- oder ausländischen Hochschule zur Promotion eingereicht. Ich übertrage der Medizinischen Fakultät das Rechte, weitere Kopien meiner Dissertation herzustellen und zu vertreiben.

Magdeburg, den 12.05.2023

Unterschrift

Curriculum vitae

Personal Data

Information not included in this version for data protection reasons.

Work Experience

since 01-01-2022	Resident doctor in the University Hospital of Magdeburg, Clinic for Hematology, Oncology and Stem Cell Transplantation (Director: Prof. Dr. med. Dimitrios Mougiakakos)
01-01-2021 – 31-12-2021	Resident doctor in Collaborative Research Center 854 (GEROK position) in the University Hospital of Magdeburg, Clinic for Hematology, Oncology and Stem Cell Transplantation (Director: Prof. Dr. med. Thomas Fischer) Research Project: *Generation and Characterization of a CALR mutant (CALRmut) „Catchup“ mouse model.*
11-2019 – 12-2020	Rural doctor in the Health Center for General Medicine in Serifos, Greece (Director: A. Kontaris)
09-2018 – 09-2019	Military service in the Greek Airforce. Resident doctor from 28-11-2018 until 16-09-2019 in the Hematology Clinic in Military Hospital “251 Air Force General Hospital” (Director: Dr. K. Anargyrou)

Education

09-2012 – 07-2018	Medical degree in the National and Kapodistrian University of Athens, Greece (Grade: “excellent - 8,95/10”)
2012	High School Final Exams, Greece

Publications

Diamantopoulos PT, **Charakopoulos E**, Symeonidis A, Kotsianidis I, Viniou NA, Pappa V, et al. Real world data on the prognostic significance of monocytopenia in myelodysplastic syndrome. *Sci Rep* 2022; 12: 17914.

Charakopoulos E, Diamantopoulos PT, Zervakis K, Giannakopoulou N, Psichogiou M, Viniou NA. A case report of a fulminant Aeromonas hydrophila soft tissue infection in a patient with acute lymphoblastic leukemia harboring a rare translocation. *Curr Med Res Opin*. 2022; 38(7):1125-1132.

Müller P, Baldauf CK, Haage TR, **Charakopoulos E**, Böttcher M, Bhuria V, Mougiakakos D, Schraven B, Fischer T. Genetic Knock-out of TNFR1 and TNFR2 in a JAK2-V617F Polycythemia Vera Mouse Model. *Hemasphere*. 2022 Apr 15;6(5):e717.

Charakopoulos E, Spyrou I, Viniou NA, et al. A case report of Hodgkin lymphoma in a patient treated with ustekinumab for psoriasis. *Medicine (Baltimore)*. 2020

Tsamakis K, Mueller C, Tsirigotis P, Tsiptsios D, Tsamakis C, **Charakopoulos E**, et al. Depression following graft-versus-host disease in a patient with acute lymphoblastic leukemia: A case report. *Molecular and Clinical Oncology.* 2020; 12(3): 208-211

Diamantopoulos PT, **Charakopoulos E**, Viniou NA, Diamantopoulou L, Gaggadi M. An unusual case report of unilateral parotid gland sarcoidosis with spontaneous remission. *Medicine (Baltimore)*. 2019; 98(49):e18172.

Charakopoulos E, Thomakos N, Sourelli D, Sideris K, Rodolakis A. Understanding the Rare Krukenberg Tumor: A Current Review. *Hellenic Journal of Obstetrics and Gynecology*. 2018; 17(4):73-83.

Language Skills

Greek	First Language
German	Large German Language Diploma (C2) -Goethe-Institut (Examination Date: 29-01-2016)
English	Certificate of Proficiency in English (C2) -University of Cambridge (Examination Date: 12-2009)

Special Skills

04-2021	Completion of Course “Laboratory Animal Science (mouse/rat) – Berlin EU Function A (formerly FELASA B)” -Humboldt-Universität zu Berlin
05-2019	Preclinical Traumamanagement (PHTLS) Provider

Magdeburg, den 12.05.2023

Emmanouil Charakopoulos

Supplements

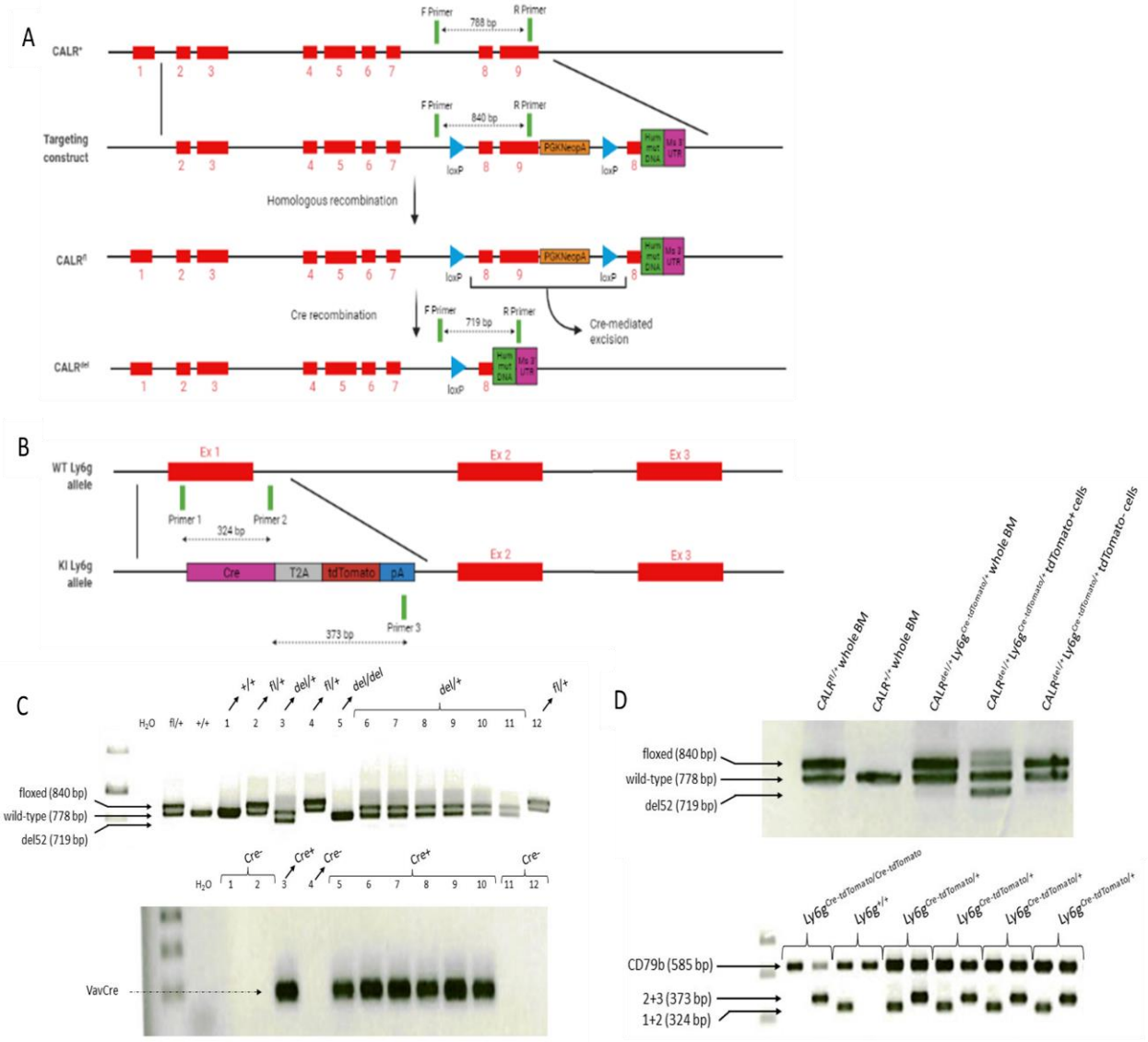

Supplementary Figure 1. (A) Diagrammatic representation of the normal murine CALR allele ($CALR^{+/+}$), the gene targeting construct, the floxed CALR knock-in allele ($CALR^{fl/+}$) after homologous recombination and the mouse-human chimeric CALR mutated gene ($CALR^{del/+}$) after Cre-mediated excision. In the modified $CALR^{fl/+}$ allele, the murine exons 8 and 9 followed by a PGKNeopA sequence are flanked by a pair of loxP sites (denoted with blue arrows). Further downstream a fused sequence of murine exon 8, the mutated human CALRdel52 region and a 3' mouse untranslated region (3' mouse UTR) have been inserted. The loxP flanked region is excised by Cre recombinase during Cre recombination. The final result of Cre recombination is the generation of a chimeric allele, which harbors the wild-type murine CALR exons 1-8 and the mutated human CALR sequence in place of exon 9. The forward and reverse primers used for PCR genotyping are denoted with green rectangles.(170) (B) Diagrammatic illustration of the WT and knock-in (KI) murine Ly6g gene. In the Catchup mouse model, exon 1 of the WT gene is replaced by a bicistronic allele harboring both Cre recombinase and the fluorescent protein tdTomato. Separation of Cre and tdTomato during translation is induced by a 2A self-cleaving peptide (T2A), which is inserted between the Cre and tdTomato sequences. A polyadenylation sequence (pA) downstream of the gene is used for transcription termination.(172) (C) PCR genotyping of CALRdel52 and VavCre recombinase in the BM of 12 CALRxVavCre mice. (D) Detection of CALRdel52 mutation (up) and characterization of the Ly6g locus in Catchup mice (down) with PCR. In $CALR^{del/+}$ $Ly6g^{Cre\text{-}tdTomato/+}$ mice, the CALRdel band is detectable after isolation of tdTomato+ cells. Characterization of the Ly6g locus requires two separate PCRs. In PCR 1, primers 1+2 are used to detect the wild-type exon 1, whereas in PCR2, primers 2+3 are employed to amplify the knock-in Cre-tdTomato sequence. Primers for the wild type CD79b gene are included as well in both PCRs as a control.(172)(A) and (B) were created with BioRender.com.

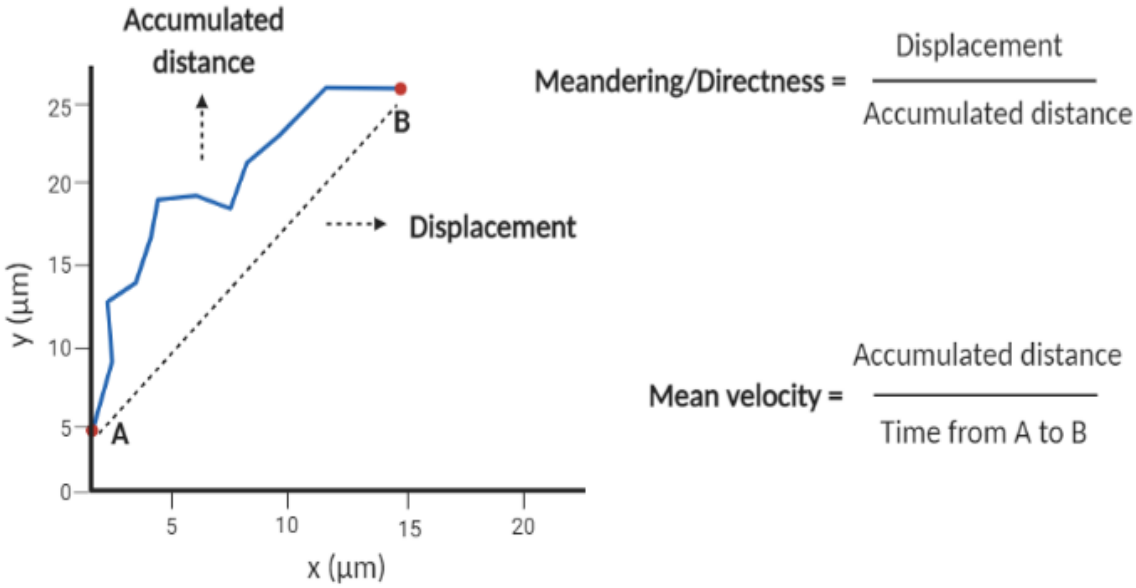

Supplementary Figure 2. During *in-vitro* time-lapse imaging, the following parameters were used to characterize the migratory movement of tdTomato^{+} cells: accumulated distance, displacement, meandering/directness and mean velocity. Accumulated distance is the overall distance in µm that cells travel as they move from point A to point B. Displacement refers to the length of a straight line connecting starting point A and ending point B. Meandering/directness represents a measure of how directly cells move and can be obtained by dividing the displacement with the accumulated distance. Mean velocity is calculated by dividing the accumulated distance with time and is expressed in µm/sec. This image was created with

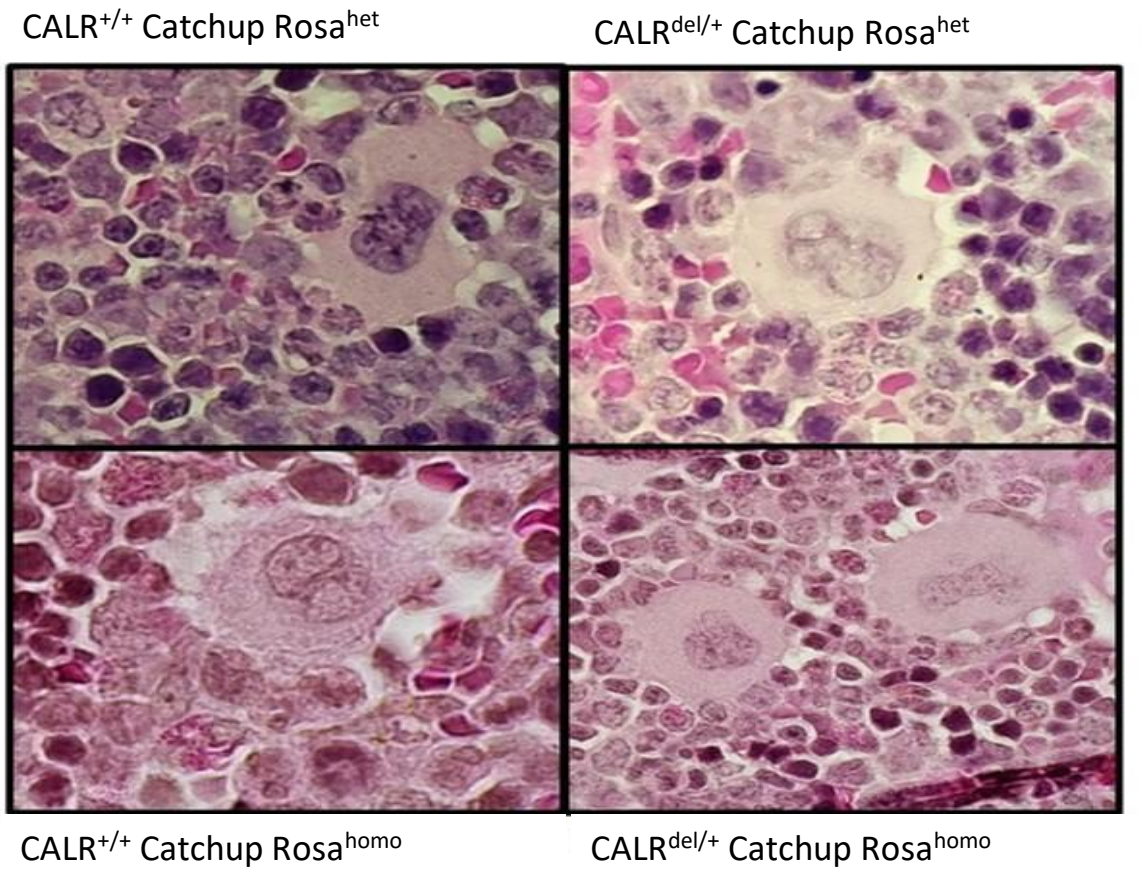

Supplementary Figure 3. Histological examination of MK morphology of 12-14 week-old $CALR^{del/+}$ Catchup mice did not reveal any signs of megakaryocyte dysplasia. Representative pictures of BM MKs of $CALR^{+/+}$ Catchup $Rosa^{tdTomato/+}$ (n = 6), $CALR^{del/+}$ Catchup $Rosa^{tdTomato/+}$ (n = 6), $CALR^{+/+}$ Catchup $Rosa^{tdTomato/tdTomato}$ (n = 2) and $CALR^{del/+}$ Catchup $Rosa^{tdTomato/tdTomato}$ (n = 4) mice; original magnification x100.

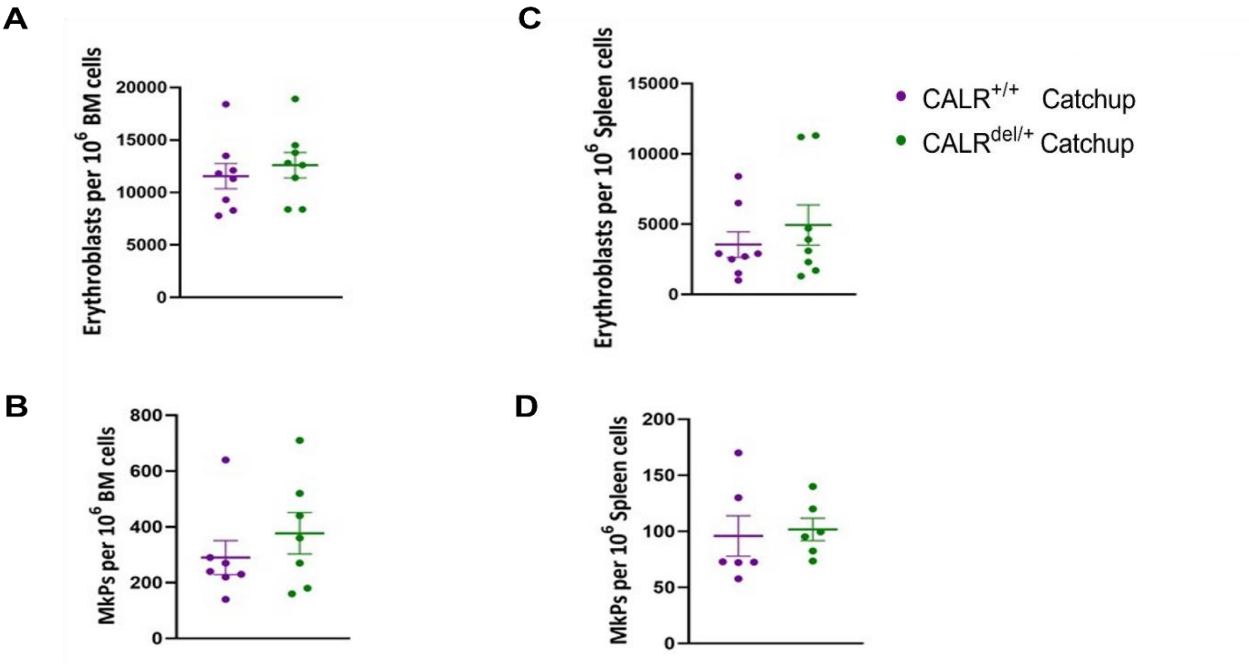

Supplementary Figure 4. Numbers of $CD71^+$ $Ter119^+$ erythroblasts and MkPs in the BM and spleen of $CALR^{del/+}$ Catchup (n = 7 for erythroblasts, n = 8 for MkPs) mice were comparable to $CALR^{+/+}$ Catchup mice (n = 7 for erythroblasts, n = 8 for MkPs). Determination of $CD71^+$ $Ter119^+$ erythroblasts (P = 0.5520) (A) and MkPs (P = 0.3832) (B) in total BM cells. Determination of $CD71^+$ $Ter119^+$ erythroblasts (P = 0.4873) (C) and MkPs (P = 0.7806) (D) in total spleen cells. Data are shown as mean ± SEM.

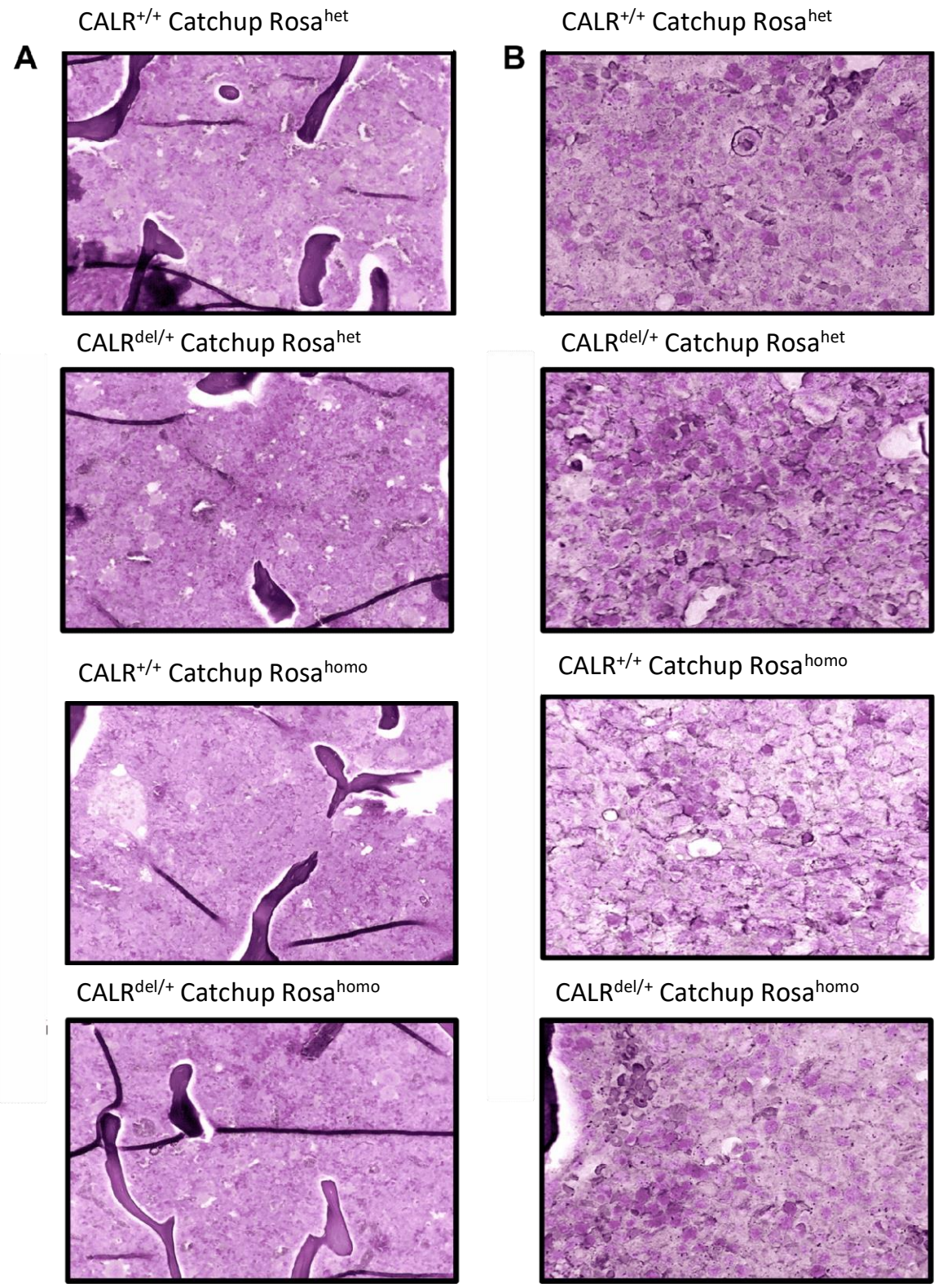

Supplementary Figure 5. Modified Gomori's staining of BM tissue sections of 12-14 week-old $CALR^{+/+}$ $Ly6g^{tdTomato/+}$ and $CALR^{del/+}$ $Ly6g^{tdTomato/+}$ mice. Pictures of BM sections from $CALR^{+/+}$ $Ly6g^{tdTomato/+}$ $Rosa^{tdTomato/+}$ (n = 2), $CALR^{del/+}$ $Ly6g^{tdTomato/+}$ $Rosa^{tdTomato/+}$ (n = 1), $CALR^{+/+}$ $Ly6g^{tdTomato/+}$ $Rosa^{tdTomato/tdTomato}$ (n = 2) and $CALR^{del/+}$ $Ly6g^{tdTomato/+}$ $Rosa^{tdTomato/tdTomato}$ (n = 2) mice; original magnification x20 (A) and x100 (B).

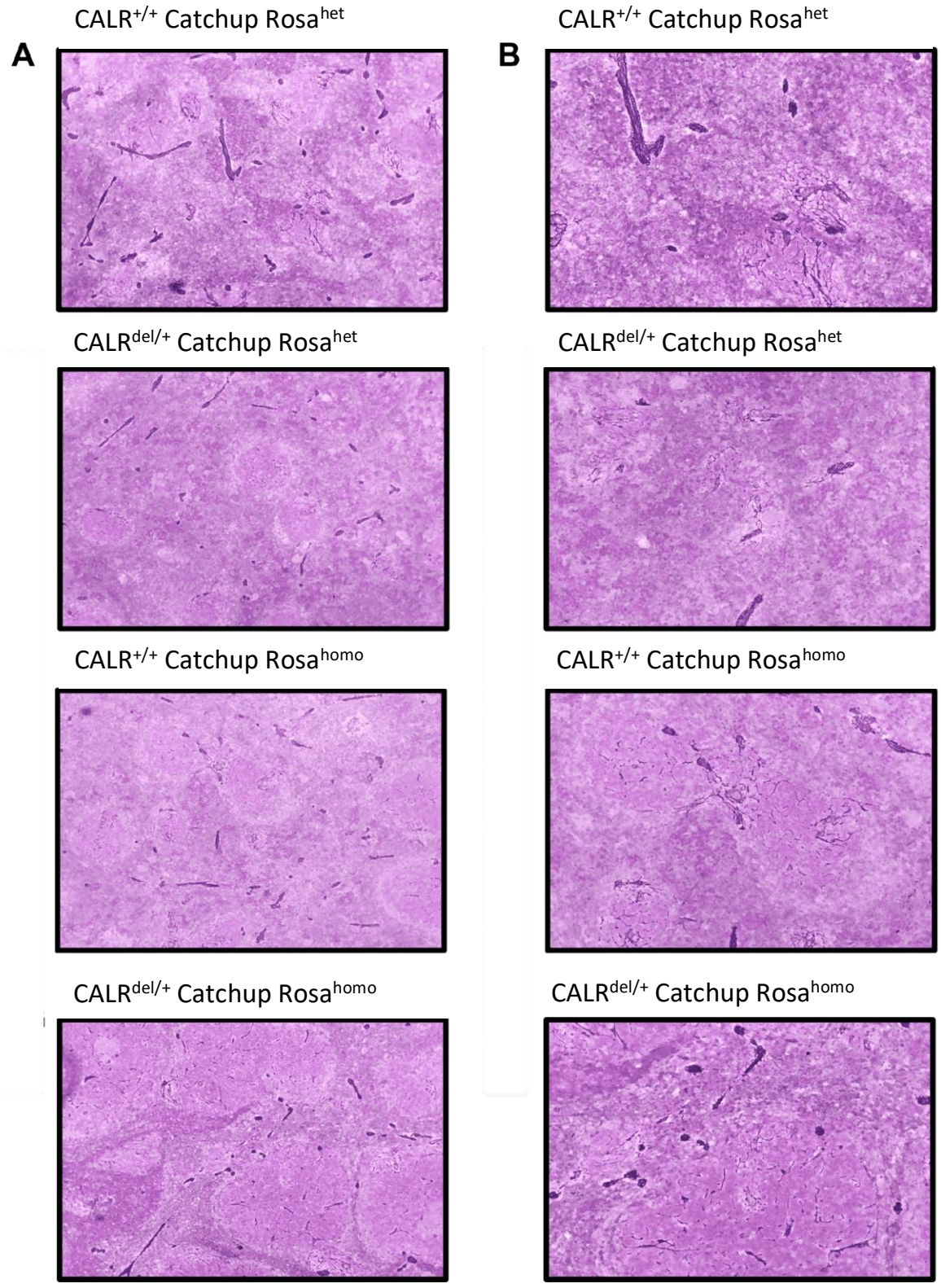

Supplementary Figure 6. Modified Gomori's staining of spleen tissue sections of 12-14 week-old $CALR^{+/+}$ $Ly6g^{tdTomato/+}$ and $CALR^{del/+}$ $Ly6g^{tdTomato/+}$ mice. Pictures of spleen sections from $CALR^{+/+}$ $Ly6g^{tdTomato/+}$ $Rosa^{tdTomato/+}$ (n = 1), $CALR^{del/+}$ $Ly6g^{tdTomato/+}$ $Rosa^{tdTomato/+}$ (n = 1), $CALR^{+/+}$ $Ly6g^{tdTomato/+}$ $Rosa^{tdTomato/tdTomato}$ (n = 2) and $CALR^{del/+}$ $Ly6g^{tdTomato/+}$ $Rosa^{tdTomato/tdTomato}$ (n = 2) mice; original magnification x10 (A) and x20 (B).

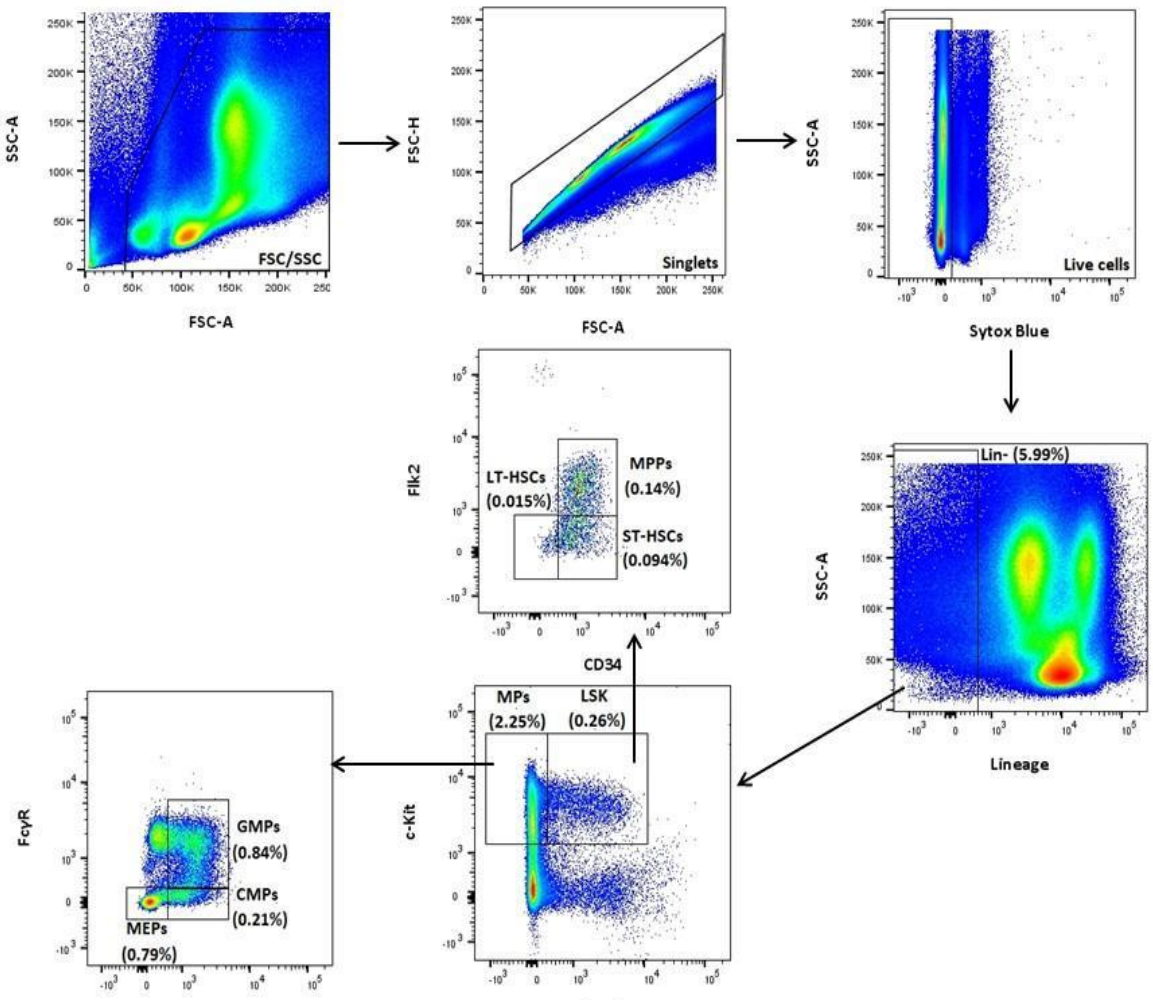

Supplementary Figure 7. Schematic representation of the gating strategy used for hematopoietic stem and progenitor cell measurement using representative pseudo-color blots of murine BM cells. The term "LSK" (Lineage markers^{-} Sca-1^{+} c-kit^{+}) refers to HSCs. The antibody-cocktail used for exclusion of cells that express lineage markers included anti-Gr-1, anti-Mac-1, anti-Ter119, anti-CD45R/B220, anti-CD3, anti-CD4, anti-CD8α, anti-CD19 and anti-IL7Rα.

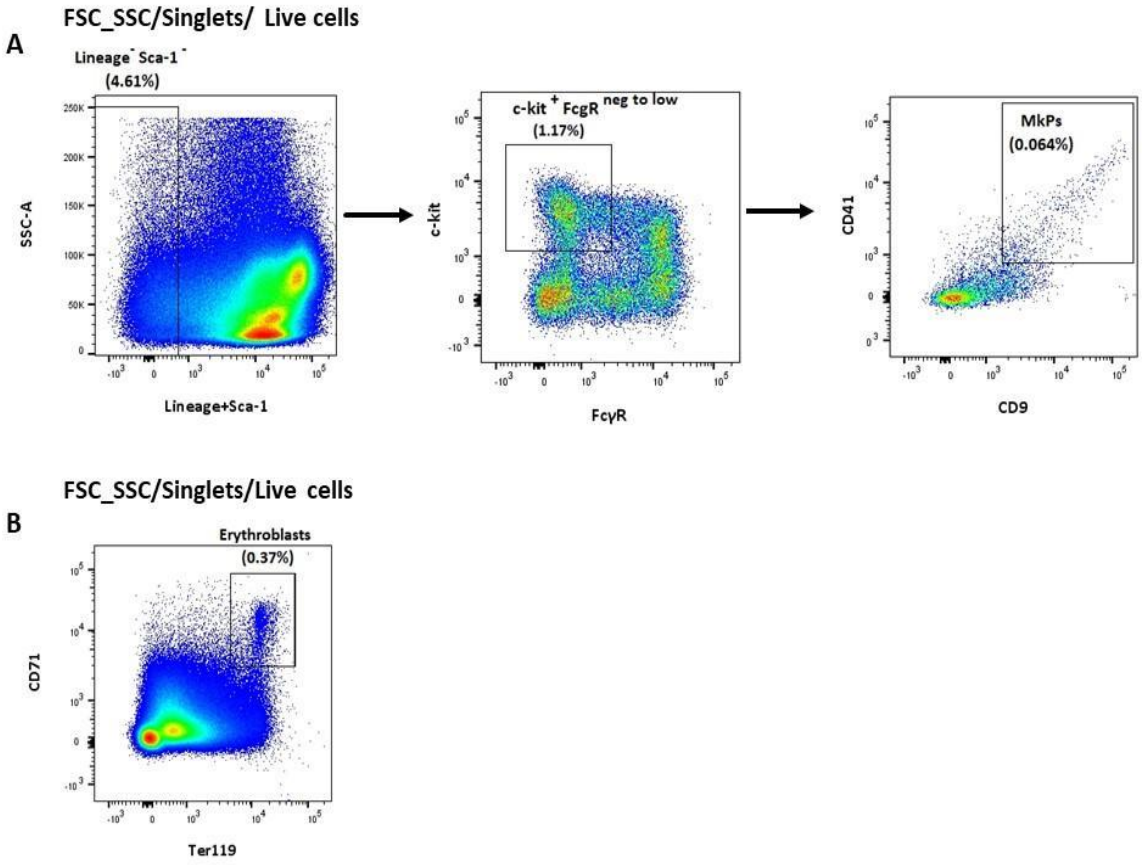

Supplementary Figure 8. Schematic representation of the gating strategy used for measurement of (A) MkPs and (B) $CD71^{+}$ $Ter119^{+}$ erythroblasts using representative pseudo-color blots of murine BM and spleen cells respectively. "FSC_SSC/Singlets/Live cells" denotes exclusion of cellular debris on FSC-A vs SSC-A, doublets on FSC-A vs FSC-H and dead cells with a Sytox dead cell stain.

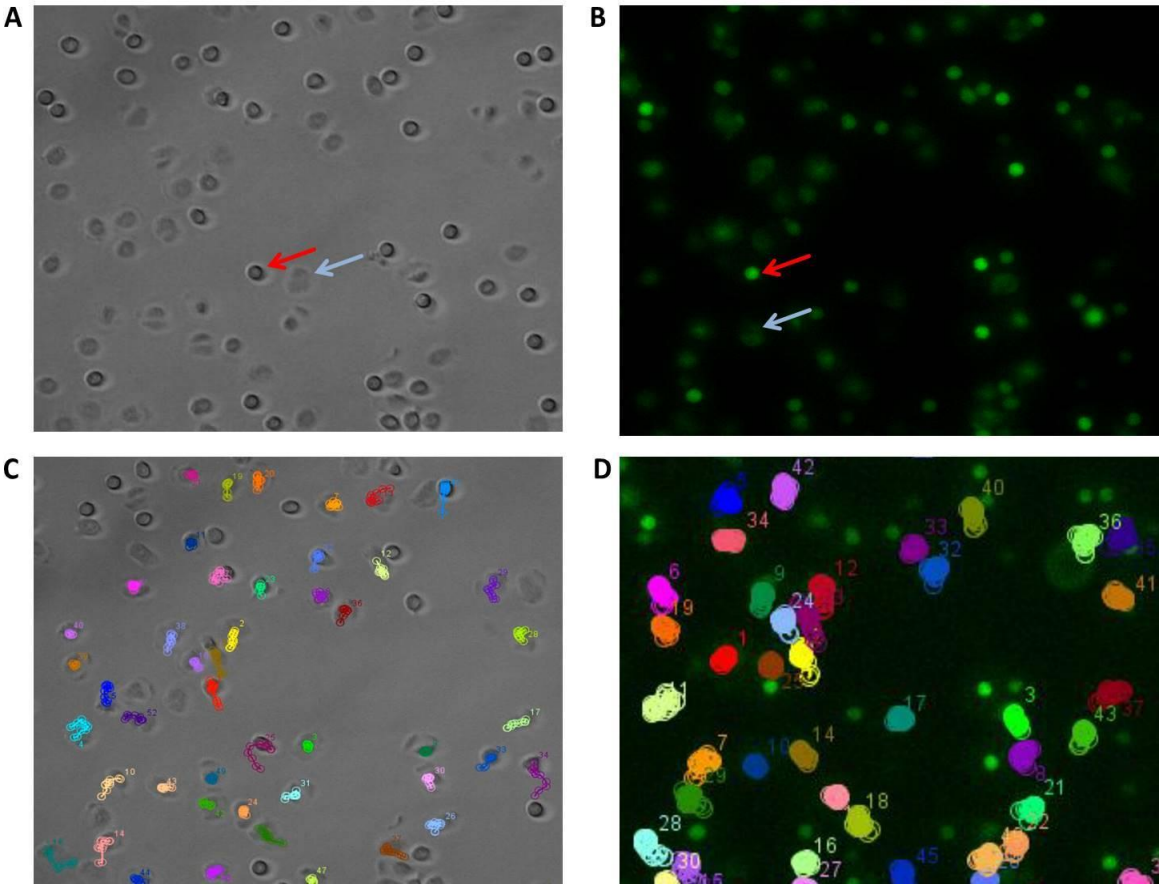

Supplementary Figure 9. An *in-vitro* time-lapse assay was employed to track migrating $CALR^{+/+}$ and $CALR^{del/+}$ $tdTomato^{+}$ cells. (A) Brightfield illumination of $tdTomato^{+}$ cells on a slide pre-coated with VCAM-1 and ICAM-1. The red arrow indicates a round non-adherent cell, whereas the blue arrow denotes a flattened firmly adherent migratory cell. (B) In the tdTomato channel, non-adherent cells (red arrow) demonstrate higher fluorescence than adherent cells (blue arrow), possibly due to flattening of the former and increase in their surface area. Manual cell tracking of migratory cells either in brightfield view (C) or in the channel for tdTomato (D).

Supplemental Table S1: No significant alterations of cytokine concentrations were observed in plasma of $CALR^{del/+}$ Catchup mice. Median cytokine concentrations in plasma of $CALR^{+/+}$ Catchup (n = 8, n = 5 for IL-4) and $CALR^{del/+}$ Catchup mice (n = 10, n = 6 for IL-4, n = 9 for IL-17), fold change and corresponding p-value. Determination by Eve Technologies, Canada (Mouse Cytokine Array/Chemokine Array 31-Plex, duplicate testing) using two-fold diluted serum samples. Data are shown as median values (unpaired, two-tailed *t*-test).

Cytokine	**$CALR^{+/del}$ Catchup mice, median [pg/ml]**	**$CALR^{+/+}$ Catchup mice, median [pg/ml]**	**Fold change**	**p-value**
Eotaxin	1155.93	1022.83	1.13	0.9929
G-CSF	461.67	515.2	0.90	0.1977
GM-CSF	30.40	34.94	0.87	0.4563
IFNγ	3.58	4.16	0.86	0.9257
IL-1α	332.06	328.19	1.01	0.8376
IL-1β	14.63	19.6	0.75	0.0664
IL-2	59.26	60.81	0.97	0.9996
IL-3	3.01	2.85	1.06	0.5910
IL-4	1.98	1.47	1.35	0.7760
IL-5	28.97	19.04	1.52	0.0867
IL-6	5.82	5.11	1.14	0.5702
IL-7	7.58	6.91	1.10	0.4371
IL-9	66.6	76.11	0.88	0.4874
IL-10	10.41	12.13	0.86	0.6206
IL-12 (p40)	15.03	16.15	0.93	0.6552
IL-12 (p70)	98.45	97.19	1.01	0.4240
IL-13	49.84	55.22	0.90	0.6608
IL-15	102.57	88.48	1.16	0.7360
IL-17	2.52	3.37	0.75	0.2941
IP-10	65.32	62.34	1.05	0.6450
KC	271.57	333.70	0.81	0.9695
LIF	2.64	2.25	1.17	0.2997
LIX	1689.66	996.55	1.70	0.3678
MCP-1	93.34	136.58	0.68	0.2513
M-CSF	31.59	32.42	0.97	0.2548
MIG	96.18	120.78	0.80	0.2469
MIP-1α	104.57	107.38	0.97	0.9011
MIP-1β	74.77	95.17	0.79	0.7410
MIP-2	361.23	342.79	1.05	0.9116
RANTES	31.02	31.71	0.98	0.3897
TNFα	15.22	19.86	0.77	0.1033
VEGF	1.44	1.32	1.09	0.5157

Supplementary Table S2. Summary of CALRdel52 mutant mouse models.

Authors	Mouse model	Zygosity	Blood counts	Spleen size	BM and Spleen composition		Histopathological analysis	
					Bone Marrow	Spleen	Bone Marrow	Spleen
Achyuthuni et al (191)	Transgenic conditional knock-in (vavCre) of mouse-human CALR-del52 chimeric oncogene	$CALR^{del52/+}$	↑PLTs starting at 6 weeks (2-fold at 52 weeks)	1.3-fold ↑ at 1 year	↑Mks at 6 months ↑LSK cells at 1 year	↑Mks ↑LSK cells ↑LT-HSCs ↑ST-HSCs ↑MPPs at 1 year	↑Mk dysplasia at 6 months	↑Mk hyperplasia ↑Mk dysplasia ↑Red pulp ↑ Lymphoid follicles at 1 year
		$CALR^{del52/del52}$	↑↑ PLTs starting at 6 weeks (4.4-fold at 52 weeks) ↑WBCs and ↓Hb at 6 months	2.25-fold ↑ at 6 months 3.3-fold ↑ at 1 year	↓Cellularity at 6 months ↑↑Mks at 6 months ↑↑LSK cells at 6 months	↑↑Mks ↑↑LT-HSCs at 6 months ↑LSK cells ↑↑ST-HSCs ↓MPPs at 1 year	↑Mk dysplasia at 6 months ↑↑Mk dysplasia at 1 year ↑Trabecular osteosclerosis ↑Reticulin (mild) at 1 year	↑↑Mk hyperplasia ↑↑Mk dysplasia ↑↑Red pulp ↑↑ Lymphoid follicles at 6 months
Ballig and et al (192)	CRISPR/Cas9	$CALR^{del52/+}$	↑PLTs (1.4-fold) at 19 weeks ↑WBCs at 52 weeks	Unremarkable	↑Mks	Unremarkable	↑Mk size Staghorn Mks	-
		$CALR^{del52/del52}$	Embryonic lethality due to defective heart development.					
Benlabiod et al (193)	Transgenic conditional knock-in (tamoxifen-inducible SCL-$CreER^{T}$) of mouse-human CALR-del52 chimeric oncogene	$CALR^{del52/+}$	↑PLTs (4-fold) 8 months post-tamoxifen ↑WBCs	Unremarkable	↓Cellularity ↑Mks ↑MkPs ↓$Ter119^{+}$ cells ↓BFU-E	↑Mks ↑MkPs	↑Mk hyperplasia	↑Mk size with polylobulation ↑Mk hyperplasia with partial disorganization ↑Reticulin
		$CALR^{del52/del52}$	↑↑PLTs (9-fold) 8 months post-tamoxifen ↑↑WBCs ↓Hb	↑2.7-fold	↓↓Cellularity ↑↑Mks ↑↑MkPs ↓↓$Ter119^{+}$ ↓↓BFU-E ↑SLAM cells	↑↑Mks ↑↑MkPs ↑$Ter119^{+}$ cells ↑CD11b+ $Gr1^{+}$ cells ↑CFU-GM ↑SLAM cells	↑↑Mk hyperplasia ↑Reticulin (mild) Neo-osteogenesis (rarely)	↑Mk size with polylobulation ↑↑Mk hyperplasia with effacement of white pulp ↑↑Reticulin
Elf et al (194)	Retroviral BMT	CALRdel52-mutated chimera	↑PLTs (1.9-fold) 16 weeks post-	-	↑Mks ↑LSK cells	-	↑Mk size Mks with hyperlobulated	-

		s	transplantation				nuclei and emperipolesis	
Li et al (170)	Transgenic conditional knock-in (Mx1 Cre) of mouse-human CALR-del52 chimeric oncogene	$CALR^{del52/+}$	↑PLTs (3-fold) ↑WBCs 3-4 months post poly I:C	Unremarkable	↑Mks ↑HSCs ↑CFU-MK ↓erythroblasts	Unremarkable	↑Mk hyperplasia Mks with hyperlobulated nuclei and clustering	Unremarkable
		$CALR^{del52/del52}$	↑↑PLTs (10-fold) ↑↑WBCs ↓Hb 3-4 months post poly I:C	↑	↑↑Mks ↑HSCs ↑MkPs ↓erythroblasts	↑HSCs ↑MkPs ↑Myeloid progenitors	↑↑Mk hyperplasia with nuclear atypia Effacement of normal hematopoiesis ↑Reticulin	↑↑Mk hyperplasia with nuclear atypia Effacement of splenic architecture
Marty et al (195)	Retroviral BMT	CALRdel52-mutated chimeras	↑PLTs (4.4-fold) 6 months post BMT ↓RBCs 1 year post BMT	2.7-fold ↑ 10 months post BMT	↓BM total cells ↑Mks ↑LSK cells ↑SLAM cells ↑CFU-MK	↑Mks ↑LSK cells ↑SLAM cells	Mk clustering Osteosclerosis Reticulin thickening 10 months post BMT	Mk clustering Osteosclerosis Reticulin thickening 10 months post BMT
Shide et al (196)	Transgenic knock-in of human CALRdel52	CALRdel52-transgenic mice	↑PLTs (2-fold) at 8 weeks	Unremarkable	↑Mks ↑MkPs ↑LT-HSCs ↑ST-HSCs ↑LSK cells ↑CMPs ↑MEPs	↑Mks	↑Mk size ↑Mk α-granules	↑Mk size ↑Mk α-granules

BFU-E, Burst Forming Unit-Erythroid; BMT, Bone Marrow Transplantation; CFU-MK, Colony Forming Unit-Megakaryocyte; CFU-GM, Colony Forming Unit-Granulocyte/Macrophage; Hb, Hemoglobin; LSK, $Lineage^{-}$ $Sca\text{-}1^{+}$ $c\text{-}kit^{+}$; LT-HSC, Long Term-Hematopoietic Stem Cell; Mk, Megakaryocyte; MkPs, Megakaryocyte Progenitors; MPP, Multipotent Progenitor; PLT, Platelet; RBC, Red Blood Cell; ST-HSC, Short Term-Hematopoietic Stem Cell; WBC, White Blood Cell

Supplemental documents (Permission to use English language and equivalency test of medical school diploma)

Bewertung ausländischer Bildungsnachweise

Sehr geehrter Herr Charakopoulos,

Sie informierten uns darüber, dass Sie beabsichtigen, in Deutschland zu promovieren. Die einschlägigen Promotionsordnungen gestatten dies im Allgemeinen, wenn ein äquivalenter Hochschulabschluss nachgewiesen werden kann. Letzteres überprüft eine dafür zuständige Zentralstelle für Ausländisches Bildungswesen in Bonn. Wir haben uns erlaubt, Ihre mitgereichten Unterlagen zu dieser Prüfung heranzuziehen.

Nach Informationen der Zentralstelle für Ausländisches Bildungswesen wird erklärt, dass Ihr Studienabschluss für Medizin an der Medizinischen Fakultät der Nationalen und Kapodistria Universität Athen/Griechenland, gleichwertig mit der deutschen ärztlichen Prüfung ist. Insofern sind wesentliche Voraussetzungen gegeben, dass Sie nach Fertigstellung Ihrer Dissertation diese als Promotionsleistung zum Dr. med. an unserer Fakultät einreichen können.

Weiterhin möchte ich Ihnen mitteilen, dass Sie die Dissertation in englischer Sprache einreichen können. Wie in der Promotionsordnung der Medizinischen Fakultät Magdeburg in § 6 Abs. 4 gefordert, soll die Dissertation zusätzlich eine deutschsprachige Zusammenfassung beinhalten.

Die übrigen Details für Ihr Promotionsvorhaben entnehmen Sie bitte der beigelegten Promotionsordnung unserer Fakultät.

Mit freundlichen Grüßen

Prof. Dr. med. Mawrin
Vorsitzender der Promotionskommission